AN INTER-BIOME COMPARISON OF STREAM NETWORK NITRATE DYNAMICS

by

ASHLEY McKENDREE HELTON

(Under the Direction of Geoffrey C. Poole)

ABSTRACT

A simulation model of stream network NO_3 dynamics was developed to scale up measurements of stream-reach NO_3 uptake in seven catchments. The model explained NO_3 dynamics well in two of seven catchments, revealing inter-biome differences in drivers of in-stream NO_3 dynamics. Where the model performed poorly, additional drivers included: spatial distribution of NO_3 sources; hydrologic delivery pathways of NO_3; surface water-groundwater exchange; downstream changes in geomorphology/flow; and variation in uptake. Where the model performed well, uptake was a stronger driver and the network removed a higher proportion of NO_3 inputs in Kansas than in North Carolina. In both catchments, small streams removed a substantial proportion of total inputs and were efficient NO_3 removers, whereas large streams removed more NO_3 mass individually. This research highlights the importance of understanding the influence of hydrology, geomorphology and biology on in-stream NO_3 dynamics in order to explain, predict and understand NO_3 uptake across biomes.

INDEX WORDS: nitrate, nitrogen, nutrient cycling, stream network, model, nitrogen uptake, inter-biome comparison

AN INTER-BIOME COMPARISON OF STREAM NETWORK NITRATE DYNAMICS

by

ASHLEY McKENDREE HELTON

B.S., University of Cincinnati, 2004

A Thesis Submitted to the Graduate Faculty of the University of Georgia in Partial Fulfillment of the Requirements for the Degree

MASTER OF SCIENCE

ATHENS, GEORGIA

2006

AN INTER-BIOME COMPARISON OF STREAM NETWORK NITRATE DYNAMICS

by

ASHLEY McKENDREE HELTON

Major Professor:	Geoffrey C. Poole
Committee:	Judith L. Meyer Miguel Cabrera

Electronic Version Approved:

Maureen Grasso
Dean of the Graduate School
The University of Georgia
August 2006

ACKNOWLEDGEMENTS

I thank my committee, Geoff Poole, Judy Meyer, and Miguel Cabrera, for their continued support in completing this research. I feel extremely fortunate to have had Geoff Poole as my advisor and mentor, and I thank him for his support, advice, and encouragement over the past two years.

I acknowledge the LINX-II research group, particularly Pat Mulholland for facilitating data sharing between myself and other LINX researchers, Jack Webster for teaching me field techniques, Clay Arango for his special attention to spatial data, and everybody in the LINX-II field teams that collected chemical and spatial data used in model development. Thanks to Wil Wollheim for advice during model development. Thanks to Chris Bennett for programming help and to Eco-metrics, Inc. for computer resources and support.

Thanks to Meyerfauna past and present for helpful input and creative ideas: Will Duncan, Gretchen Loeffler Peltier, Norm Leonard, Monica Palta, Elizabeth Sudduth, Krista Jones and Theresa Thom. Thanks to my office-mates who make life in the Ecology Building much more interesting: Gretchen Loeffler Peltier, John Davis, Cindy Tant, Will Duncan…

I thank my family: my mom, my grandmother, and my sisters for their continued support over the years. I am especially grateful to my husband, Nick, for all of his love and support.

This research was funded as part of the Lotic Intersite Nitrogen eXperiments funded by the National Science Foundation (DEB #0111410).

TABLE OF CONTENTS

LIST OF TABLES

LIST OF FIGURES

CHAPTER1

INTRODUCTION

Humans have substantially altered the global nitrogen (N) cycle. Human activities, such as increased fertilizer application, propagation of N-fixing crops, and fossil fuel combustion, have at least doubled the natural rate of N fixation into biologically available forms (Vitousek et al. 1997). Human activities have also released large amounts of N from long-term storage, through drainage of wetlands, land clearing and conversion, and burning of biomass (Vitousek et al. 1997; Matson et al. 1987). One consequence of increasing the supply of bioavaliable N to landscapes is that the rate at which N is leached to surface water increases, which, in turn, increases the transfer of N through rivers to estuaries and coastal areas. In effect, human activity has increased riverine N inputs to the ocean by about 3-fold for all of North America (Howarth 1998), and the links between increased N loads and eutrophication and hypoxia in coastal ecosystems have been well documented (Turner and Rabalais 1994; Scavia et al. 2003; Turner et al. 2005).

Nitrate-nitrogen (NO_3-N) is of particular concern because, since NO_3-N is the most soluble and mobile form of N, it is easily leached by precipitation into groundwater and streams. Anthropogenic changes in stream NO_3-N concentration account for most of the total human impact on riverine N export (worldwide, Caraco and Cole 1999; Mississippi river, Goolsby and Battaglin 2001). For example, the total N concentration has nearly doubled, whereas the NO_3-N concentration has increased by a factor of 10 in the lower Mississippi since estimated pre-European settlement concentrations (Goolsby and Battaglin 2001). Furthermore, NO_3-N

concentrations have doubled in the Mississippi river basin since 1965 and have increased 3- to 10- fold in rivers of the Northeastern United States since the early 1900s (Vitousek et al. 1997).

However, streams and rivers are not simply inactive conduits transporting nutrients and other materials to receiving water bodies. They play an important role in N delivery to coastal ecosystems since they act to store, transport and transform N moving from upland to coastal areas. Recent mass balance studies indicate that riverine N flux measurements account for only 20 to 25% of anthropogenic N inputs to the landscape (Howarth et al. 1996), and that in-stream removal may account for a substantial proportion of landscape N removal (Howarth et al. 1996; VanBreemen et al. 2002). Recent landscape models of N dynamics have been used to estimate stream network N attenuation across large river basins. These studies show that in-stream N removal is substantial across river networks (Alexander et al. 2000; de Wit 2001; Seitzinger et al. 2002; Donner et al. 2004) and that N removal efficiency and magnitude vary throughout the network depending on stream size (Alexander et al. 2000; Wollheim et al. 2006). Small streams remove a larger proportion of their direct N inputs (Alexander et al. 2000; Wollheim et al. 2006); whereas, on average, large streams remove greater masses of N (Seitzinger et al. 2002; Wollheim et al. 2006).

On the stream-reach scale, N amendment studies, in which a particular form of N (or a stable N isotope, e.g., Mulholland et al. 2004) is added to single reaches of small streams (Stream Solute Workshop 1990), are performed to quantify N removal from the water column via denitrification and biotic and abiotic uptake (e.g., Dodds et al. 2000; Hamilton et al. 2001; Merriam et al. 2002; Böhlke et al. 2004; Royer et al. 2004; Payne et al. 2005). Controls of N uptake on the reach-scale have been studied extensively. Some notable studies have explored the relationships between N uptake and an array of physical and biological variables, including

transient storage (Valett et al. 1996; Hall et al. 2002), N concentration in the water column (Dodds et al. 2002), carbon and N stoichiometry (Dodds et al. 2004), whole stream metabolism (Hall and Tank 2003), riparian vegetation and algal growth (Sabater et al. 2000), aullochthonous inputs (Webster et al. 2000), and channel complexity and geomorphic variability (Doyle et al. 2003).

Researchers have expended much effort quantifying reach-scale N uptake and understanding controls of N dynamics on the stream reach scale. However, much less is known about in-stream N dynamics on the stream network scale. Over 200 nitrate and ammonium amendment experiments have been published (Ensign and Doyle In Revision); whereas only a handful of landscape-scale models have dealt explicitly with N processing across river networks (see Wollheim et al. 2006). Furthermore, landscape-scale studies generally use a statistical approach to estimate in-stream losses (e.g., SPARROW model, Smith et al. 1997), whereas studying N processing on the reach-scale requires a more mechanistic approach (e.g., nutrient spiraling, Newbold et al. 1981). Thus, the goal of this research is to scale up *in situ* measurements of NO_3-N uptake to the stream network scale among seven 3^{rd} to 6^{th} order stream networks in seven different biomes across the United States and Puerto Rico (Figure 1.1), which correspond to the second Lotic Intersite Nitrogen eXperiment study sites (LINX-II).

I developed a simulation model of stream network NO_3-N dynamics to scale up reach-scale measurements of biological NO_3-N uptake made during the LINX-II field experiments. The simulation model is based on classic flow accumulation network hydrology, in which water accumulates in streams from topographically contributing drainage areas, and NO_3-N uptake schema that incorporates changes in physical parameters in a downstream direction. The model was used as a reference condition in order to compare drivers of stream network NO_3-N

dynamics amongst biomes and to determine the relative influence of uptake as a driver of NO_3 dynamics among stream networks (Chapter 2) and to determine the whole-network NO_3 removal and the spatial distribution of NO_3 removal among stream sizes for a subset of the stream networks (Chapter 3). This research extends large river network estimates of in-stream N attenuation (e.g., Alexander et al. 2000) into smaller headwater streams and extends measurements of reach-scale N removal to mechanistic predictions of N removal on the stream network scale, thus making initial linkages between reach-scale and landscape-scale estimates of in-stream N removal.

References

Alexander, R. B., R. A. Smith, and G. E. Schwarz. 2000. Effect of stream channel size on the delivery of nitrogen to the Gulf of Mexico. Nature **403**:758-761.

Böhlke, J. K., J. W. Harvey, and M. A. Voytek. 2004. Reach-scale isotope tracer experiment to quantify denitrification and related processes in a nitrate-rich stream, midcontinent United States Limnology and Oceanography **49**:821-838.

Caraco, N. F., and J. J. Cole. 1999. Human impact on nitrate export: An analysis using major world rivers. Ambio **28**:167-170.

de Wit, M. J. M. 2001. Nutrient fluxes at the river basin scale. I: the PolFlow model. Hydrological Processes **15**:743-759.

Dodds, W. K., M. A. Evans-White, N. M. Gerlanc, L. Gray, D. A. Gudder, M. J. Kemp, A. L. López, D. Stagliano, E. A. Strauss, J. L. Tank, M. R. Whiles, and W. M. Wollheim. 2000. Quantification of the Nitrogen Cycle in a Prairie Stream. Ecosystems **3**:574-589.

Dodds, W. K., A. J. López, W. B. Bowden, S. Gregory, N. B. Grimm, S. K. Hamilton, A. E. Hershey, E. Martí, W. H. McDowell, J. L. Meyer, D. Morrall, P. J. Mulholland, B. J. Peterson, J. L. Tank, H. M. Valett, J. R. Webster, and W. Wollheim. 2002. N uptake as a function of concentration in streams. Journal of the North American Benthological Society **21**:206-220.

Dodds, W. K., E. Martí, J. L. Tank, J. Pontius, S. K. Hamilton, N. B. Grimm, W. B. Bowden, W. H. McDowell, B. J. Peterson, H. M. Valett, J. R. Webster, and S. Gregory. 2004. Carbon and nitrogen stoichiometry and nitrogen cycling rates in streams. Oecologia **140**:458-467.

Donner, S. D., C. J. Kucharik, and M. Oppenheimer. 2004. The influence of climate on in-stream removal of nitrogen. Geophysical Research Letters **31**:doi: 10.1029/2004GL020477.

Doyle, M. W., E. H. Stanley, and J. M. Harbor. 2003. Hydrogeomorphic controls on phosphorus retention in streams. Water Resources Research **39**:doi:10.1029/2003WR002038.

Ensign, S. H., and M. W. Doyle. In Revision. Nutrient spiraling in streams and river networks. Journal of Geophysical Research – Biogeosciences.

Goolsby, D. A., and W. A. Battaglin. 2001. Long-term changes in concentrations and flux of nitrogen in the Mississippi River Basin, USA. Hydrological Processes **15**:1209-1226.

Hall, R. O. J., E. S. Bernhardt, and G. E. Likens. 2002. Relating nutrient uptake with transient storage in forested mountain streams Limnology and Oceanography **47**:255-265.

Hall, R. O. J., and J. L. Tank. 2003. Ecosystem metabolism controls nitrogen uptake in streams in Grand Teton National Park, Wyoming Limnology and Oceanography **48**:1120-1128.

Hamilton, S. K., J. L. Tank, D. F. Raikow, W. M. Wollheim, B. J. Peterson, and J. R. Webster. 2001. Nitrogen uptake and transformation in a midwestern U.S. stream: A stable isotope enrichment study. Biogeochemistry **54**:297-340.

Howarth, R. W. 1998. An assessment of human influences on fluxes of nitrogen from the terrestrial landscape to the estuaries and continental shelves of the North Atlantic Ocean. Nutrient Cycling in Agroecosystems **52**:213-223.

Howarth, R. W., G. Billen, D. Swaney, A. Townsend, N. Jaworski, K. Lajtha, J. A. Downing, R. Elmgren, N. Caraco, T. Jordan, F. Berendse, J. Freney, V. Kudeyarov, P. Murdoch, and Z. Zhao-Liang. 1996. Regional nitrogen budgets and riverine N and P fluxes for the drainages to the North Atlantic: Natural and human influences. Biogeochemistry **35**.

Matson, P. A., P. M. Vitousek, J. J. Ewel, M. J. Mazzarino, and G. P. Robertson. 1987. Nitrogen Transformations Following Tropical Forest Felling and Burning on a Volcanic Soil. Ecology **68**:491-502.

Merriam, J. L., W. H. McDowell, J. L. Tank, W. M. Wollheim, C. L. Crenshaw, and S. L. Johnson. 2002. Characterizing nitrogen dynamics, retention and transport in a tropical rainforest stream using an in situ 15N addition. Freshwater Biology **47**:143-160.

Mulholland, P. J., H. M. Valett, J. R. Webster, S. A. Thomas, L. W. Cooper, S. K. Hamilton, and B. J. Peterson. 2004. Stream denitrification and total nitrate uptake rates measured using a field 15N tracer addition approach Limnology and Oceanography **49**:809-820.

Newbold, J. D., J. W. Elwood, R. V. O'Neill, and W. Van Winkle. 1981. Measuring Nutrient Spiralling in Streams. Canadian Journal of Fisheries & Aquatic Sciences **38**:860-863.

Payne, R. A., J. R. Webster, P. J. Mulholland, H. M. Valett, and W. K. Dodds. 2005. Estimation of stream nutrient uptake from nutrient additions experiments. Limnology and Oceanography: Methods **3**:174-182.

Royer, T. V., J. L. Tank, and M. B. David. 2004. Transport and Fate of Nitrate in Headwater Agricultural Streams in Illinois Journal of Environmental Quality **33**:1296-1304

Sabater, F., A. Butturini, I. Muñoz, A. Romaní, S. Sabater, E. MartÍ, and J. Wray. 2000. Effects of riparian vegetation removal on nutrient retention in a Mediterranean stream. Journal of the North American Benthological Society **19**:609-620.

Scavia, D., N. N. Rabalais, R. E. Turner, D. Justic´, and J. William J. Wiseman. 2003. Predicting the response of Gulf of Mexico hypoxia to variations in Mississippi River nitrogen load Limnology and Oceanography **48**:951-956.

Seitzinger, S. P., R. V. Styles, E. W. Boyer, R. B. Alexander, and G. Billen. 2002. Nitrogen retention in rivers: model development and application to watersheds in the northeastern U.S.A. Biogeochemistry **57**:199-237.

Smith, R. A., G. E. Schwarz, and R. B. Alexander. 1997. Regional interpretation of water-quality monitoring data. Water Resources Research **33**:2781-2798.

Stream Solute Workshop. 1990. Concepts and methods for assessing solute dynamics in stream ecosystems. Journal of the North American Benthological Society **9**:95-119.

Turner, R. E., and N. N. Rabalais. 1994. Coastal eutrophication near the Mississippi river delta. Nature **368**:619-621.

Turner, R. E., N. N. Rabalais, E. M. Swenson, M. Kasprzak, and T. Romaire. 2005. Summer hypoxia in the northern Gulf of Mexico and its prediction from 1978 to 1995. Marine Environmental Research **59**:65-77.

Valett, H. M., J. A. Morrice, C. N. Dahm, and M. E. Campana. 1996. Parent Lithology, Surface-Groundwater Exchange, and Nitrate Retention in Headwater Streams. Limnology and Oceanography **41**:333-345.

Van Breemen, N., E. W. Boyer, and C. L. Goodale. 2002. Where did all the nitrogen go? Fate of nitrogen inputs to large watersheds in the northeastern U.S.A. Biogeochemistry **57**:267-293.

Vitousek, P. M., J. D. Aber, R. W. Howarth, G. E. Likens, P. A. Matson, D. W. Schindler, W. H. Schlesinger, and D. G. Tilman. 1997. Technical Report: Human Alteration of the Global Nitrogen Cycle: Sources and Consequences. Ecological Applications **7**:737-750.

Webster, J. R., J. L. Tank, J. B. Wallace, J. L. Meyer, S. L. Eggert, T. P. Ehrman, B. R. Ward, B. L. Bennett, P. F. Wagner, and M. E. McTammany. 2000. Effects of litter exclusion and wood removal on phosphorus and nitrogen retention in a forest stream. Verh. Internat. Verein. Limnol. **27**:1337-1340.

Wollheim, W. M., C. J. Vorosmarty, B. J. Peterson, S. P. Seitzinger, and C. S. Hopkinson. 2006. Relationship between river size and nutrient removal. Geophysical Research Letters **33**:doi:10.1029/2006GL025845.

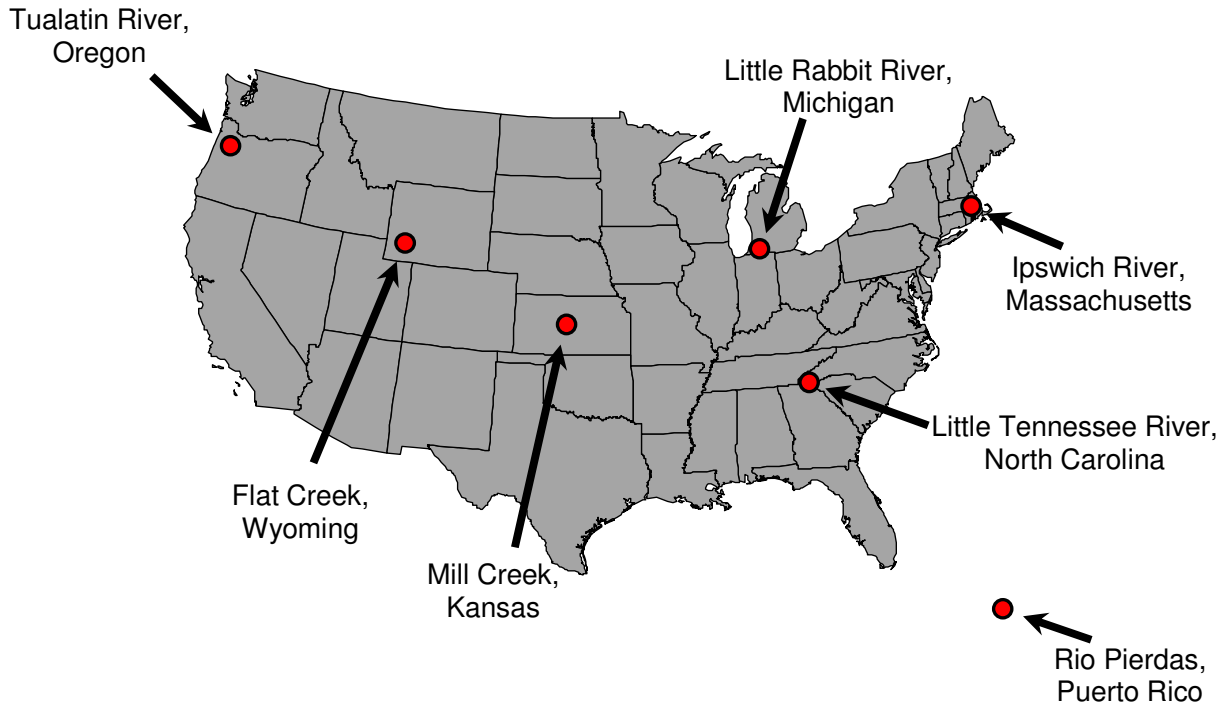

Figure 1.1: Locations of study stream networks, which correspond to LINX-II study sites.

CHAPTER 2

INTER-BIOME COMPARISON OF CATCHMENT-SCALE DRIVERS OF STREAM NETWORK NITRATE DYNAMICS[1]

---

[1]Helton, A.M., G.C. Poole, J.L. Meyer, C. Arango, L.R. Ashkenas, C.Dahm, W. K. Dodds, S. Gregory, N. B. Grimm, R. O. Hall, S. H. Hamilton, S. L. Johnson, W. H. McDowell, P. J. Mulholland, B. J. Peterson, J. L. Tank, H. M. Valett, and J. R. Webster. To be submitted to an undecided journal.

Abstract

The goal of this research was to identify and compare stream network-scale drivers of (nitrate-nitrogen) NO_3-N dynamics among seven 3rd to 6th order stream networks in different biomes across the United States and Puerto Rico. We attempted to scale up reach-scale *in situ* measurements of biological NO_3-N uptake to the stream network scale in each study catchment using a simulation model based on conceptualizations about stream networks commonly used in landscape modeling. We used this model as a common frame of reference to compare NO_3-N dynamics across study networks. The model explained NO_3-N dynamics well in two (North Carolina and Kansas) of the seven networks, revealing differences among biomes in drivers of in-stream NO_3-N dynamics. In the North Carolina stream network, the model did not require biological uptake to explain landscape NO_3-N dynamics; hydrologic delivery and transport were sufficient. Conversely, in the Kansas stream network, the model did require biological uptake to explain landscape NO_3-N dynamics. Where the model performed poorly, we found that additional drivers not incorporated in the model included: 1) the spatially explicit distribution of anthropogenic sources of N to streams; 2) the influence of multiple hydrologic pathways of nutrient delivery to streams; 3) the relative roles of the hyporheic zone versus the stream bed in nutrient processing; 4) discontinuities and abrupt changes in downstream channel geometry and flow because of urbanization and natural features; and 5) variation in biological and environmental factors that drive biological uptake across stream networks. This study illustrates the importance of incorporating hydrologic, geomorphologic, chemical, and biological drivers of nutrient dynamics into conceptual models used for hypothesis generation, research design and stream network models.

Introduction

Recent research in lotic systems has focused on understanding the role streams play in retaining, removing and transforming nutrients. Both reach-scale field experiments (e.g., Peterson et al. 2001) and stream network-scale models (e.g., Alexander et al. 2000) have shown that streams remove a high proportion of nitrogen (N) delivered from the landscape. However, field experiments involving N amendments to whole stream reaches have primarily dealt with in-stream removal resulting from streambed water column interactions in perennial stream reaches within a narrow range of environmental conditions (e.g., small streams during base flow, Fisher et al. 2004); whereas landscape-scale models focus on predicting N export from watersheds over coarse spatial and temporal scales. The limited settings under which field conditions are measured coupled with the coarse scale of landscape models make incorporating field observations into stream network-scale models difficult.

Nevertheless, stream network-scale models have recently begun integrating in-stream processing into their predictions of N export from large watersheds. In-stream N removal in these models is predicted from the relationship between parameterized removal coefficients and stream channel characteristics, such as channel geometry, stream flow or channel slope. Equations that describe in-stream N removal may be empirically derived using a mass balance approach (e.g., SPARROW, Smith et al. 1997; Alexander et al. 2000), empirically derived using literature estimates of sediment denitrification and mass balance in-stream losses (e.g., RIV-N, Seitzinger et al. 2002) or estimated during model calibration (e.g., PolFlow, de Wit 2001; Darracq and Destouni 2005). However, none of these network-scale studies have incorporated biological processing from whole reach N amendment experiments. Depending on assumptions about stream network structure and about the relationships between in-stream removal and

patterns of N delivery, hydrology and geomorphology, estimated N removal in stream networks can be highly variable among predictions made for the same stream network with different models (Alexander et al. 2002; Wollheim et al. 2006).

Although predicted removal can be highly variable and the precise equations used to relate in-stream removal to physical characteristics of stream channels differ (Wollheim et al. 2006), stream network-scale models of N dynamics generally share common underlying assumptions about N delivery to streams, hydrology, and geomorphology that drive modeled patterns of in-stream N removal. N delivery to streams is estimated from either uniform loads from the landscape (e.g., Caraco and Cole 1999; Seitzinger et al. 2002) or spatially explicit loads (e.g., Alexander et al. 2000; Van Drecht et al. 2003). Spatial heterogeneity of loading has been shown by some researchers to have only a small to moderate impact on the overall proportion of N retained by the stream network (Alexander et al. 2002; Seitzinger et al. 2002), whereas other researchers have suggested that adequately describing the spatial distribution of N delivery is necessary to avoid major biases in nutrient removal estimates (Johnes and Butterfield 2002; Lindgren and Destouni 2004).

There are models that have relatively detailed representations of hydrologic delivery of N to streams (e.g., SPARROW, Smith et al. 1997; PolFlow, de Wit 2001); however stream network models invest little in describing geomorphic and hydrologic variation within stream channels that drives in-stream biological processing. Stream network models generally assume that channel geometry changes predictably and continuously downstream in proportion to flow (e.g., $w = aQb$, $d = cQd$ where w = width, d = depth, Q = flow, a and c are width and depth coefficients, respectively, and b and d are width and depth exponents, respectively; Leopold and Maddock 1953). For example, Alexander et al. (2000) and Seitzinger et al. (2002) both use the

depth coefficient and exponent derived by Leopold and Maddock (1953) from data describing 112 streams across the United States. Other models that utilize channel geometry use the same equations parameterized with different datasets (e.g., Donner et al. 2002; Donner et al. 2004; Wollheim et al. In Review).

Stream network models also assume that flow changes continuously from headwater streams to the watershed outlet. Some models (e.g., Smith et al. 1997; Alexander et al. 2000; Seitzinger et al. 2002) use estimated stream flow from the EPA-USGS Reach File Version 1 (RF1) (W.E. Gates and Associates Inc 1982; Alexander et al. 1999). In the RF1 streams, lateral flows based on water yields derived from U.S. Geological Survey gauging data and upstream contributions were summed from upstream to downstream so that flow increased continuously downstream. Where measured flows decreased downstream a loss function was applied in the main stem to continuously decrease flow to the observed value at the downstream gage. Other models include a more detailed water runoff model, but once the flow enters the stream channel it increases continuously downstream (PolFlow, de Wit 2001; Donner et al. 2002; Darracq and Destouni 2005).

Although each approach is slightly different in its precise equations used to predict in-stream removal, all of the models described above are grounded in assumptions about in-stream hydrology and geomorphology that may ignore more complicated geomorphologic and hydrologic dynamics that drive network-scale patterns of in-stream processing. Recently researchers have suggested that stream networks are composed of heterogeneous discontinuous hydrogeomorphic reaches connecting the headwaters to the outlet that drive abrupt changes in biological communities and ecosystem functioning through the network (Poole 2002; Benda et al. 2004; Thorpe et al. 2006). The portrayal of streams as physically and ecologically continuous

ignores differential geology, tributary effects and geomorphic influences (Thorpe et al. 2006). In fact, stream network-scale ecosystem structure and processing may be driven by the geomorphic structure of the stream network (Benda et al. 2004; Ganio et al. 2005).

Therefore, the goal of this research was to identify and compare stream network-scale drivers of NO_3-N dynamics among seven 3rd to 6th order stream networks in different biomes across the United States and Puerto Rico. We attempted to scale up reach-scale *in situ* measurements of biological NO_3-N uptake to the stream network scale in each study catchment using a simulation model based on conceptualizations about stream networks commonly used in landscape modeling, which include relatively uniform N delivery to streams and continuous and predictable downstream changes in channel geometry and flow. Then, we used this model as a common frame of reference to compare NO_3-N dynamics across study networks. Where the model was sufficient to scale up measurements of reach-scale NO_3-N biological uptake, we examined the relative influence of uptake as a driver of landscape-scale NO_3-N dynamics. Where the model was inadequate, we used the model results to discern additional drivers of NO_3-N dynamics not incorporated by the simulation model. Identifying prominent drivers of NO_3-N dynamics across diverse landscapes allowed us to highlight opportunities for improving widely held conceptualizations about stream network N dynamics.

Methods

Overview

We conducted a formal test of commonly applied conceptualizations of in-stream N dynamics to determine where the assumptions about hydrology, geomorphology and biology were adequate to describe network-scale patterns of in-stream NO_3-N concentrations and to differentiate drivers of NO_3-N dynamics among stream networks. To test our conceptual model,

we developed a simulation model that represents our conceptual model of stream network NO_3-N dynamics. We used an inverse modeling approach to determine the spatial distribution of NO_3-N loading rates to streams necessary to recreate the observed patterns of NO_3-N concentration across seven stream networks. We implemented two different model scenarios: one that described hydrologic delivery and transport of NO_3-N within a given geomorphic network structure and one that added the biotic uptake of NO_3-N to hydrologic delivery and transport.

We assessed the performance of our simulation model (and thus, the appropriateness of the underlying conceptual model) using two lines of evidence: 1) the frequency of predicted extreme NO_3-N loading rate values; and 2) the correlations between simulated NO_3-N loading rates and patterns of land use known to influence NO_3-N loading rates to streams. We used the model results to conduct an inter-biome comparison of the seven stream networks. Where the model appeared to explain the drivers of NO_3-N dynamics, we tested the relative influence of uptake on landscape-scale patterns of NO_3-N. Where the model was deemed inadequate, we attempted to discern important dynamics in each catchment that were not incorporated by the conceptual model.

Model Development

Underlying conceptual model

The underlying conceptual model on which the simulation model is based encompasses general assumptions about hydrology, geomorphology and biology. In particular, the model is based on five major assumptions: 1) channel geometry changes predictably and continuously downstream in proportion to flow; 2) biological uptake per unit area increases monotonically with concentration; 3) streams gain water as they flow downstream from their drainage areas; 4)

water and NO_3-N yield per unit area are uniform for each contributing area (Figure 2.1); and 5) hydrologic flux within the network is at steady state. Based on these general assumptions we tested whether or not the model yielded realistic NO_3-N loading rates to streams given an observed distribution of NO_3-N concentration for a given stream network.

Implementation

We used the Network Exchange Objects (NEO) modeling system (Poole and Bennett, In Preparation) to develop a simulation model of NO_3-N loading, transport, and biotic uptake within stream networks. The NEO system incorporates concepts from the agent-based modeling paradigm (e.g., Grimm 1999) to simulate rule-based fluxes of "resources" through systems represented as networks. To develop the stream NO_3-N model, stream networks were compartmentalized into segments, defined as the length of stream between tributary junctions (Figure 2.2). The model routes NO_3-N and water from contributing drainage areas and through the stream network segment by segment from the headwaters to the outlet, and NO_3-N is removed from each segment via uptake by the stream bed (Figure 2.3). Additionally, our field data suggested that water withdrawals are important hydrologic drivers in some of the study basins (see Parameterization, below). In these networks, NO_3-N is removed in proportion to withdrawn water.

The NO_3-N concentration ($[NO_3]$, M L^{-3}) for any stream segment is equal to the following equation:

$$[NO_3]_p = NO3_p/Q_p \quad (1)$$

where $NO3_p$ is the mass of NO_3-N in stream segment p (M, where M is a measure of mass) and Q_p is the discharge of stream segment p (L^3T^{-1}, where L is a measure of length and T is a

measure of time). The model calculates NO_3 and Q using a simple steady state mass balance approach in which incoming flows are subtracted from outgoing flows for each stream segment.

The stream flow for each segment is calculated by subtracting outgoing flows from incoming flows according to the following equation:

$$Q_p = \Sigma Q_{p-i} + A_p * Y_p - Q_w - Q_{p+1} \quad (2)$$

where Q_p is the discharge of stream segment p (L^3T^{-1}), ΣQ_{p-i} is the sum of the discharges from contributing upstream segments (L^3T^{-1}), $A_p * Y_p$ represents discharge from the adjacent drainage area, where A_p is the adjacent drainage area of stream segment p (L^2), and Y_p is the water yield to stream segment p ($L^3L^{-2}T^{-1}$), Q_w is the water withdrawal from segment p (L^3T^{-1}), and Q_{p+1} is the discharge of water to the next downstream segment. The term Q_w is only applicable in two of the seven stream networks (Oregon and Wyoming) because there are instances in which measured flow decreases downstream (see Parameterization below).

The mass of NO_3-N for each segment is also calculated by subtracting outgoing NO_3-N from incoming NO_3-N according to the following equation:

$$NO3_p = \Sigma NO3_{p-i} + NO3Load_p - NO3Removed_p - NO3Withdrawal_p - NO3_{p+1} \quad (3)$$

where $NO3_p$ is the mass of NO_3-N in stream segment p (M), $\Sigma NO_3\text{-}N_{p-i}$ is the mass of NO_3-N from contributing upstream segments (M), $NO_3\text{-}NLoad_p$ is the mass of NO_3-N received by stream segment p from lateral sources (M), $NO_3\text{-}NRemoved_p$ is the mass of NO_3-N removed from stream segment p by in-stream processing (M), $NO_3\text{-}NWithdrawal_p$ is the mass of NO_3-N removed by water withdrawals (M). NO_3-NLoad for each stream segment is equal to the areal loading rate (L_p, ML^{-2}) multiplied by the adjacent drainage area of the stream segment (A_p, L^2). NO_3-NWithdrawal represents NO_3-N removed from each segment with water withdrawal and is removed in proportion to NO_3-N concentration so that removing NO_3-N by withdrawal does not

alter the NO_3-N concentration within a stream segment. The term NO_3-NWithdrawal is only applicable in two of the seven stream networks.

For each stream segment, NO_3-NRemoved is equal to the mass of NO_3-N in the stream segment times the fractional removal of NO_3-N which is determined by the following equation recently applied by Wollheim et al. (2006):

$$R = 1 - e^{(-v_f/H_L)} \quad (4)$$

where R is the fraction of NO_3-N removed, v_f is the average vertical velocity of NO_3-N molecules through the water column or the mass transfer coefficient (LT^{-1}), and H_L is the hydraulic load (LT^{-1}). The mass transfer coefficient is defined as the ratio of the areal NO_3-N uptake rate (U, $ML^{-2}T^{-2}$) to in-stream NO_3-N concentration (ML^{-3}). It represents uptake normalized by the concentration in the water column and thus is a measure of the biological and chemical demand for NO_3-N relative to the amount of NO_3-N available (Stream Solute Workshop 1990). The hydraulic load is the ratio of discharge into the stream segment (L^3T^{-1}) to the surface area of the water body. For a stream segment, surface area (L^2) equals the segment length multiplied by average width. Therefore, H_L is a measure of the rate of water passage through the water body relative to the benthic surface area available for NO_3-N removal. We chose this equation to represent NO_3-N removal because it explicitly integrates biological and chemical processing parameters directly measured in field experiments (v_f) and separates biological and chemical controls of removal (v_f) from hydrological controls (H_L) thereby eliminating the dependence of v_f on river size exhibited by in-stream removal equations used in many models (see additional discussion in Wollheim et al. 2006).

Model Application

Study Basins

We selected seven stream networks that contained or were in close proximity to stream reaches used in the second Lotic Intersite Nitrogen eXperiment (LINX-II; Table 2.1, Figure 2.4 – 2.10). Sampling for [NO_3-N] in the stream network was performed concurrently to $^{15}NO_3$-N tracer field experiments, in which *in situ* biological NO_3-N uptake rates were measured across stream reaches. This ensured that environmental conditions were similar in modeled catchments and experimental streams during sampling events.

Catchments were also chosen based on flow at their outlets during the time of LINX-II experiments. Because the relative importance of streambed dynamics in a stream is influenced by the ratio of discharge to streambed area (Dahm et al. 1998), comparing basins with approximately the same base flow discharge provided a more uniform comparison across basins than basin area or stream order. Depending on climate, drainage density, branching pattern, and the definition of first order streams (e.g., from 1:24,000 USGS maps versus perennial channels on the ground), the size of a 5th or 6th order stream and its catchment may vary remarkably across different climatic and geologic settings (Hughes and Omernik 1983). In particular, we targeted streams with base flows of 1000-5000 L s^{-1}, which provided a manageable sized watershed for gathering landscape data and had discharges approximately two orders of magnitude larger than streams in which the LINX-II $^{15}NO_3$-N field experiments were conducted.

In order to relate estimated NO_3-N loading rates to streams with land cover, catchments were also selected to have at least some proportion of agricultural, urban and forested land cover that was relatively well-distributed throughout the basin. Lastly, catchments were selected with minimal identified point sources and water withdrawals as well as an absence of major main

stem dams. Despite these efforts, 'ideal' study landscapes are impossible to find. Several sites had minor (or even occasional major) deviations from these ideals, as outlined in Discussion, below.

Model Parameterization

The simulation model requires the following stream network characteristics: network topology, drainage areas, hydrology, stream segment geometry, distribution of in-stream NO_3-N concentration, and biological uptake (v_f). A summary of catchment-scale geomorphic variables is given in Table 2.2 and Table 2.3.

Network structure: Although 1:100,000 or 1:500,000 hydrography datasets are typically used in stream network models (e.g., Alexander et al. 2000; de Wit 2001; Seitzinger et al. 2002), 1:24,000 digital hydrography datasets were obtained for each catchment since the catchments modeled in this study are small relative to catchments modeled in other studies. Each stream network was divided into segments, defined as the length of stream between tributary junctions. Segment flow direction was determined and, for each segment, the upstream "contributing" segments and the downstream "receiving" segment were recorded to enable the model to route flow and NO_3-N through the network.

Drainage Basin Delineation: Watershed boundaries for each [NO_3-N] sampling location and each stream segment were delineated from 30-meter raster digital elevation models (USGS National Elevation Data Set, available online at http://seamless.usgs.gov) using the Spatial Analyst extension in ArcView GIS software (Version 3.3, Environmental Systems Research Institute, Redlands CA 2002). Before delineating watersheds, elevation datasets were modified by lowering the elevation values of mapped steam channels to force flow direction maps to match existing 1:24,000 hydrography (e.g., King et al. 2005). Watershed boundaries were used

to determine contributing drainage areas for [NO_3-N] sampling locations and adjacent drainage areas for stream segments (Figure 2.1a-c). For sampling locations, the contributing drainage area is defined as the contributing basin area, but excluding areas that drain to any sampling location further upstream (Figure 2.1b). For stream segments, the adjacent drainage area is the drainage area contributing directly to each stream segment, not including area draining to upstream reaches (Figure 2.1c).

Hydrology: In order to effectively estimate water yield across the catchment, each catchment was divided into five to ten sub-catchments and discharge was measured at each sub-catchment outlet and at the catchment outlet during the time NO_3-N samples were collected (Figure 2.11). Water yield ($L^3\ L^{-2}\ T^{-1}$) for each sub-catchment was calculated by subtracting upstream measured flows and dividing the difference by the contributing drainage area. Each segment within a sub-catchment's contributing drainage area was assigned that sub-catchment's water yield (Figure 2.11).

In portions of two stream networks (Oregon and Wyoming) flows decreased in a downstream direction, creating the appearance of negative water yields in some contributing drainage areas. For those stream segments, we incorporated specific water withdrawals along the main stem. First, we assigned all segments in catchments with negative water yields the water yield value from the next upstream catchment. Then, we removed water and an amount of NO_3-N proportionate to the in-stream NO_3-N concentration from the main stem segments between the upstream and downstream measured flow in order to decrease the flow from the higher upstream observed flow to the lower downstream observed flow.

Stream segment geometry: Stream segment length was measured for each segment from the 1:24.000 digital hydrography dataset for each network. Average width was estimated for

each segment based on the equation $w = aQ^b$ from Leopold et al. (1964) where Q is the stream flow in the segment and a and b are the width coefficient and width exponent, respectively. The width coefficient and exponent were parameterized for each stream network using measured discharge and width data from each catchment (Table 2.3). Where insufficient width and/or flow data was available to quantify the relationship, the width coefficient and exponent were parameterized based on a combination of width and flow measurements from all sites (see Table 2.3).

[NO_3-N] sampling locations: Surveys of in-stream NO_3-N concentrations were performed concurrently with hydrologic measurements to describe the distribution of NO_3-N concentration throughout the stream network. A total of 30-50 sampling locations were distributed throughout each catchment, with one located at the outlet of the catchment, one each at the outlet of each sub-catchment, and the remainder in representative streams within the sub-catchments and along the main stem (Figures 2.4 – 2.10). Our objective was to choose sampling locations that were well-distributed among adjacent land-use types, across stream orders, and between sub-catchments. Each stream network was sampled for two consecutive years, except the Wyoming stream network, which was sampled for one year.

NO_3-N sampling was performed under similar field conditions (base flow) during the same season (summer) as the LINX-II $^{15}NO_3$-N field experiments. Sampling parameters included conductivity and temperature readings as well as water samples at every sampling location, analyzed for NO_3-N, ammonium-nitrogen, and total dissolved nitrogen, total nitrogen, total phosphorus, soluble reactive phosphorus, and chloride (Appendix A).

Biological Processing: LINX-II $^{15}NO_3$-N injection experiments were performed on three stream reaches within or near each stream network for three years, for a total of nine stream

reaches within each biome. [NO_3-N] sampling was performed during two of the three years of injection experiments. In this study we used NO_3-N uptake rates (U, $ML^{-2}T^{-1}$) and NO_3-N concentrations from the first two years of experiments for Massachusetts, Michigan, Oregon, Wyoming and Puerto Rico and data from all three years for Kansas and North Carolina. We used additional published uptake rates from North Carolina (Earl et al. Submitted) and Wyoming (Hall and Tank 2003). For a detailed description of techniques used in the LINX-II $^{15}NO_3$-N field experiments to determine U, see Mulholland et al. (2004).

Vertical velocity (v_f) was parameterized for each site as the slope of the linear relationship forced through zero between areal NO_3-N uptake rates and in-stream NO_3-N concentrations ($U = v_f$ [NO_3-N]). Both linear relationships between uptake and concentration (O'Brien et al. Submitted) and higher order kinetics (e.g., Michaelis-Menten kinetics, Dodds et al. 2002) have been observed. However, higher order kinetics were not evident in the data used to parameterize this model (Table 2.3). Linear regressions between NO_3-N uptake rates and concentrations were performed using R-Statistical Software (Version 2.2.1, R Foundation for Statistical Computing 2005; Table 2.3).

Scenario descriptions and model runs

The model was implemented under two scenarios. The first scenario described hydrologic delivery and transport of NO_3-N within each network (i.e., biological uptake = 0). The second scenario incorporated biological uptake (i.e., vf = U/[NO_3-N]) as well as hydrologic delivery and transport. We used the model to estimate the distribution of NO_3-N loading rates across each of the seven stream networks for each year where in-stream [NO_3-N] samples were collected for both scenarios for a total of 26 model runs (Table 2.5). For each model run, modeled discharge and NO_3-N were initialized to zero for each stream segment. NO_3-N and

water were allowed to accumulate from the landscape and passed through the stream network until the model reached steady state conditions, so that the model ran for as many iterations as required for water flowing from the most upstream segment in the first iteration to reach the outlet in the final iteration.

We used a model-independent parameter optimiser, Parameter ESTimation (PEST; Version 10.1, S.S. Papadopoulos and Associates, Inc. 2006) to determine the spatially-explicit pattern of NO_3-N loading rates required to reproduce the observed patterns of in-stream NO_3-N concentrations across each stream network. PEST determined areal NO_3-N loading rates for the contributing area of each sampling location and assigned the loading rate to each stream segment within a sampling location's contributing area (Figure 2.1b). Loading rates were not permitted to drop below zero.

This approach constitutes an inverse modeling approach, since we used the model to estimate model parameters. Landscape-scale models of nutrient fluxes generally use estimates of landscape loading rates as model input so that in-stream concentrations are some function of landscape loading (i.e., $[NO_3\text{-N}] = f(\text{Loading})$; e.g., Smith et al. 1997). However, in our model we make no *a priori* estimates of NO_3-N loading rates, and we use PEST to compute the pattern of loading for a given distribution of NO_3-N concentration (i.e., $\text{Loading} = f([NO_3\text{-N}])$). For any particular distribution of NO_3-N concentration there must be some distribution of loading to the stream network that recreates that particular pattern of concentration. We used the model to estimate that pattern of loading.

Model Output Analysis

We used the estimated loading rate parameter values to test the effectiveness of the underlying conceptual model in describing network-scale NO_3-N dynamics for the seven stream

networks. Because the number of NO_3-N concentration samples collected was limited for each stream network, we did not have NO_3-N concentrations to corroborate the model. Thus, we assessed the performance of our simulation model using two lines of evidence: 1) the frequency of predicted extreme NO_3-N loading rate values; and 2) the correlations between simulated NO_3-N loading rates and patterns of land use known to influence NO_3-N loading rates to streams.

Assessment of extreme loading rates: We calculated the percent of extreme high and extreme low loading rates for each stream network for each model scenario (Figure 2.12). Extreme high loading rates were defined as those that were greater than the highest reported value of N loading to streams in the published literature (6.46 kg km^{-2} day^{-1}, Table 2.4). Extreme low loading rates were defined as loading rates that were predicted at the lower model boundary (i.e., loading rates equal to zero).

Extreme loading rates are important indicators of unreasonable parameter estimation because extreme loading rates are indicative of some deviation of conditions in the stream network from model assumptions. Extreme loading rates occur under two conditions: 1) where there are rapid increases in downstream NO_3-N concentration (Figure 13a), and 2) where there are rapid decreases in downstream NO_3-N concentration (Figure 13b). When in-stream concentration increases rapidly, the model compensates for that increase by assigning an unreasonably high NO_3-N loading rate to that sampling location's contributing area. This creates extreme high concentrations of NO_3-N in unsampled tributaries within the contributing area. Unsampled tributaries (i.e., tributaries without upstream sampling locations) are not constrained by measured NO_3-N concentrations and thus are subject to unrealistic estimates of NO_3-N concentrations. Another example is when NO_3-N concentrations decrease faster than the model is capable of predicting based on the in-stream removal function. The model compensates for

rapidly decreasing NO_3-N concentration by decreasing the estimated loading rate, which is indicative of some unaccounted for mechanism of removal. Thus, extreme loading rates indicate some unexplained patterns of addition or removal of NO_3-N to or from the stream network not incorporated by the model. Therefore, quantifying the proportion of extreme loading rates allows us to determine the relative performance of the model among the stream networks.

Land cover analysis: Linear regressions were performed between NO_3-N loading rates and percent agricultural and percent urban land covers for each catchment for each year under both modeling scenarios. Researchers have established that nutrient loading rates to streams are related to patterns of land cover (e.g., Jones et al. 2001). Thus, we expected that in catchments where the simulation model adequately describes NO_3-N dynamics that simulated NO_3-N loading rates would be related to land cover.

30 meter resolution land cover datasets were collected from several different sources. USGS National Land Cover Datasets developed from Landsat TM imagery (NLCD; available online at http://seamless.usgs.gov) were collected for North Carolina, Michigan, Wyoming, and Kansas. The most up-to-date NLCD coverage was obtained for each of these catchments, which included 2001 coverage for North Carolina and 1992 coverage for Michigan, Wyoming and Kansas. Land cover for Massachusetts was obtained from the Massachusetts Geographic Information System (MassGIS 2005, available online at http://www.state.ma.us/mgis/massgis.htm) land use coverage from 1999 derived from 1:25,000 areal photography. 1990 land cover for Oregon was obtained from the Institute for a Sustainable Environment at the University of Oregon (ISE 1999, available online at http://www.fsl.orst.edu/pnwerc/wrb/access.html). We used a land cover dataset developed by

Helmer et al. (2002) for Puerto Rico, which was mapped from Landsat TM imagery taken during 1991 and 1992.

Land cover for each catchment was reclassified into urban, which included all urban and suburban land uses, and agricultural, which included all agricultural land uses (see Appendix B for reclassification schemes). Simple linear regressions between loading rates and both reclassified urban and agricultural land covers were performed using R Statistical Software (Table 2.6; Version 2.2.1, R Foundation for Statistical Computing 2005) for each catchment for each year for both model scenarios. If estimated loading rates were reasonable across each stream network, then they should have strong, significant relationships to percent agricultural land cover, urban land cover or both.

Basin specific analyses: We performed basin specific analyses to discern differences in landscape-scale drivers of stream network NO_3-N dynamics among the seven stream networks. Where the model adequately described NO_3-N dynamics, we determined the relative importance of uptake in stream networks as a driver of NO_3-N dynamics. Where the model did not adequately explain NO_3-N dynamics, we discerned probable drivers of NO_3-N dynamics not represented by the simulation model, and therefore not encompassed by our conceptual model. Where the model performed well, ANCOVAs were performed using SAS software (Version 8, SAS Institute, Inc. Cary, NC 1999) and we calculated the total proportion of NO_3-N removed in the stream networks as simulated by the model. Where the model did not perform well, various statistical analyses were performed as needed to illustrate differences among the catchments, including box-and-whisker plots and ANOVAs which were performed using R Statistical Software (Version 2.2.1, R Foundation for Statistical Computing 2005). Additional spatial analyses were performed in ArcView GIS Software (Version 3.3, Environmental Systems

Research Institute, Redlands CA 2002). The supporting logic behind and details of these analyses are site specific and depend on the results from the simulation model. We therefore described the details of the additional spatial and statistical analyses in the Results section, below.

Results

The model adequately described NO_3-N dynamics in two of the seven stream networks (North Carolina and Kansas, Table 2.7). However, the model performed poorly in the remaining five stream networks (Oregon, Wyoming, Michigan, Massachusetts and Puerto Rico, Table 2.7). We used the model results to identify unique landscape-scale drivers of NO_3-N dynamics among the seven stream networks.

North Carolina: There were no extreme high loading rate values and the proportion of the loading rates equal to zero was the lowest of the seven modeled catchments under both scenarios for the North Carolina stream network (Figure 2.12). North Carolina loading rates had a significant positive relationship with both percent agricultural and urban land cover for both years under both scenarios (Table 2.6; Figure 2.14). Since the conceptual model seemed to explain NO_3-N dynamics in the North Carolina (Table 2.7), an analysis of covariance (ANCOVA) was performed to test the differences between the linear regressions of loading rates on percent agricultural land among the model scenario without and the model scenario with in-stream NO_3-N removal. The relationship between loading rates and percent agricultural land cover was not significantly different between the two model scenarios for either year (ANCOVA, 2003: $p=0.34$, 2004: $p = 0.10$). In the North Carolina catchment, 16 and 28 percent of NO_3-N inputs were removed from the stream network in 2003 and 2004, respectively.

Kansas: There were no extreme high loading rate values for the Kansas stream network for either year or model scenario and the proportion of the loading rates equal to zero was also low for the model scenario with biological uptake (Figure 2.12). Kansas NO_3-N loading rates had a significant positive relationship with percent agricultural land cover for both years for the model scenario that incorporated biological uptake, but the relationship was not significant for the scenario without uptake (Table 2.6; Figure 2.15). No significant relationships existed between loading rates and percent urban land cover (Table 2.6), which is reasonable since there was less than one percent urban land cover throughout the catchment (Table 2.2). As in North Carolina, since the conceptual model seemed to explain NO_3-N dynamics (Table 2.7), an analysis of covariance (ANCOVA) was performed to test for differences between the linear regressions of loading rates on percent agricultural land among the model scenario without and the model scenario with in-stream NO_3-N removal. The relationships between loading rates and percent agricultural land cover were significantly different between the two scenarios for both years (ANCOVA, $p<0.001$). The Kansas stream network removed 80 and 71 percent of NO_3-N inputs during 2003 and 2004, respectively.

Oregon: The Oregon stream network had extreme high and low loading rates (Figure 2.12), and a weak but significant positive relationship between loading rates and percent agricultural land cover (Table 2.6). Extreme high NO_3-N concentrations in the Oregon stream network suggested that there were sources of NO_3-N to the stream network not incorporated by the model (Figure 13a). Figure 2.16 illustrates the extreme values by comparing the observed versus simulated distribution of NO_3-N concentrations throughout the stream network. This is because concentrated sources of NO_3-N loading to the main stem were not accounted for in the model, which drive loading rates for stream segments in those contributing areas to extreme high

values. Additional known sources unaccounted for in the model along the main stem include four waste water treatment plants and dairy farming operations. In the future we will be consulting Oregon researchers to identify and quantify point sources in the network.

Wyoming: The Wyoming stream network had no high extreme loading rates, but did have a high proportion of extreme low loading rates (Figure 2.12). NO_3-N loading rates did have a significant relationship with percent agricultural land cover for both scenarios (Table 2.6); however, this relationship was driven by two leverage points with high percent agricultural land cover (Figure 2.17a) and loading rates were not normally distributed so the normality assumption of linear regression was violated. Field observations suggested that a combination of irrigation withdrawal and loss of water to the aquifer deplete flow downstream in the main stem of the Wyoming stream network. Main stem flow was plotted against the distance along the stream channel from the most upstream main stem sampling location to the outlet to illustrate the change in flow downstream (Figure 2.17b). The stream network did not adhere to assumptions about hydrology since streams were highly influenced by surface-groundwater exchange, and thus the parameterized loading rates were nonsensical. The influence of groundwater exchange, anthropogenic water withdrawal or both resulted in a high proportion of zero loading rates in the Wyoming stream network.

Michigan: The Michigan stream network had a combination of extreme high and low loading rates (Figure 2.12), and there were no significant relationships with percent land cover (Table 2.6). Three factors violated model assumptions in the Michigan stream network: 1) high density animal operations; 2) agricultural tile drainage; and 3) groundwater flow. First, 47.5 percent of the Michigan catchment is pasture, and there are a substantial number of concentrated feeding lots and other high density animal operations. For example, Allegan County (the

primary county in which the Little Rabbit River catchment is located) contains 4.1% of cattle, 17% of hogs and 60% of chickens in Michigan, but makes up only 1.9% of Michigan's land area (USDA 2002). High density animal operations create concentrated sources of NO_3-N (e.g., Kim et al. 2003) and thus violate the assumption that NO_3-N loading rates are diffuse and uniform per unit area.

Second, 30.6 percent of the Michigan catchment is row crop, and most of row crop in the catchment is tile drained. Tile drainage is the practice of removing excess water from the subsurface of agricultural soils, in which a network of below-ground pipes collect infiltrating water and route it to nearby lakes, rivers or streams. In bypassing the natural flow of water from the surface to the water table, drainage systems often prevent the natural filtration of water provided by soils and wetlands. This drainage system ultimately changes pathways of hydrologic delivery of NO_3-N to stream channels, which violates the assumptions in the model that water and NO_3-N yield are diffuse and uniform.

Finally, the Michigan stream network is strongly influenced by groundwater, and ground water flow direction varies from surface water flow patterns, ultimately disconnecting the stream network from its surficial contributing area during periods without overland runoff (Figure 2.18). Groundwater flow paths between sampling locations for a sub-section of the Michigan stream network were determined in ArcView GIS software (Version 3.3, Environmental Systems Research Institute, Redlands CA 2002). 1:24,000 water table contour datasets representing the elevation of the water table were obtained for Allegan County in Michigan (Michigan Department of Environmental Quality 2005, available online at http://gwmap/rsgis/msu.edu), and a groundwater flow direction grid was created from the water table contours. Groundwater flow paths between a subset of sampling locations were determined by mapping the least cost paths

between sampling locations using the groundwater flow direction grid, and they indicated that groundwater flow paths did not corresponded to surface water flow paths represented by the hydrography layer. Concentrated agricultural operations, tile drainage systems and groundwater flow paths indicated that water and NO_3-N do not accumulate in-streams uniformly from the contributing drainage area in the Michigan stream network.

Massachusetts: In the Massachusetts stream network, there was a high proportion of extreme low NO_3-N loading rates (Figure 2.12), and there were no significant relationships between NO_3-N loading rates and percent land cover (Table 2.6). The Massachusetts catchment violates model assumptions of hydrology and stream channel geometry. The Massachusetts catchment has approximately 18% wetland cover, whereas other catchments have less than 3% wetland cover (Figure 2.19, Table 1.2). Wetlands may act as NO_3-N sinks, preventing NO_3-N from being transported to downstream segments. Distances along the stream network from each sampling location to the closest upstream wetland were measured for the Massachusetts stream network. NO_3-N loading rates were grouped into three categories: high, low and zero loading rates and an analysis of variance (ANOVA) was performed to test for differences among loading groups based on their proximity to upstream wetlands. Loading rates were significantly lower for sampling locations located closer to upstream wetlands (ANOVA; $p<0.05$).

The Massachusetts stream network also has a high number of water withdrawals (Figure 2.19). The Massachusetts catchment has a large area of developed land in headwater areas which may yield high NO_3-N runoff to streams. High NO_3-N water from developed areas may be removed by downstream water withdrawals and replaced with low NO_3-N runoff from more natural areas, which would also result in under-estimated loading rates to stream networks.

Puerto Rico: In the Puerto Rico stream network, there were some extreme high and low loading rate values for both years (Figure 2.12). We found only one significant relationship with percent agricultural land cover, and it occurred for the first model scenario during the second year of sampling (Table 2.6). However, this relationship was driven by one extreme NO_3-N loading rate (Figure 2.20a). The Puerto Rico stream network has 32.4 percent urban land cover, which is much greater than any other study catchment (Table 2.2). Factors caused by urbanization, that may drive stream network NO_3-N dynamics, are unaccounted for in the simulation model. For the Puerto Rico stream network, geomorphology and biological processing were highly variable. For most catchments, uptake increased linearly as a function of NO_3-N concentration (r^2 = 0.47-0.99, Table 2.3); however, in the Puerto Rico network, NO_3-N uptake did not fit a linear relationship with NO_3-N concentration (r^2 = 0.01). Also, flow explained much less variation in width than other study catchments (Table 2.3; Figure 20b). This indicated that biological processing in Puerto Rico streams was influenced by factors other than NO_3-N concentration and that channel geometry did not change continuously downstream in proportion to flow. The variation in channel geometry is likely due to channel modifications associated with urbanization. From field observations, Puerto Rico also has a high density of straight pipe sewage lines from residential buildings to streams. These sewage inputs ultimately change the distribution of NO_3-N loading to streams, violating the assumption that loading is diffuse and uniform.

Discussion

Realistic loading rates (Figure 2.12) and significant relationships between loading rates and land cover (Table 2.6) suggested that our conceptual model was appropriate for the North Carolina and Kansas stream networks during base flow conditions. In catchments where the

influence of groundwater-surface water interaction on hydrology and NO_3-N processing is minimal, loading is relatively uniform, and geomorphology changes predictably with flow, the current conceptual model of network-scale N processing is sufficient to explain stream network NO_3-N dynamics.

In the North Carolina stream network, the model did not require biological uptake to explain landscape NO_3-N dynamics; hydrologic delivery and transport were sufficient (Figure 2.14). Conversely, in the Kansas stream network, the model did require biological uptake to explain landscape NO_3-N dynamics; hydrologic delivery and transport alone were insufficient (Figure 2.15). Biological uptake either was (Kansas) or was not (North Carolina) a strong driver of network NO3-N dynamics

According to the model results, the North Carolina stream network removed 16 and 28% of NO_3-N delivered from the landscape in 2003 and 2004, respectively, whereas the Kansas stream network removed 80 and 71% of NO_3-N delivered. As might be expected, when in-stream removal is relatively low, incorporating removal into the model does not significantly improve the ability of the model to explain stream network NO_3-N dynamics. However, when in-stream removal is high, incorporating removal into the model substantially improves the model's explanatory power. For stream networks with high in-stream removal, it is essential to integrate in-stream processing to accurately simulate stream network NO_3-N dynamics.

In stream networks where the model performed poorly, we analyzed various hydrologic, geomorphologic and biological characteristics of the stream networks, that helped explain why the simulation model (and hence the conceptual model) was insufficient, which differed among stream networks. Both the Oregon and Michigan stream networks had non-uniform distributions of loading to the stream network due to point sources (Figure 2.16) and high density agricultural

operations, respectively. Non-uniform anthropogenic inputs of NO_3-N to streams produce a non-uniform distribution of loading rates. However, the conceptual model represented here assumes uniform NO_3-N delivery rates to streams across each contributing area. Researchers have recognized the importance of understanding the spatial distribution of load in predicting stream network N removal (Alexander et al. 2002; Wollheim et al. 2006), but have attributed the spatial distribution of load with having only a small to modest effect on whole network removal. Other researchers have suggested that landscape heterogeneity plays a larger role in the uncertainty of nutrient export (Lindgren and Destouni 2004). This study illustrates that describing the spatial distribution of loading rates to streams is essential to reasonably predict the patterns of in-stream NO_3-N concentrations, which influence the magnitude of in-stream NO_3-N removal.

Sub-surface hydrology may influence both NO_3-N delivery to and processing within streams. For any stream, the relative influence of the hyporheic zone on the overall rate of in-stream processing is determined by both the rate of biological activity within the hyporheic zone and the fraction of stream water moving through the hyporheic zone (Findlay 1995). In Wyoming, a combination of aquifer recharge and irrigation deplete stream water as Flat Creek flows downstream (Figure 2.17), resulting in additional mechanisms of removal not incorporated by the model. Associated exchange of water between the channel and the hyporheic exchange may increase N removal from stream water by increasing residence time, which increases contact with benthic biota that process nutrients. The retention of solutes is greater in the hyporheic zone than in the channel (Triska et al. 1989), and recent research has shown a correlation between the magnitude of interaction with the hyporheic zone and reach-scale nutrient retention (Valett et al. 1996; Hill et al. 1998). This suggests that NO_3-N processing within the hyporheic zone may be an important driver of NO_3-N removal across the Wyoming stream network, and that

incorporating the influence of groundwater-surface water exchange in stream network models of NO_3-N dynamics is essential for networks where channel and hyporheic water are readily exchanged.

Groundwater interacts with surface water in nearly all landscapes (Winter 1999), and groundwater flow paths influence the delivery of NO_3-N to streams (Hill 1989; Poiani et al. 1996). Groundwater flow generally follows topography, and digital elevation models are commonly used to model ground water flow (Baker et al. 2003). However, when topography is relatively flat and groundwater flows through unconsolidated lithology, the water table may fluctuate independently of surface topography, particularly during periods of low precipitation (Western et al. 1999). Also, anthropogenic modifications, such as tile drainage systems, in which water is routed from agricultural fields to streams through a network of sub-surface pipes, disconnect the channel from its surficial drainage area. The Michigan stream network has the smallest elevation difference between headwaters and outlet (Table 2.2), groundwater flows relatively independently from surface water (Figure 2.18) and a large portion of the Michigan catchment is tile drained, ultimately disconnecting the stream network from its surficial contributing area during periods without overland runoff. Stream network models of N dynamics predict in-stream N concentrations based on N sources within topographically defined contributing drainage areas. This assumption is valid as long as subsurface flow paths correspond to surface flow paths. However, during base flow in some types of geologic settings or anthropogenically influenced systems, groundwater flow may become decoupled from surficial topography so that N in groundwater may cross drainage divides in route to streams. A more thorough understanding of groundwater flow paths in settings where streams are highly influenced by groundwater or anthropogenic sub-surface modifications may greatly increase the

ability of models to predict NO_3-N delivery to streams and hence patterns of in-stream NO_3-N removal.

Inconsistencies also arise between the stream network and the simulation model where there are discontinuous changes in channel geometry and/or flow or where channel geometry is not related to flow by common geomorphic equations (e.g., $w = aQ^b$). In Massachusetts, wetland cover accounts for 20% of total land cover and wetlands are significantly associated with extreme low NO_3-N loading rates. When streams flow through wetland areas, water slows down and the stream spreads out into the wetland area, ultimately increasing water residence time and surface area available for processing. Wetlands act as N sinks, both preventing N from upstream contributing streams from being transported downstream and preventing N runoff from the adjacent drainage area from reaching stream channels. N retention is higher in wetlands than in lakes and rivers, mainly because of higher residence time (Saunders and Kalff 2001), which suggests that in-stream removal is higher than estimated by the model when streams intersect wetlands.

Another example of unrepresented changes in channel geometry applies to catchments with high urbanization. Downstream changes in channel size relative to stream discharge may not always behave as simple power functions (Ebisemiju 1991), particularly in highly urbanized catchments (Gregory et al. 1992). Furthermore, streams flowing through patches of urbanized areas and relatively undisturbed areas can exhibit disjunct patterns of channel shape (Chin and Gregory 2001; Jeje and Ikeazota 2002). In Puerto Rico, urban land cover accounts for 42% of total catchment land cover, which is over two times higher than any of the other networks (Table 2.2), and the Puerto Rico stream network exhibited the weakest relationship between observed width and flow (Table 2.3; Figure 2.20b). In highly urbanized catchments there is a need to

create methodology to better predict variation in channel shape in order to accurately predict in-stream processing.

The simulation model assumes that the biological demand for N increases linearly with concentration ($U = v_f * [NO_3\text{-}N]$). This assumption is grounded in nutrient spiraling theory (Stream Solute Workshop 1990), has been observed in the field (O'Brien et al. Submitted), has been used in stream network models of N dynamics (Wollheim et al. 2006), and fit the data for all but one study catchment well (Table 2.3). In Puerto Rico, areal uptake was not linearly related to NO_3-N concentration (Table 2.3), suggesting that biological uptake is a function of some other in-stream or environmental conditions. Recent research has suggested that other resources may drive biological demand. For example, N uptake rates may be dependent upon stoichiometric relationships with other dissolved nutrients (Dodds et al. 2004; Cross et al. 2005). Relationships between stream ecosystem metabolism (Hall and Tank 2003) and the biomass of in-stream biota (Hall et al. 2003) and in-stream N processing have also been observed. Biological uptake has complex physiochemical and biological drivers which may need to be incorporated into models of in-stream processing.

Opportunities for improving widely held conceptualizations of factors driving network-scale dynamics: The stream networks in this study represent a wide range of naturally occurring variation in hydrology, geomorphology and biology (Table 2.1). However, the simulation model (and hence our conceptual model) does not encompass the range of possible conditions represented by stream networks. This study highlights the reality that different streams have different hydrologic, geomorphologic and biological drivers of in-stream processing, and that integrating a more diverse array of possible drivers into our conceptual thinking about streams at

the landscape scale will improve our ability to understand, explain and predict nutrient processing across stream networks.

Integrating the following ideas into common conceptual models of stream network N dynamics will greatly increase the applicability of our conceptual models to hypothesis generation, research design and landscape modeling to describe in-stream processing: 1) the spatially explicit distribution of anthropogenic sources of N to streams; 2) the influence of multiple hydrologic pathways of nutrient delivery to streams; 3) the relative roles of the hyporheic zone versus the stream bed in nutrient processing; 4) discontinuities and abrupt changes in downstream channel geometry and flow because of urbanization and natural features; and 5) variation in biological and environmental factors that drive biological uptake across stream networks. We suggest that incorporating a more complete understanding of stream networks that encompasses hydrologic, geomorphologic and chemical drivers of in-stream processes into core conceptual models of stream network loading, transport and processing will allow more reliable scaling of site-level measurements. For any stream network, considering the unique distribution of N in streams, channel geomorphology, residence time (hydrology), biological activity, and network topology will increase our understanding stream N dynamics on a landscape-scale. And, since stream networks retain a large proportion of their incoming N (Peterson et al. 2001; Alexander et al. 2000), understanding stream N dynamics on a landscape-scale is a key to understanding N export from a diversity of landscapes through rivers to estuaries and coastal ecosystems.

References

Alexander, R. B., J. W. Brakebill, R. E. Brew, and R. A. Smith. 1999. ERF1—Enhanced River Reach File 1.2. U.S. Geological Survey Open-File Report 99-457, Reston, VA.

Alexander, R. B., P. J. Johnes, E. W. Boyer, and R. A. Smith. 2002. A comparison of models for estimating the riverine export of nitrogen from large watersheds. Biogeochemistry 57:295-339.

Alexander, R. B., R. A. Smith, and G. E. Schwarz. 2000. Effect of stream channel size on the delivery of nitrogen to the Gulf of Mexico. Nature 403:758-761.

Arheimer, B., L. Andersson, and A. Lepisto. 1996. Variation of nitrogen concentration in forest streams -- influences of flow, seasonality and catchment characteristics. Journal of Hydrology 179:281-304.

Bailey, R.G. (2005) Identifying ecoregion boundaries. Environmental Management. 34 (1): S14 - S26.

Baker, M. E., M. J. Wiley, P. W. Seelbach, and M. L. Carlson. 2003. A GIS Model of Subsurface Water Potential for Aquatic Resource Inventory, Assessment, and Environmental Management. Environmental Management 32:706-719.

Benda, L., N. L. Poff, D. Miller, T. Dunne, G. Reeves, G. Pess, and M. Pollock. 2004. The network dynamics hypothesis: How channel networks structure riverine habitats. BioScience 54:413-427.

Caraco, N. F., and J. J. Cole. 1999. Human impact on nitrate export: An analysis using major world rivers. Ambio 28:167-170.

Chin, A., and K. J. Gregory. 2001. Urbanization and adjustment of ephemeral stream channels. Annals of the Association of American Geographers 91:595-608.

Cross, W. F., J. P. Benstead, P. C. Frost, and S. A. Thomas. 2005. Ecological stoichiometry in freshwater benthic systems: recent progress and perspectives. Freshwater Biology 50:1895-1912.

Dahm, C. N., N. B. Grimm, P. Marmonier, H. M. Valett, and P. Vervier. 1998. Nutrient dynamics at the interface between surface waters and groundwaters. Freshwater Biology 40:427-451.

Darracq, A., and G. Destouni. 2005. In-stream nitrogen attenuation: Model-aggregation effects and implications for coastal nitrogen impacts. Envionrnmental Science and Technology 39:3716-3722.

de Wit, M. J. M. 2001. Nutrient fluxes at the river basin scale. I: the PolFlow model. Hydrological Processes 15:743-759.

Dodds, W. K., A. J. López, W. B. Bowden, S. Gregory, N. B. Grimm, S. K. Hamilton, A. E. Hershey, E. Martí, W. H. McDowell, J. L. Meyer, D. Morrall, P. J. Mulholland, B. J. Peterson, J. L. Tank, H. M. Valett, J. R. Webster, and W. Wollheim. 2002. N uptake as a function of concentration in streams. Journal of the North American Benthological Society 21:206-220.

Dodds, W. K., E. Martí, J. L. Tank, J. Pontius, S. K. Hamilton, N. B. Grimm, W. B. Bowden, W. H. McDowell, B. J. Peterson, H. M. Valett, J. R. Webster, and S. Gregory. 2004. Carbon and nitrogen stoichiometry and nitrogen cycling rates in streams. Oecologia 140:458-467.

Donner, S. D., M. T. Coe, J. D. Lenters, and T. E. Twine. 2002. Modeling the impact of hydrological changes on nitrate transport in the Mississippi River Basin from 1955 to 1994. Global Biogeochemical Cycles 16:doi: 10.1029/2001GB001396.

Donner, S. D., C. J. Kucharik, and M. Oppenheimer. 2004. The influence of climate on in-stream removal of nitrogen. Geophysical Research Letters 31:doi: 10.1029/2004GL020477.

Ebisemiju, F. S. 1991. Some comments on the use of spatial interpolation techniques in studies of man-induced river channel changes. Applied Geography 11:21-34.

Fenneman, N.M (1914) Physiographic boundaries within the United States. Annals of the Association of American Geographers. 4:84–134.

Findlay, S. 1995. Importance of Surface-Subsurface Exchange in Stream Ecosystems: The Hyporheic Zone. Limnology and Oceanography 40:159-164.

Fisher, S. G., R. A. Sponseller, and J. B. Heffernan. 2004. Horizons in stream biogeochemistry: Flowpaths to progress. Ecology 85:2369-2379.

Ganio, L. M., C. E. Torgersen, and R. E. Gresswellc. 2005. A geostatistical approach for describing spatial pattern in stream networks. Frontiers in Ecology and the Environment 3:138-144.

Gregory, K. J., R. J. Davis, and P. W. Downs. 1992. Identification of river channel change due to urbanization. Applied Geography 12:299-318.

Grimm, V. 1999. Ten years of individual-based modelling in ecology: what have we learned and what could we learn in the future? Ecological Modelling 115:129-148.

Hall, R. O., J. L. Tank, and M. F. Dybdahl. 2003. Exotic snails dominate nitrogen and carbon cycling in a highly productive stream. Frontiers in Ecology and the Environment 1:407-411.

Hall, R. O. J., and J. L. Tank. 2003. Ecosystem metabolism controls nitrogen uptake in streams in Grand Teton National Park, Wyoming Limnology and Oceanography 48:1120-1128.

Helmer, E. H., O. Ramos, T. D. M. Lopez, M. Quinones, and W. Diaz. 2002. Mapping the forest type and land cover of Puerto Rico, a component of the Caribbean Biodiversity Hotspot. Caribbean Journal of Science 38:165-183.

Hill, A. R. 1989. Ground water flow paths in relation to nitrogen chemistry in the near-stream zone. Hydrobiologia 206:39-52.

Hill, A. R., C. F. Labadia, and K. Sanmugadas. 1998. Hyporheic Zone Hydrology and Nitrogen Dynamics in Relation to the Streambed Topography of a N-Rich Stream. Biogeochemistry 42:285-310.

Hughes, R. M., and J. M. Omernik. 1983. An alternative for characterizing stream size. Pages 87-101 in T. D. Fontaine III and S. M. Bartell, editors. Dynamics of Lotic Ecosystems, Chapter 5. Ann Arbor Science, Ann Arbor, Michigan.

Jeje, L. K., and S. I. Ikeazota. 2002. Effects of Urbanisation on Channel Morphology: The Case of Ekulu River in Enugu, South Eastern Nigeria. Singapore Journal of Tropical Geography 23:37-51.doi: 10.1111/1467-9493.00117.

Johnes, P. J., and D. Butterfield. 2002. Landscape, regional and global estimates of nitrogen flux from land to sea: Errors and uncertainties. Biogeochemistry 57:429-476.

Jones, K. B., A. C. Neale, M. S. Nash, R. D. V. Remortel, J. D. Wickham, K. H. Riitters, and R. V. O'Neill. 2001. Predicting nutrient and sediment loadings to streams from landscape metrics: A multiple watershed study from the United States Mid-Atlantic Region. Landscape Ecology 16:301-312.

Kim, R.H., J. Lee, and H.W. Chang. 2003. Characteristics of organic matter as indicators of pollution from small-scale livestock and nitrate contamination of shallow groundwater in an agricultural area. Hydrological Processes 12: 2485-2496.

King, R. S., M. E. Baker, D. F. Whigham, D. E. Weller, T. E. Jordan, P. F. Kazyak, and M. K. Hurd. 2005. Spatial considerations for linking watershed land cover to ecological indicators in streams. Ecological Applications 15:137-153.

Leopold, L. B., and T. Maddock. 1953. The hydraulic geometry of streams and some physiographic implications. U.S. Geological Survey Professional Paper 252.

Leopold, L. B., M. G. Wolman, and J. P. Miller. 1964. Fluvial Processes in Geomorphology. Freeman Press, San Francisco.

Lindgren, G. A., and G. Destouni. 2004. Nitrogen loss rates in streams: Scale-dependence and up-scaling methodology. Geophysical Research Letters 31:doi:10.1029/2004GL019996.

Mulholland, P. J., H. M. Valett, J. R. Webster, S. A. Thomas, L. W. Cooper, S. K. Hamilton, and B. J. Peterson. 2004. Stream denitrification and total nitrate uptake rates measured using a field 15N tracer addition approach Limnology and Oceanography 49:809-820.

O'Brien, J., W. K. Dodds, K. C. Wilson, J. N. Murdock, and J. Eichmiller. Submitted. The transport, cycling, and retention of nitrate in streams: 15N experiments across a gradient of nitrate concentrations.

Peterson, B. J., W. M. Wollheim, P. J. Mulholland, J. R. Webster, J. L. Meyer, J. L. Tank, E. Marti, W. B. Bowden, H. M. Valett, A. E. Hershey, W. H. McDowell, W. K. Dodds, S. K. Hamilton, S. Gregory, and D. D. Morrall. 2001. Control of Nitrogen Export from Watersheds by Headwater Streams. (Cover story). Science 292:86.

Poiani, K. A., B. L. Bedford, and M. D. Merrill. 1996. A GIS-based index for relating landscape characteristics to potential nitrogen leaching to wetlands. Landscape Ecology 11:237-255.

Poole, G. C. 2002. Fluvial landscape ecology: addressing uniqueness within the river discontinuum. Freshwater Biology 47:641-660.

Saunders, D. L., and J. Kalff. 2001. Nitrogen retention in wetlands, lakes and rivers. Hydrobiologia 443:205-212.

Seitzinger, S. P., R. V. Styles, E. W. Boyer, R. B. Alexander, and G. Billen. 2002. Nitrogen retention in rivers: model development and application to watersheds in the northeastern U.S.A. Biogeochemistry 57:199-237.

Smith, R. A., G. E. Schwarz, and R. B. Alexander. 1997. Regional interpretation of water-quality monitoring data. Water Resources Research 33:2781-2798.

Stream Solute Workshop. 1990. Concepts and methods for assessing solute dynamics in stream ecosystems. Journal of the North American Benthological Society 9:95-119.

Thorpe, J. H., M. C. Thoms, and M. D. Delong. 2006. The riverine ecosystem synthesis: Biocomplexity in river networks across space and time. River Research and Applications 22:123-147.

Triska, F. J., V. C. Kennedy, R. J. Avanzino, G. W. Zellweger, and K. E. Bencala. 1989. Retention and Transport of Nutrients in a Third-Order Stream in Northwestern California: Hyporheic Processes. Ecology 70:1893-1905.

Valett, H. M., J. A. Morrice, C. N. Dahm, and M. E. Campana. 1996. Parent Lithology, Surface-Groundwater Exchange, and Nitrate Retention in Headwater Streams. Limnology and Oceanography 41:333-345.

USDA, United States Department of Agriculture. 2002 Census of Agriculture. National Agricultural Statistics Service. Available online: http://www.nass.usda.gov/Census_of_Agriculture/index.asp

Van Drecht, G., A. F. Bouwman, J. Knoop, A. Beusen, and C. Meinardi. 2003. Global modeling of the fate of nitrogen from point and nonpoint sources in soils, groundwater, and surface water. Global Biogeochemical Cycles 17:2621-2620.

W.E. Gates and Associates Inc. 1982. Estimation of streamflows and the Reach File.

Western, A. W., R. B. Grayson, G. Bloschl, G. R. Willgoose, and T. A. McMahon. 1999. Observed spatial organization of soil moisture and its relation to terrain indices. Water Resources Research 35:797-810.

Winter, T. C. 1999. Relation of streams, lakes and wetlands to groundwater flow systems. Hydrogeology Journal 2:28-45.

Wollheim, W. M., C. J. Vorosmarty, B. J. Peterson, P. A. Green, S. P. Seitzinger, J. Harrison, A. F. Bouwman, M. Meybeck, and J. P. M. Syvitski. In Review. A Spatially Distributed Framework for Aquatic Modeling of the Earth System (FrAMES). Global Biogeochemical Cycles.

Wollheim, W. M., C. J. Vorosmarty, B. J. Peterson, S. P. Seitzinger, and C. S. Hopkinson. 2006. Relationship between river size and nutrient removal. Geophysical Research Letters 33:doi:10.1029/2006GL025845.

Table 2.1: Geographic descriptions of study sites. [1]See Fenneman (1914) or Bailey (2005) for a description of physiographic provinces within the United States

Site Location	Site Abbreviation	Stream	Biome	Physiographic Province [1]
Western North Carolina and Northeastern Georgia	NC	Little Tennessee River	Warm temperate deciduous forest	Southern Appalachians
Coastal Massachusetts	MA	Ipswich River	Cool, temperate deciduous forest	New England Coastal Plain
Southern Michigan and Northern Indiana	MI	Little Rabbit River	Cool, temperate deciduous forest	North Central Till plain
Central Kansas	KS	Mill Creek	Grassland	Great Plains
Western Oregon	OR	Tualatin River	Humid coniferous	Cascade Mountains
Puerto Rico	PR	Rio Pierdas	Moist evergreen tropical forest	Montane to Coastal Plain
Western Wyoming	WY	Flat Creek	Semi-arid coniferous	Rocky Mountains

Table 2.2 : Geomorphic and land cover descriptors of study catchments. % Ag = percent agricultural land cover, % Urb = percent urban land cover, %Wet = percent wetland cover. [1] Represents urban and barren land cover.

Site Abbreviation	Watershed Area (km^2)	Drainage Density ($km\ km^{-2}$)	Minimum Elevation (meters)	Maximum Elevation (meters)	% Ag	% Urb	% Wet
NC	361	1.23	603	1651	10.4	6.5	0.15
KS	1008	1.87	276	489	26.7	0.62	0.41
WY	400	0.50	1891	3391	3.3	1.2	2.5
OR	1828	0.78	18	1058	4.1	16.3	0.79
MI	126	1.13	193	255	78.3	1.8	2.6
MA	381	1.35	0	129	10.4	13.5	18.2
PR	40	1.68	3	313	29.7	42.4[1]	1

Table 2.3: Site-specific model parameter values. Width coefficient (a) and width exponent (b) derived for each site, w = aQb, where w = width and Q = discharge. Mass transfer coefficient (vf) derived for each catchment, U = vf[NO_3], where U = areal NO3 uptake. ND = insufficient data, 'All Sites' relationship used. ns Not Significant, * p<0.05, **p<0.001

Site	Year	Width Coefficient	Width Exponent	R-squared	Mass transfer coefficient (m s^{-1})	R-squared	Uptake (v_f) Data Sources
North Carolina	2003	6.2775	0.4403	0.81 **	1.995E-06	0.57 **	LINX-II, Earl et al. (Submitted)
	2004	7.30339	0.45163	0.9 **			
Kansas	2003	ND	ND	-	5.90E-06	0.99 **	LINX-II
	2004						
Wyoming	2005	7.0038	0.331	0.5 **	1.37E-04	0.64 **	LINX-II, Hall and Tank (2003)
Oregon	2003	ND	ND	-	2.37E-06	0.45 **	LINX-II
	2004						
Michigan	2003	10.41546	0.45403	0.93 **	3.58E-06	0.98 **	LINX-II
	2004	8.00106	0.40341	0.85 **			
Massachusetts	2003	7.4322	0.2721	0.37 *	1.13E-06	0.99 **	LINX-II
	2004						
Puerto Rico	2004	6.6324	0.3476	0.27 *	3.53E-06	0.01 ns	LINX-II
	2005						
All Sites	-	7.1733	0.3478	0.74 **	3.00E-06	0.52 **	LINX-II, Earl et al. (Submitted), Hall and Tank (2003)

Table 2.4: Literature estimates of N loading to streams. All literature loading rates were reported on an annual time scale, but we report them here as daily rates. Data reported as mean (range) when the reference included data from more than one watershed. % Ag = percent agricultural land cover, % Urban = percent urban land cover, TN = total nitrogen, NO_3-N = nitrate-nitrogen, DIN = dissolved inorganic nitrogen

[1] Loading rates to streams reported here were estimated by adding estimated riverine denitrification and stream export.
[2] Loading rates to streams reported here are NO_3-N leaching estimates from agricultural land
[3] Loading rates to streams reported here are NO_3-N leaching estimates from forest land
[4] Loading rates to streams reported here were estimated by adding in-stream TN yield and 10% of watershed TN storage

Watershed	Location	Basin Area (km^2)	% Ag	% Urban	Loading to Streams (kg N $km^{-2}day^{-1}$)	Nitrogen Species	Reference
Ipswich River basin	Northeastern Massachusetts	404	7	35	1.85	TN	Williams et al. 2004
					0.67	NO_3-N	
small Sierra Nevada watersheds	Sierra Nevada Mountains, California	2.6 (0.2 - 19.6)	-	-	0.50 (0.30 - 0.71)	DIN	Sickman et al. 2002
small Rocky Mountains watersheds	Rocky Mountains, Colorado and Wyoming	4.3 (0.3 - 11.7)	-	-	0.68 (0.22-1.18)	DIN	
16 Northeast U.S. watersheds	Along a longitudinal profile from Maine to Virginia	15 520 (475 - 70189)	19 (1 - 61)	5 (0 - 22)	2.89 (1.38 - 6.31)[1]	TN	Van Breeman et al. 2002
					4.60 (2.14 - 6.46)[2]	NO_3-N	
					0.59 (0.39 - 0.85)[3]	NO_3-N	
18 Southeast U.S. watersheds	Georgia, Mississippi and Alabama	1841 (9 - 8481)	17 (2 - 42)	1 (0.1 - 5)	1.93 (1.16 - 3.32)[4]	TN	Harned et al. 2004

Table 2.5: Simulated NO_3-N loading rates to streams. Loading rates are reported as mean (range).

Site	Year	Number of Observations	NO_3-N loading to streams (kg N km^{-2} day^{-1})	
			No Removal	Removal
North Carolina	2003	55	0.50 (0.02 - 2.58)	0.58 (0.02 - 3.14)
	2004	57	0.16 (0 - 0.74)	0.20 (0 - 0.86)
Kansas	2003	25	0.03 (0 - 0.12)	0.13 (0 - 0.61)
	2004	25	0.21 (0 - 0.72)	0.92 (0.01 - 2.88)
Wyoming	2005	17	0.23 (0 - 3.29)	0.21 (0 - 1.60)
Oregon	2003	44	0.37 (0 - 6.8)	0.74 (0 - 11.50)
	2004	50	0.59 (0 - 8.4)	0.95 (0 - 11.79)
Michigan	2003	35	1.19 (0 - 5.01)	2.40 (0 - 9.57)
	2004	31	5.51 (0 - 36.66)	8.88 (0 - 72.43)
Massachusetts	2003	46	0.09 (0 - 0.66)	0.14 (0 - 0.95)
	2004	38	0.30 (0 - 3.17)	0.41 (0 - 4.70)
Puerto Rico	2004	37	2.51 (0 - 15.97)	3.19 (0 - 19.93)
	2005	34	0.94 (0 - 7.48)	1.47 (0 - 8.03)

Table 2.6: R-squared values for regressions between loading rates and percent land cover.

ns Not significant, * $p < 0.05$, ** $p < 0.01$, ***$p < 0.001$, **** $p < 0.0001$

Site	Year	Agricultural Land Cover		Urban Land Cover	
		No Removal	Removal	No Removal	Removal
North Carolina	2003	0.58 ****	0.57 ****	0.14 **	0.13 **
	2004	0.63 ****	0.64 ****	0.18 **	0.16 **
Kansas	2003	0.11 ns	0.30 **	0.04 ns	0.0005 ns
	2004	0.02 ns	0.40 ***	0.08 ns	0.12 ns
Wyoming	2005	0.23 *	0.42 **	0.01 ns	0.02 ns
Oregon	2003	0.10 *	0.10 *	0.008 ns	0.0007 ns
	2004	0.03 ns	0.03 ns	0.00001 ns	0.00003 ns
Michigan	2003	0.04 ns	0.04 ns	0.003 ns	0.00005 ns
	2004	0.0005 ns	0.0001 ns	0.03 ns	0.02 ns
Massachusetts	2003	0.0009 ns	0.0006 ns	0.06 ns	0.08 ns
	2004	0.00004 ns	0.0003 ns	0.09 ns	0.10 ns
Puerto Rico	2004	0.02 ns	0.03 ns	0.005 ns	0.005 ns
	2005	0.15 *	0.10 ns	0.08 ns	0.06 ns

Table 2.7 : Summary of results from model verification analyses.

√ indicates the stream network passed model verification. X indicates the stream network did not pass model verification.

Study Basin	Extreme Loading Rate Assessment	Land Cover Analysis
North Carolina	√	√
Kansas	√	√
Oregon	**X**	**X**
Wyoming	**X**	**X**
Michigan	**X**	**X**
Massachusetts	**X**	**X**
Puerto Rico	**X**	**X**

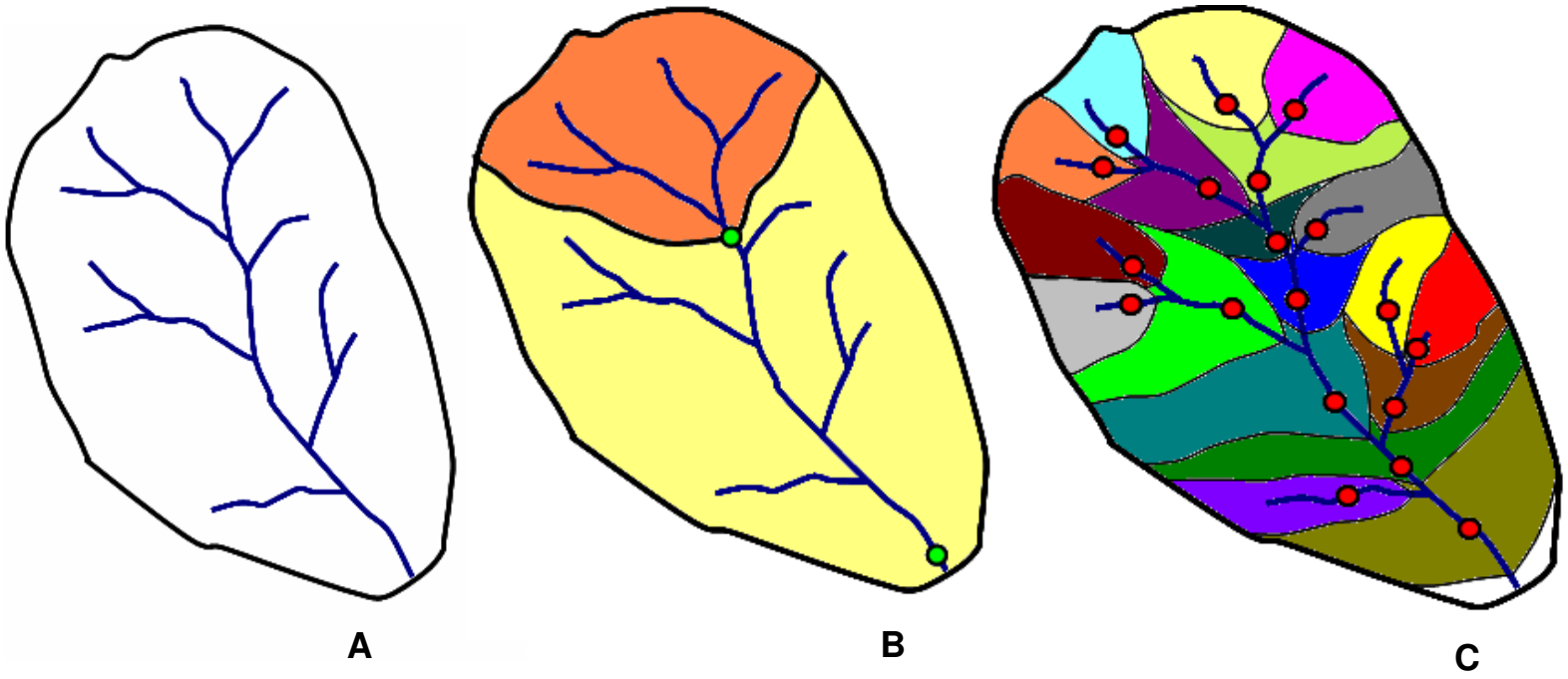

Figure 2.1: Example of watershed area, contributing drainage area and adjacent area. A) Watershed area for the entire network. B) Contributing drainage areas for each sampling location (represented by green circles). Stream segments within the same contributing areas have equal NO_3-N loading rates. C) Adjacent drainage areas for each stream reach.

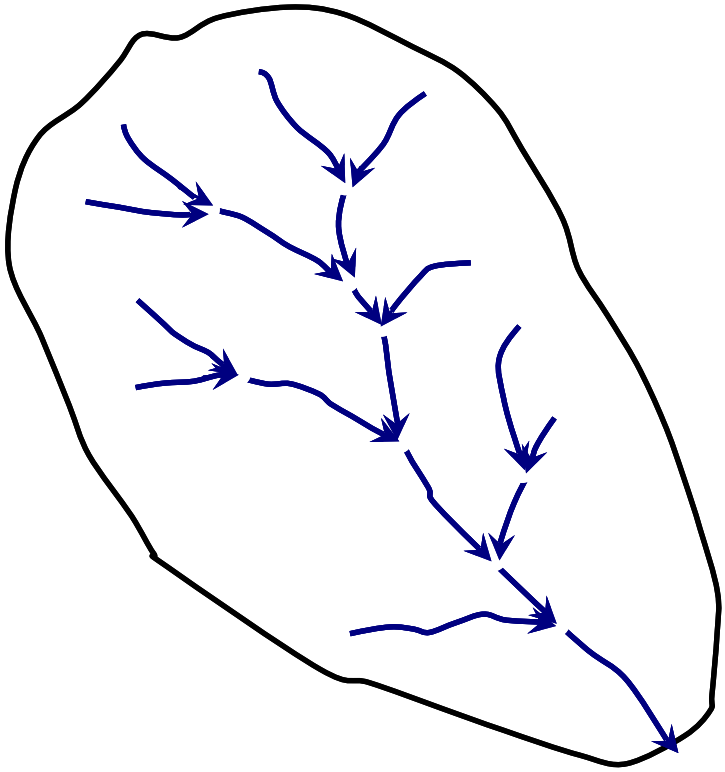

Figure 2.2: Example of a modeled stream network. Stream networks are divided into segments between tributary junctions. Each red circle represents a stream segment.

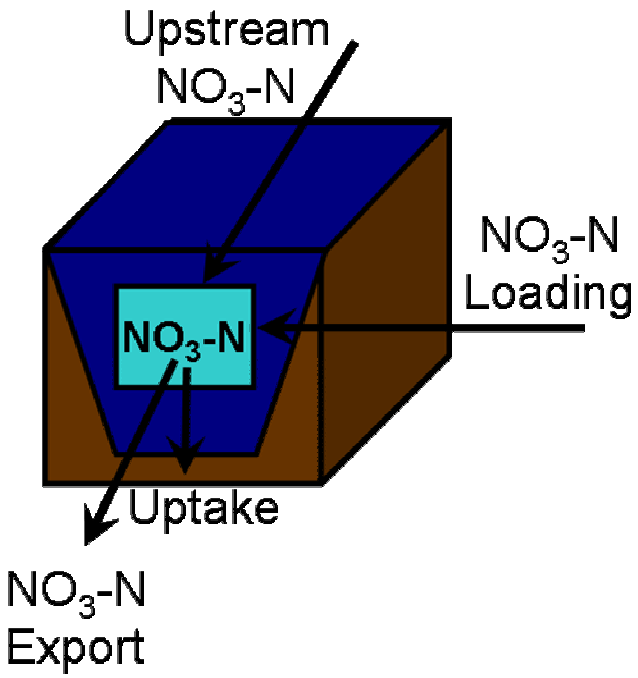

Figure 2.3: Box-and-arrow diagram of water and NO_3-N flow through a stream segment.

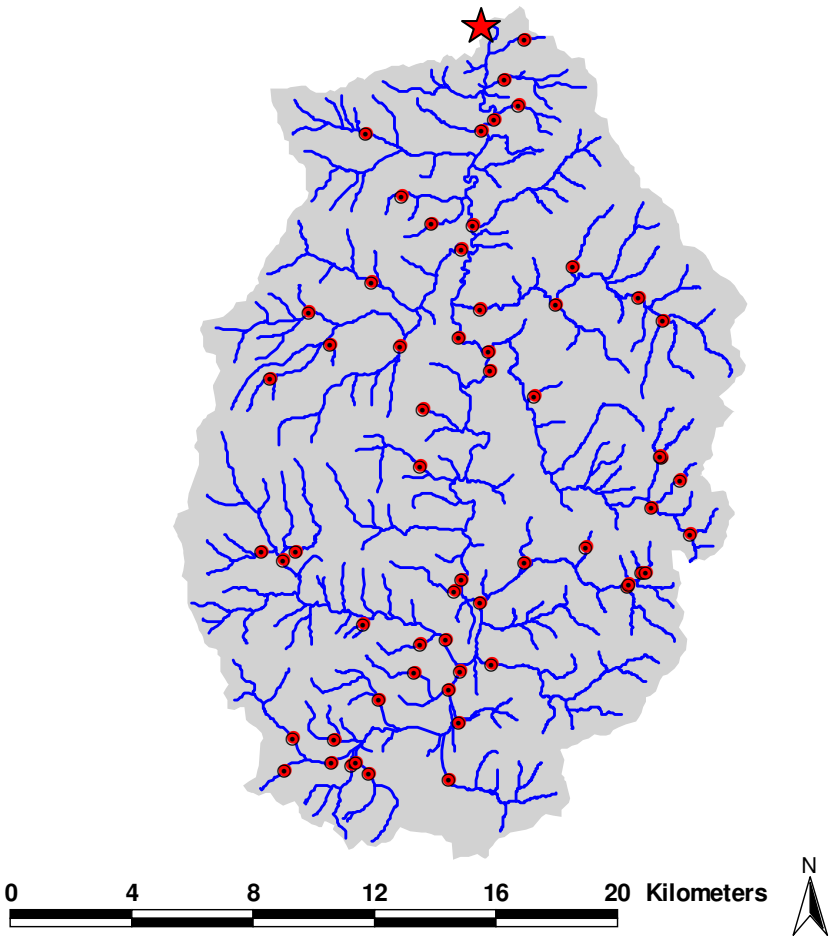

Figure 2.4: Map of the Little Tennessee River catchment, North Carolina. Red circles represent synoptic sampling locations. Star represents outlet.

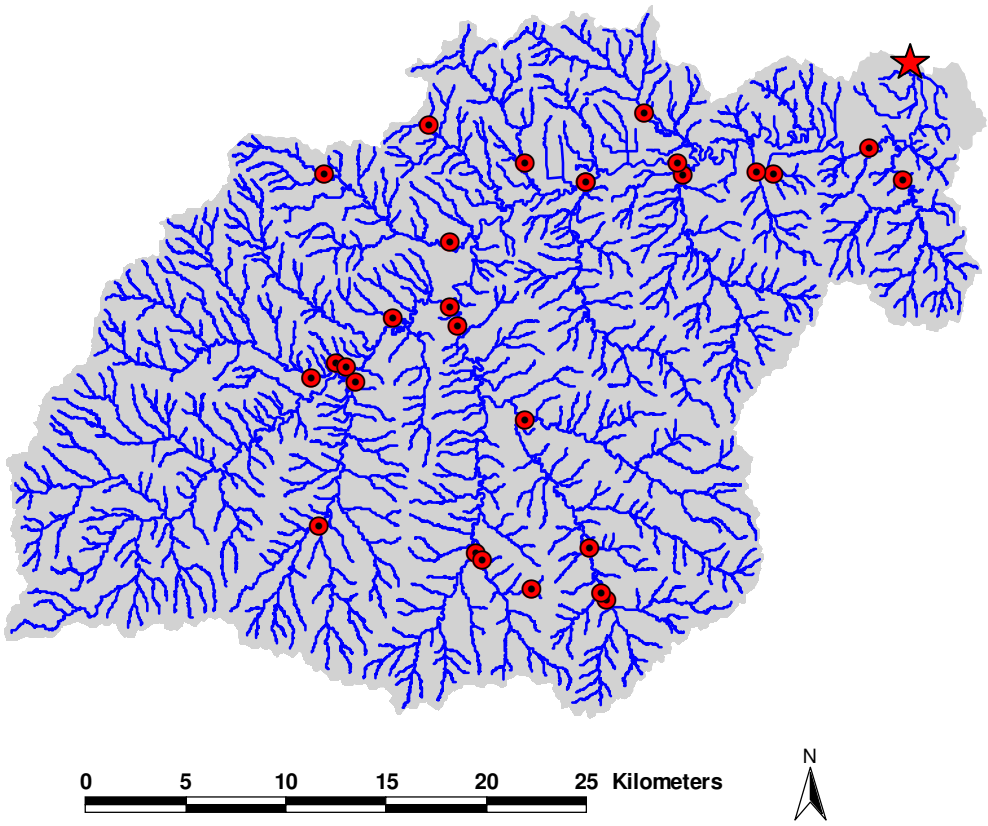

Figure 2.5: Map of the Mill Creek catchment, Kansas. Red circles represent synoptic sampling locations. Star represents outlet.

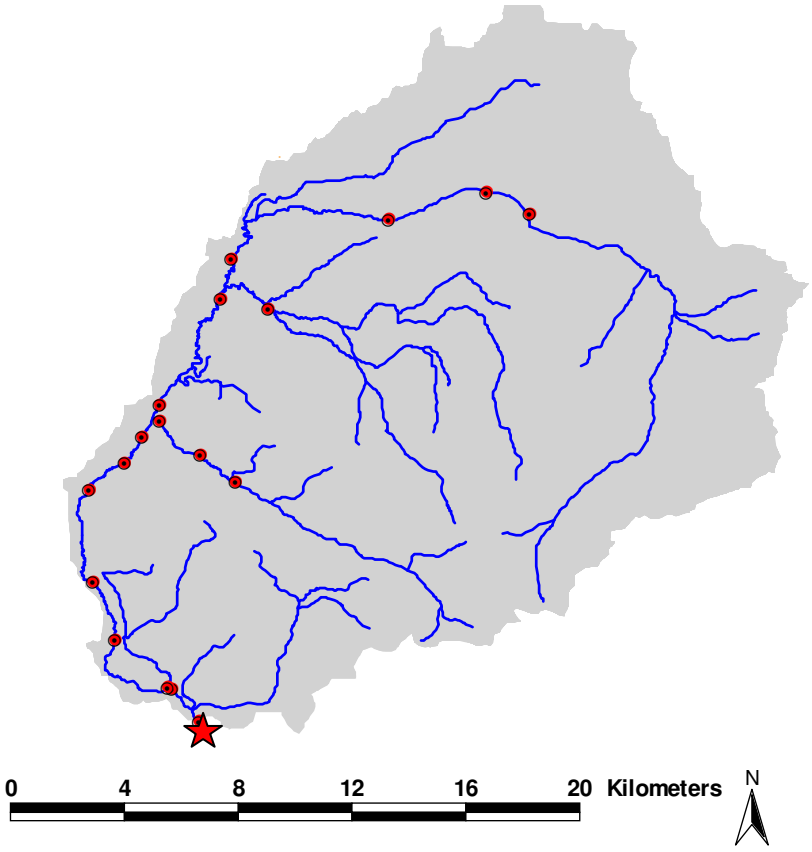

Figure 2.6: Map of the Flat Creek catchment, Wyoming. Red circles represent synoptic sampling locations. Star represents outlet.

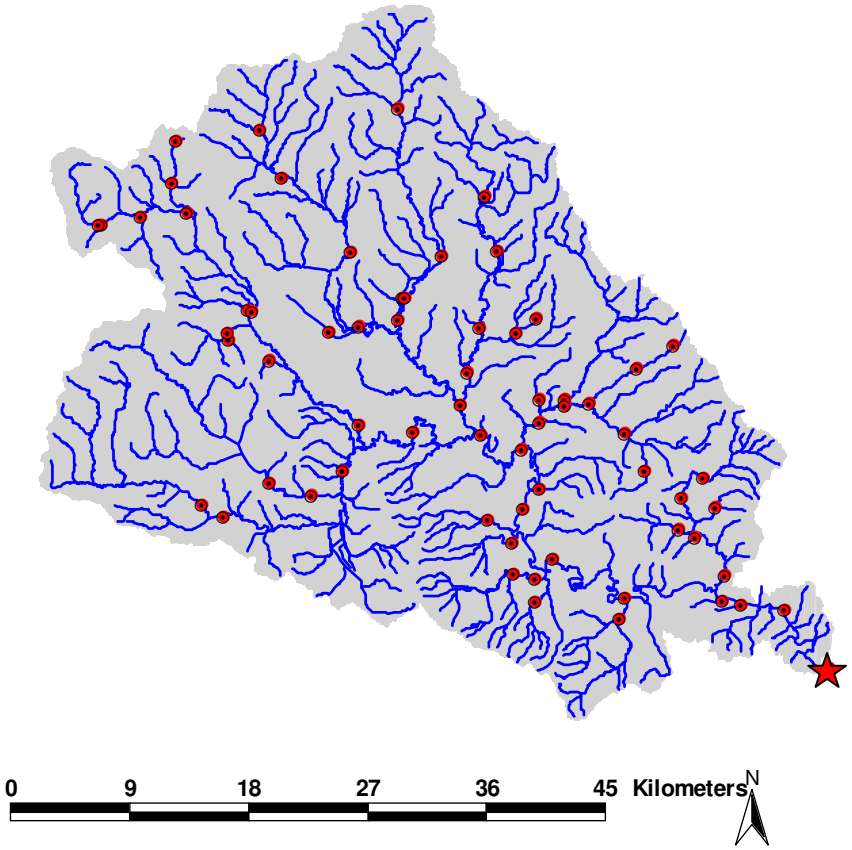

Figure 2.7: Map of the Tualatin River catchment, Oregon. Red circles represent synoptic sampling locations. Star represents outlet.

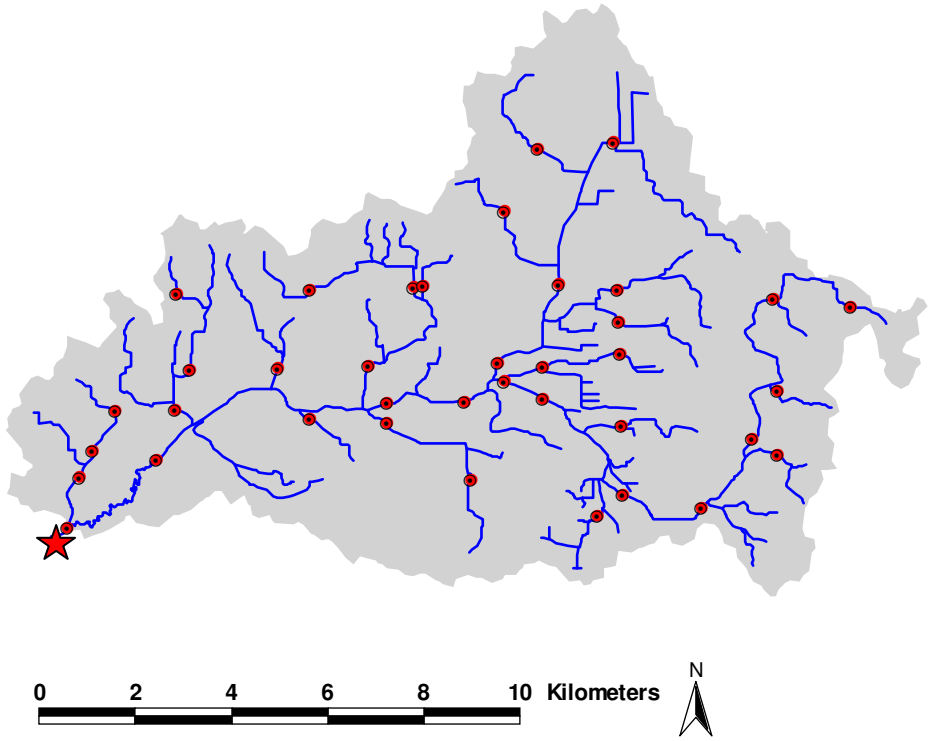

Figure 2.8: Map of the Little Rabbit River catchment, Michigan. Red circles represent synoptic sampling locations. Star represents outlet.

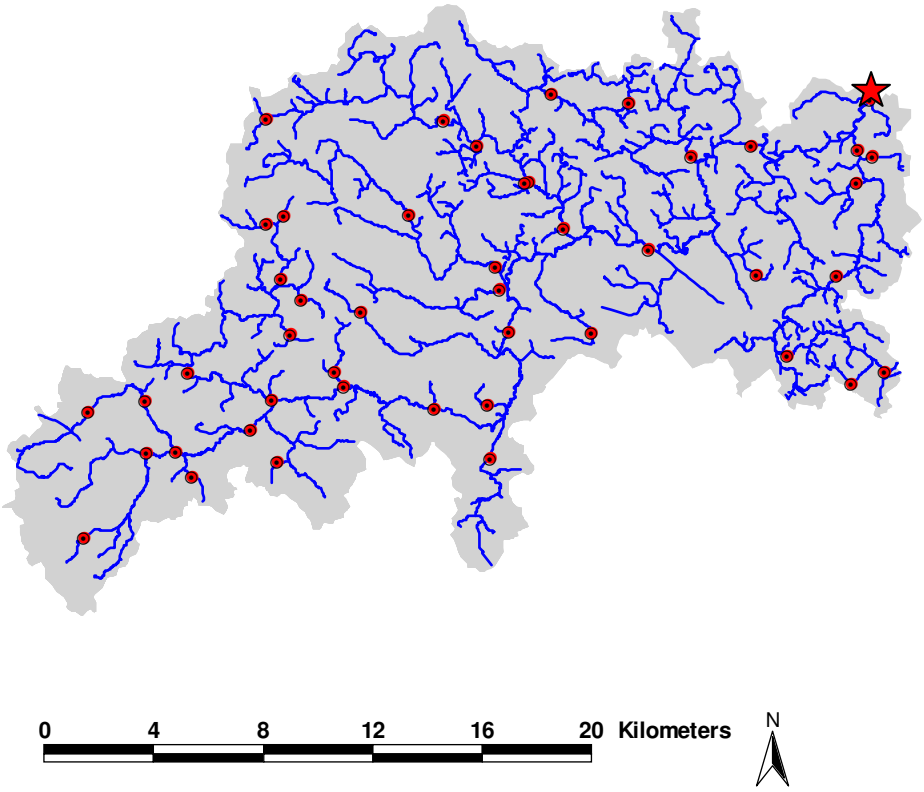

Figure 2.9: Map of the Ipswich River catchment, Massachusetts. Red circles represent synoptic sampling locations. Star represents outlet.

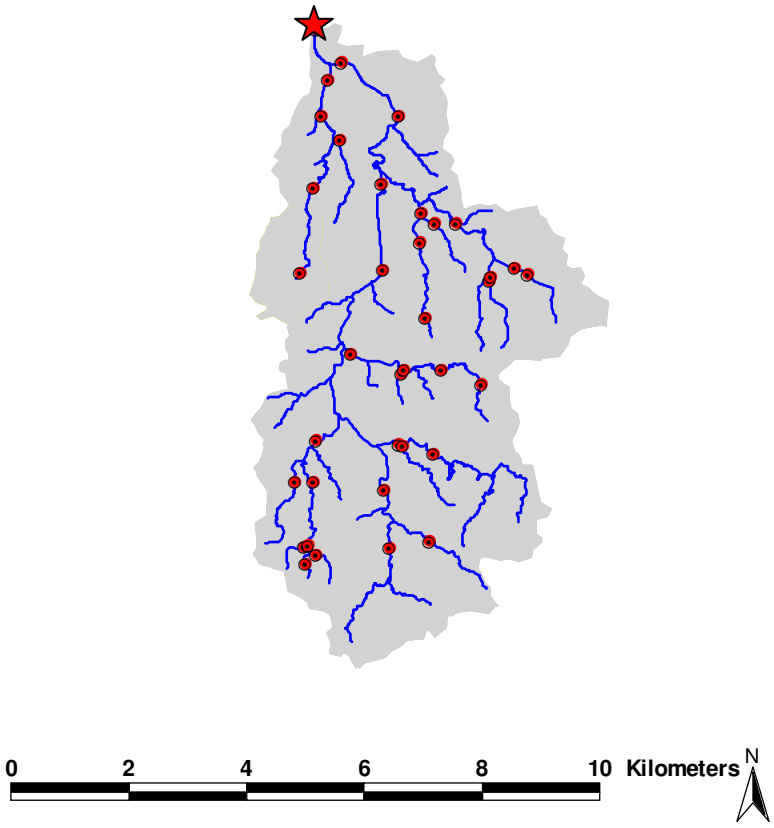

Figure 2.10: Map of the Rio Pierdas catchment, Puerto Rico. Red circles represent synoptic sampling locations. Star represents outlet.

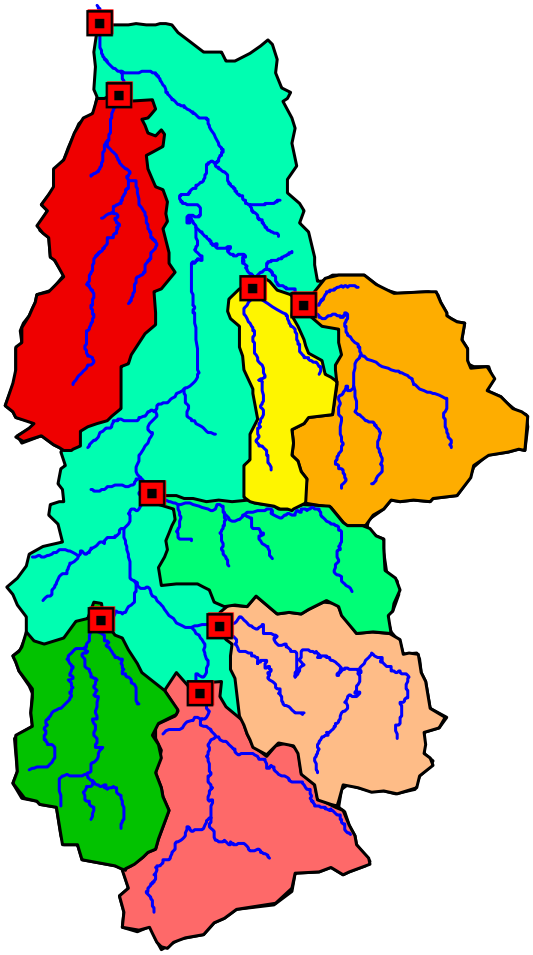

Figure 2.11: Example of sub-catchment divisions within a sampled stream network. Flow is measured at the outlet of each sub-catchment (represented by red squares). The water yield determined from each gauging location is assigned to each stream segment within that gauging location's contributing area, represented here by different colors.

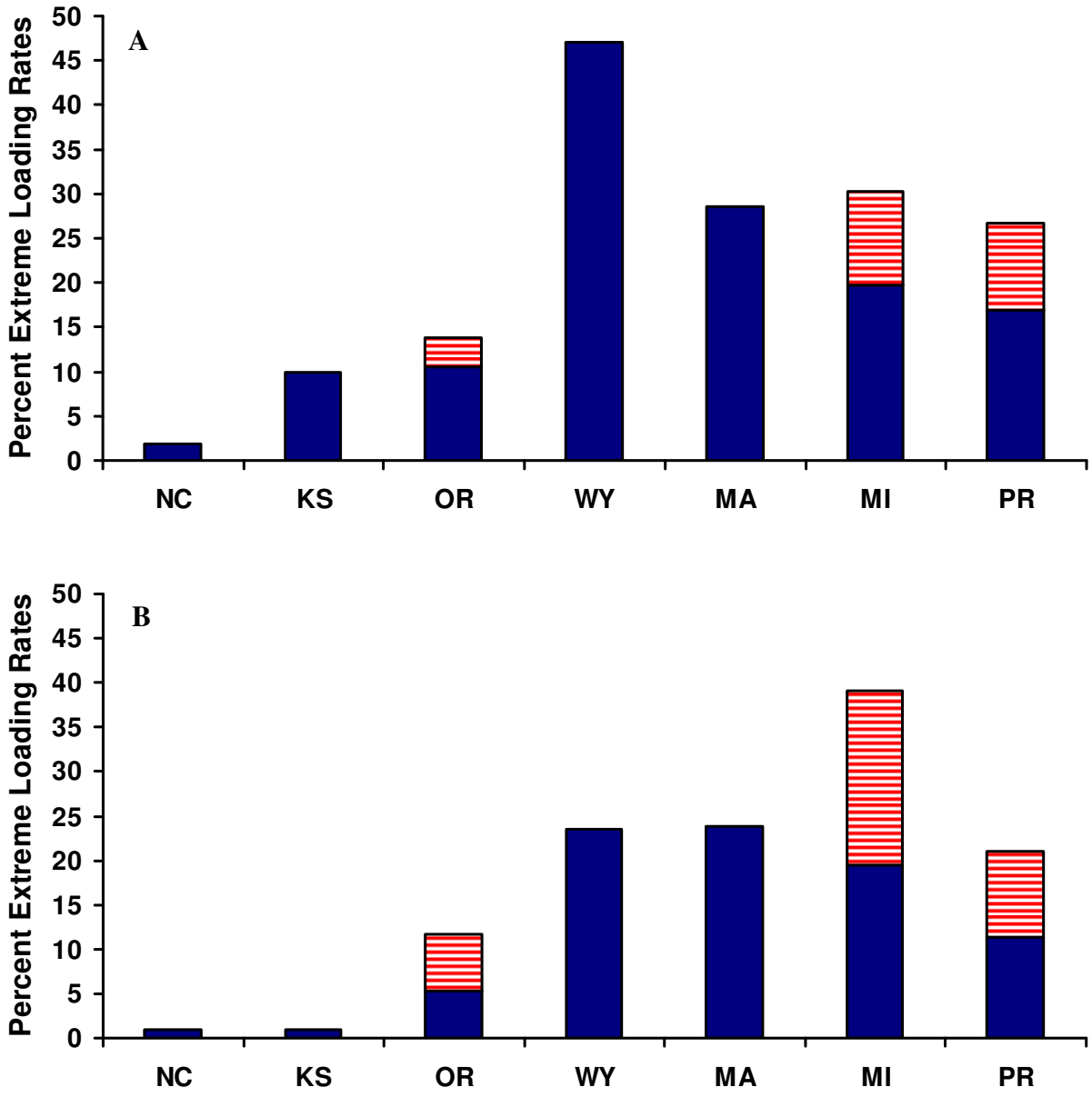

Figure 2.12: Percent of extreme loading rates for each catchment. A) Model scenario without uptake and B) Model scenario with uptake. Solid blue = extreme low loading rates and red stripes = high extreme loading rates. Extreme low loading rates = 0 and high loading rates are greater than 6.46 kg km^{-2} day^{-1}, the absolute highest reported loading rate derived from an extensive literature search.

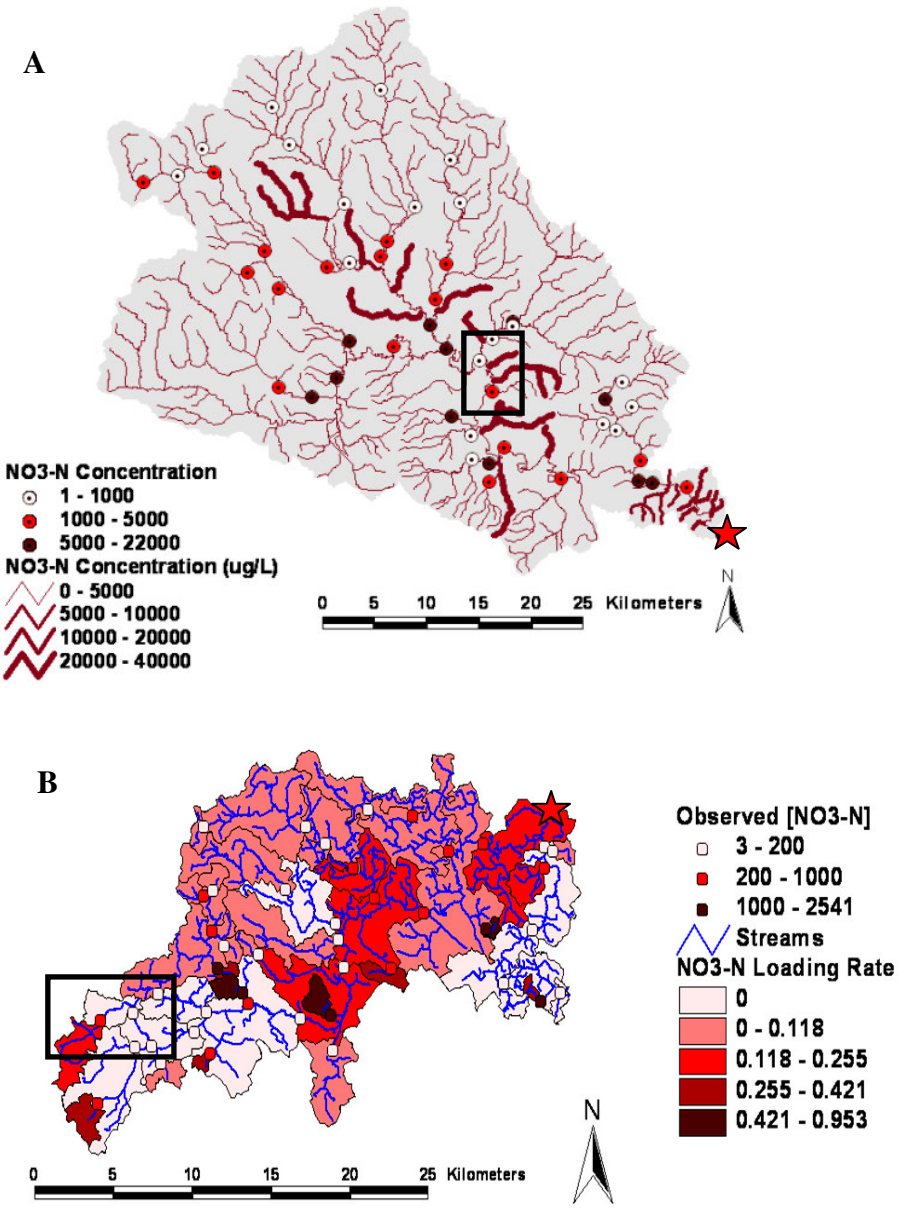

Figure 2.13: Examples of extreme simulated NO_3-N loading rate values. A) Oregon stream network observed and simulated NO_3-N concentrations. Star represents outlet. Rapid downstream increases in observed NO_3-N concentrations create extreme high (i.e., >6.46 kg $km^{-2}day^{-1}$) simulated loading rates, and B) Massachusetts stream network observed NO_3-N concentrations and simulated loading rates. Star represents outlet. Rapid downstream decreases in observed NO_3-N concentrations create extreme low (i.e., zero) simulated loading rates.

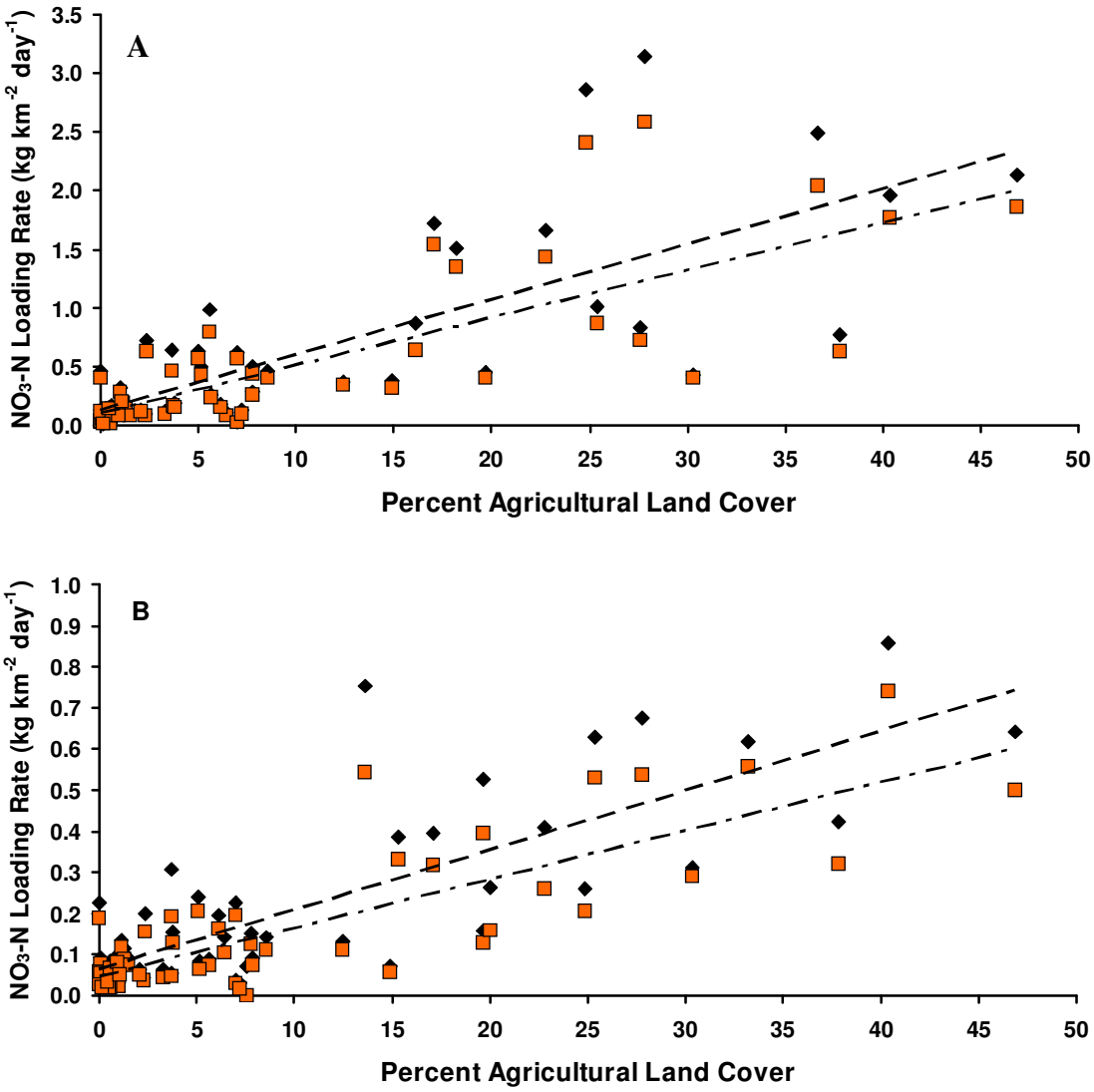

Figure 2.14: NO_3-N loading rates versus percent agricultural land cover for 2003 (A) and 2004 (B) for the North Carolina stream network. Filled squares = Scenario 1: No in-stream removal, Filled diamonds = Scenario 2: In-stream removal. There were no significant differences between linear regressions for either year (ANCOVA, 2003: p=0.34, 2004: p = 0.10).

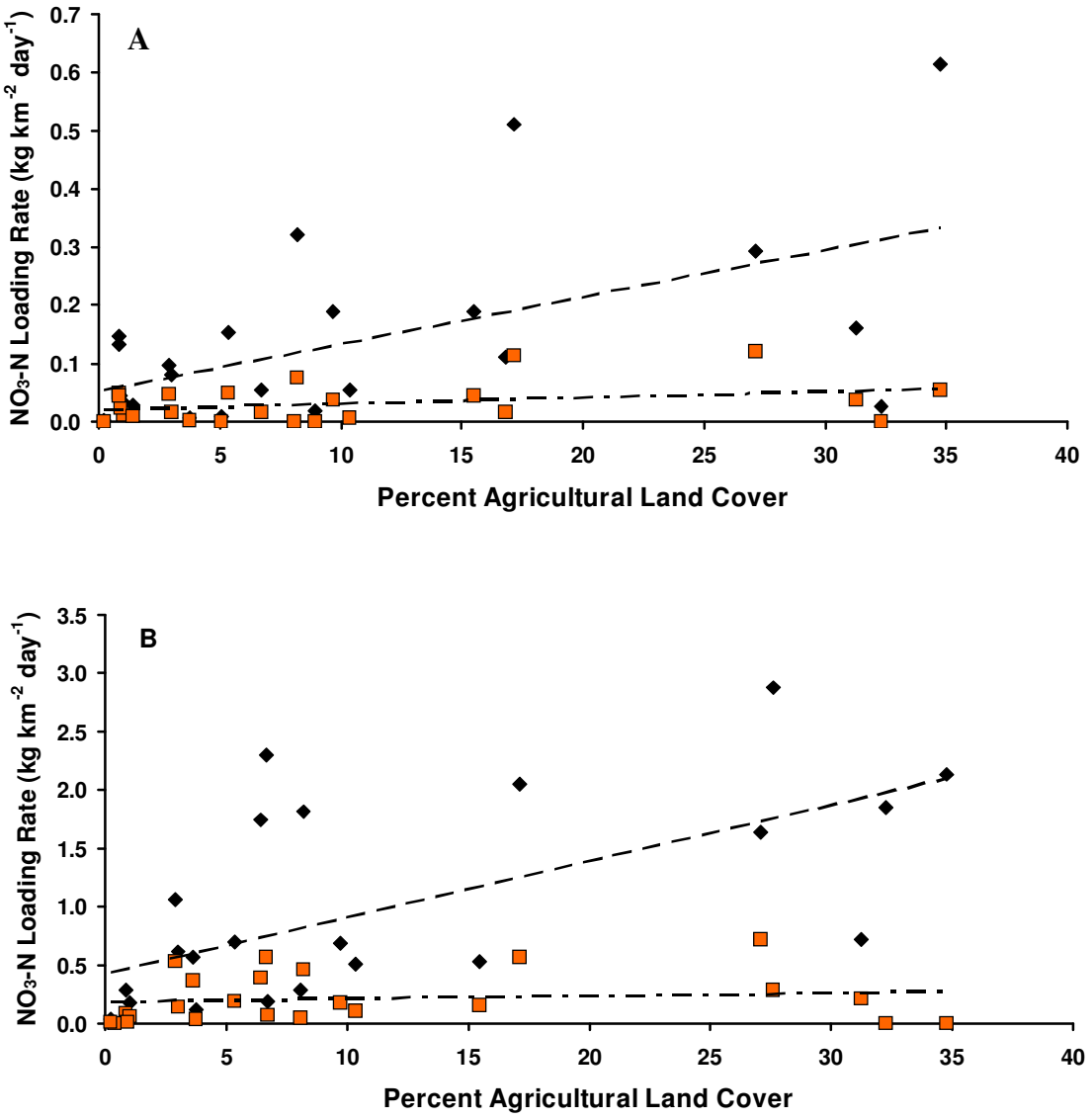

Figure 2.15: NO_3-N loading rates versus percent agricultural land cover for 2003 (A) and 2004 (B) for the Kansas stream network. Filled squares = Scenario 1: No in-stream removal, Filled diamonds = Scenario 2: In-stream removal. The relationships were significantly different between the two scenarios for both years (ANCOVA, $p<0.001$).

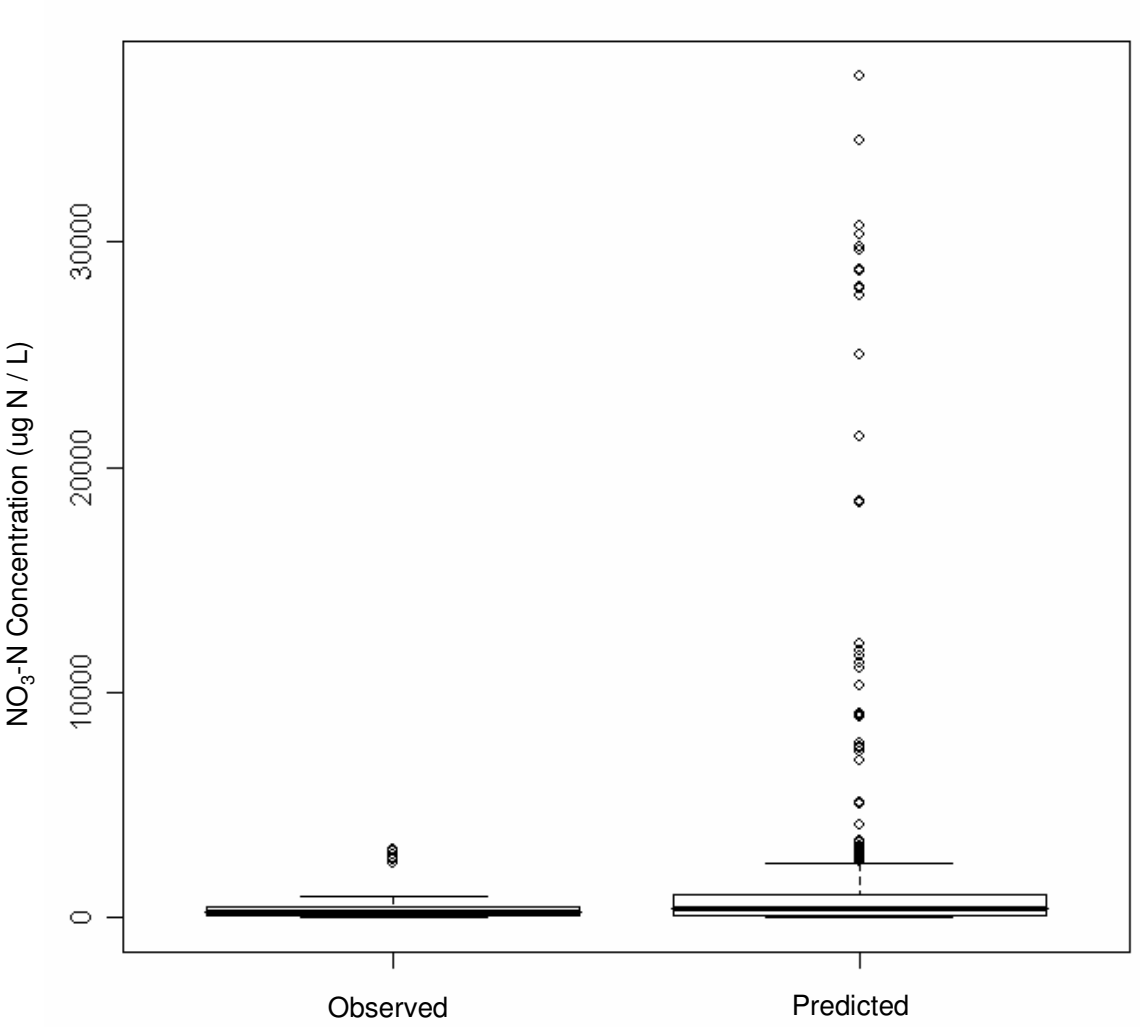

Figure 2.16: Box-and-whisker plot of observed (n = 44= number of [NO_3-N] samples) and simulated (n = 522 = number of stream segments) NO_3-N concentrations in the Oregon stream network.

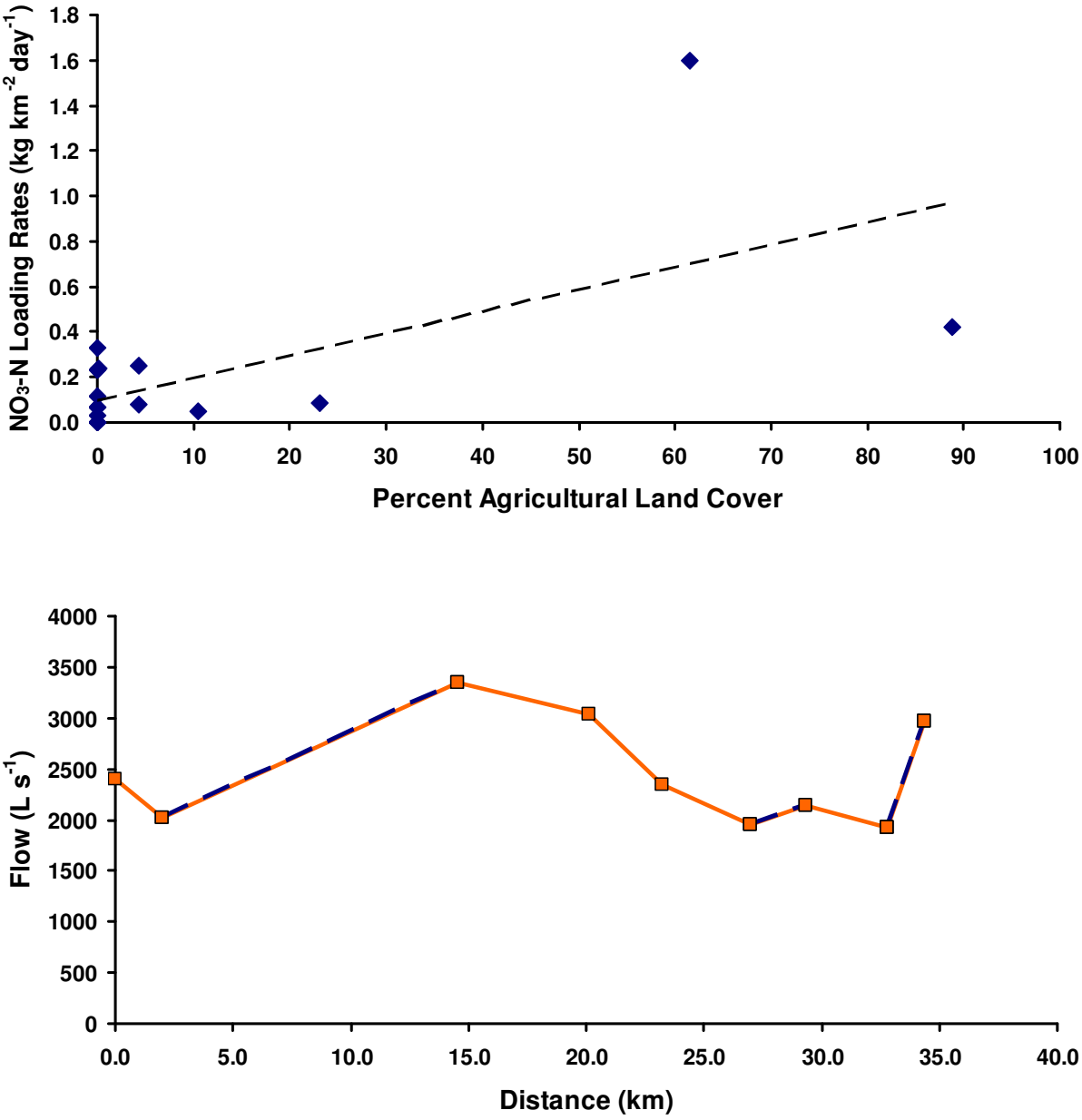

Figure 2.17: A) NO_3-N loading rates to streams versus percent agricultural land cover for Wyoming for the second scenario. B) Flow from the most upstream sampling location on the Flat Creek main stem (distance = 0) to the catchment outlet. Dashed lines show decreases in river discharge as water moves downstream.

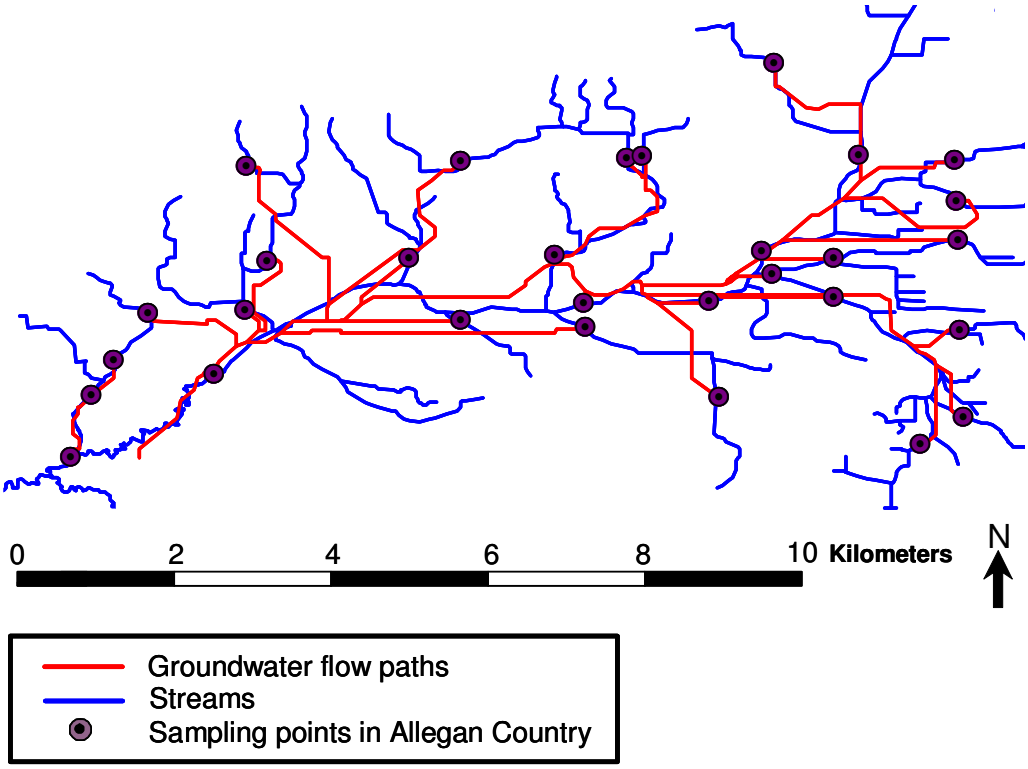

Figure 2.18: Map of surface and groundwater flow paths for sampling locations on the Little Rabbit River in Allegan County, Michigan.

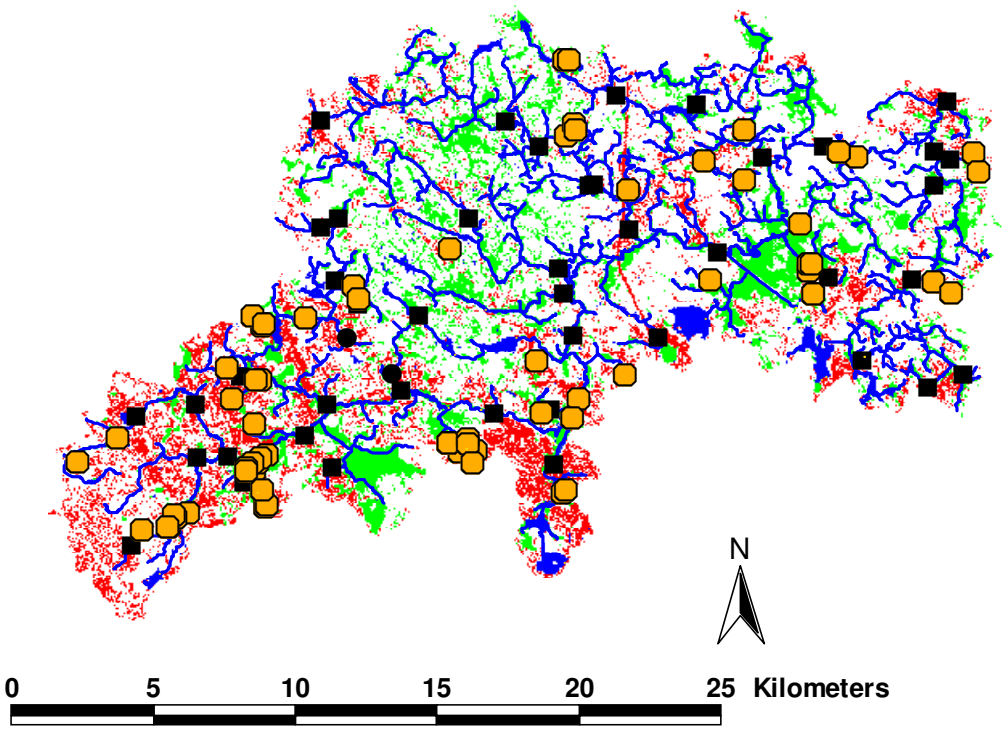

Figure 2.19: Map of wetland distribution (green), urban land cover (red), water withdrawals (orange circles) and [NO_3-N] sampling locations (black squares) in the Ipswich River catchment, Massachusetts.

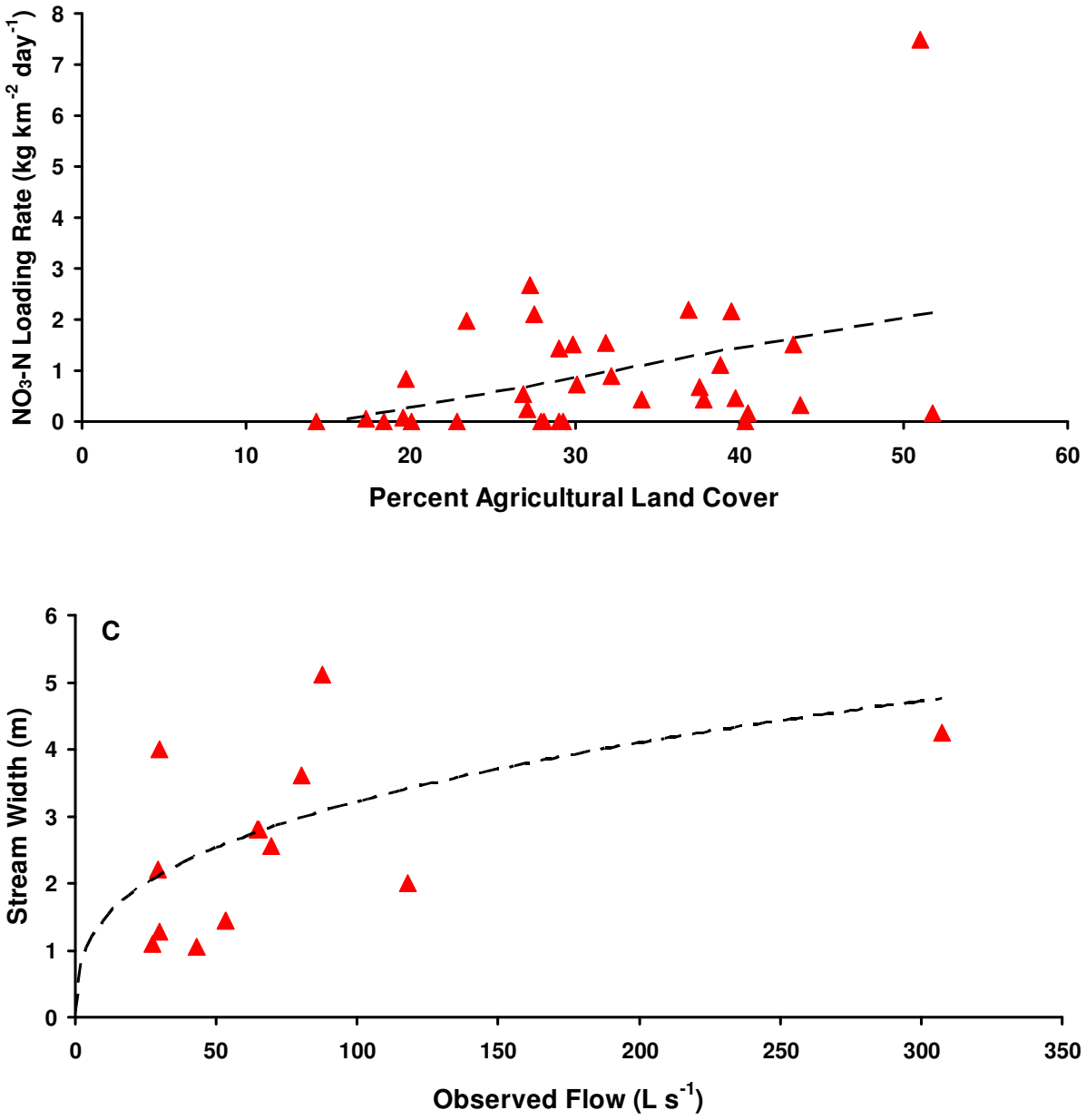

Figure 2.20: A) NO_3-N loading rates versus percent agricultural land cover for the Puerto Rico stream network for the first modeling scenario. B) Relationship used to parameterize the stream geometry equation for the Puerto Rico stream network.

CHAPTER 3

PATTERNS OF IN-STREAM NO_3-N REMOVAL WITHIN AND AMONG A 5^{TH} AND 6^{TH} ORDER STREAM NETWORK[1]

---

[1]Helton A.M., G.C. Poole, J.L. Meyer, W. K. Dodds, P. J. Mulholland, H. M. Valett, and J. R. Webster. To be submitted to an undecided journal.

Abstract

The goal of this research was to scale up *in situ* measurements of reach-scale biological activity to estimate stream network-scale removal and the spatial distribution of NO_3-N removal throughout the network, extending the predictions of river network models into smaller stream networks using experimental data. We used a stream network model that simulates in-stream processing and NO_3-N transport through stream networks 1) to examine differences in network-scale in-stream NO_3-N removal among two stream networks, Little Tennessee River in North Carolina and Mill Creek in Kansas; and 2) to determine the relative importance of stream size throughout each network. We found that network-scale removal varied between sites and years. The Kansas stream network removed a higher proportion of its NO_3-N inputs because it had more stream length available for processing, greater biological activity, and longer residence times. Both stream networks removed higher proportions of their NO_3-N inputs during years with lower discharges. For both networks, small streams removed a substantial proportion of total inputs and were efficient NO_3 removers. Individually, large streams removed more NO_3 mass. This study illustrates the importance of understanding the drivers of inter-annual, inter-site and stream size differences in biological processing on network-scale NO_3-N dynamics.

Introduction

Estimates of increased anthropogenic nitrogen (N) inputs to streams (e.g.,Vitousek 1997), riverine N fluxes (e.g.,Howarth 1998) and their effects on aquatic systems (e.g., eutrophication, Turner and Rabalais 1994; hypoxia, Turner et al. 2005) are well established; however, the precise fate of a large portion of N input to aquatic systems is poorly understood. Recent mass balance studies indicate that riverine N flux measurements account for only 20 to 25% of anthropogenic N inputs to the landscape (Howarth et al. 1996), and that in-stream removal may

account for a substantial proportion of landscape N removal (Howarth et al. 1996; Van Breemen et al. 2002).

Several current stream network models of N dynamics have been used to estimate stream network N attenuation across large river basins. These studies have found that in-stream N removal is substantial across river networks. Estimates of in-stream N removal in regional drainages in the Mississippi River basin range from 10 to 60% (SPARROW model, Alexander et al. 2000) and from 18 to 50% (Donner et al. 2004) of N inputs to surface waters. Likewise, Seitzinger et al. (Riv-N model; 2002) predicted that 37 to 76% of N input to sixteen river networks in the Northeastern United States was removed within the streams, and Alexander et al. (SPARROW model; 2002) predicted that 7 to 54% of N delivered to streams was removed for the same sixteen watersheds. For the Rhine and Elbe river basins, de Wit (PolFlow model; 2001) predicted that 14 to 45% of input to surface water was removed in the river network. Although network-scale removal is variable depending on both the model used and the particular stream network, these modeling studies all agree that stream networks remove a substantial proportion of their incoming N.

Some river network modeling studies also suggest that N removal in streams may vary among streams of different sizes in larger river basins. Small streams generally remove a higher proportion of their incoming N (per unit length, Wollheim et al. 2006; per stream reach, Seitzinger et al. 2002; per unit of water travel time, Alexander et al. 2000). Although larger stream reaches remove smaller fractions of their direct N inputs, they remove larger masses of N because more N passes through them (Seitzinger et al. 2002; Wollheim et al. 2006). For example, N that is not removed from smaller streams in addition to N from the landscape flows through larger streams. Much less N flows through smaller streams because smaller streams do

not receive as much N from upstream reaches. However, the influence of streams of different sizes on basin-wide removal depends on their level of biological activity and their channel geometry (Wollheim et al. 2006); therefore the relative importance of different sized streams likely varies among catchments.

Recently, reach-scale N amendment experiments have also focused on quantifying in-stream N losses (e.g., Mulholland et al. 2004). This research suggests that very small headwater streams may remove over 50% of their N inputs (Peterson et al. 2001). However, these studies are generally performed over a narrow range of environmental conditions (e.g., small streams during base flow, Fisher et al. 2004), no relationship has been observed experimentally between stream size and in-stream removal rates (Wollheim et al. 2001), and N uptake measurements from these studies have not been incorporated into catchment-scale models.

Thus, our goal was to scale up *in situ* measurements of reach-scale biological activity to estimate stream network-scale removal and the spatial distribution of NO_3-N removal throughout the network, extending the predictions of river network models into smaller stream networks using experimental data. We used a recently developed stream network model that simulates in-stream processing and NO_3-N transport through stream networks 1) to examine differences in network-scale in-stream NO_3-N removal among two stream networks, Little Tennessee River in North Carolina and Mill Creek in Kansas; and 2) to determine the relative importance of stream size throughout each network.

Methods

Overview

We used a simulation model of stream network NO_3-N dynamics to determine the spatial distribution of NO_3-N loading rates to streams necessary to recreate the observed patterns

of NO_3-N concentration across stream networks (Chapter 1). In this study, we used model results from two stream networks in which the model adequately explained stream network NO_3-N dynamics (Chapter 1) to determine 1) how whole network in-stream NO_3-N removal varied between years for each catchment and among the two catchments; and 2) how in-stream NO_3-N removal was distributed throughout each of the two stream networks among streams of different sizes.

Model Development

The simulation model of NO_3-N loading, transport and biotic uptake was developed using the Network Exchange Objects (NEO) modeling system (Poole and Bennett, In Preparation). Stream networks were divided into segments, which were defined as the length of stream between tributary junctions. The model routes NO_3-N and water from contributing drainage areas and through the stream network segment by segment from the headwaters to the outlet, and NO_3-N is removed from each segment via uptake by the stream bed (Figure 3.1). For a complete description of water and NO_3-N transport equations, see Chapter 1.

The fractional removal of NO_3-N from the water column for each segment was determined by the following equation recently applied by Wollheim et al. (2006):

$$R = 1 - e^{(-v_f/H_L)} \quad (1)$$

where R is the fraction of NO_3-N removed, v_f is the average vertical velocity of NO_3-N molecules through the water column or the mass transfer coefficient (LT^{-1}, where L is a measure of length and T is a measure of time), and H_L is the hydraulic load (LT^{-1}). The mass transfer coefficient is defined as the ratio of the areal NO_3-N uptake rate (U, $ML^{-2}T^{-2}$, where M is a measure of mass) to in-stream NO_3-N concentration (ML^{-3}), which represents uptake normalized by the concentration in the water column. Thus, v_f is a measure of the demand for NO_3-N

relative to the amount of NO_3-N available (Stream Solute Workshop 1990), and represents biological activity throughout the stream network. The hydraulic load is the ratio of discharge into the stream segment (L^3T^{-1}) to the surface area of the stream segment. For a stream segment, surface area equals the segment length multiplied by average width (L^2). Therefore, H_L is a measure of the rate of water passage through the stream segment relative to the benthic surface area available for NO_3-N removal, and represents the physical controls of NO_3-N removal in each stream segment.

We chose this particular equation to represent NO_3-N removal because it explicitly integrates biological processing parameters directly measured in field experiments (v_f) and separates biological controls of removal (v_f) from hydrological controls (H_L). This eliminates the dependence of v_f on river size exhibited by in-stream removal equations used in many models (Wollheim et al. 2006), making this equation ideal to analyze the effects of stream size on in-stream NO_3-N removal.

Model Application

Study Basins

In this study, we used model results from Chapter 1 for the North Carolina and Kansas stream networks. Little Tennessee River is located in western North Carolina with its headwaters in Northeastern Georgia (Figure 3.2). The watershed area is approximately 360 km^2 and is predominately forested (Table 3.1). Mill Creek is located in central Kansas and is approximately 1010 km^2 (Figure 3.3). The land cover is predominately grassland with a substantial proportion of agriculture (Table 3.1). Both stream networks contained or were in close proximity to stream reaches used in the second Lotic Intersite Nitrogen eXperiment (LINX-II), and NO_3-N sampling in the stream networks was performed concurrently to $^{15}NO_3$-N

tracer field experiments, in which *in situ* biological NO_3-N uptake rates were measured across stream reaches. We selected these two stream networks for further analyses because the simulation model explained NO_3-N dynamics across these two stream networks well (Chapter 1).

Parameterization

The simulation model requires a description of stream network topology, drainage areas, hydrology, stream segment geometry, distribution of in-stream NO_3-N concentration, and biological uptake (v_f), which are described in Chapter 1. 1:24,000 digital hydrography datasets were used to determine stream segment length and network topology. Watershed boundaries, contributing areas to sampling locations and adjacent drainage areas to stream reaches (Figure 3.4) were delineated from 30-meter raster digital elevation models (USGS National Elevation Data Set, available online at http://seamless.usgs.gov). Surveys of in-stream NO_3-N concentrations were conducted to describe the distribution of NO_3-N concentration throughout the stream network for both North Carolina and Kansas stream networks for two consecutive years. Stream flow was derived from water yield estimates which were determined from measured stream flows during NO_3-N sampling according to Chapter 1. Average segment width was estimated for each segment based on the equation $w = aQ^b$ from Leopold et al. (1964) parameterized for each stream network where Q is the stream flow in the segment and a and b are the width coefficient and width exponent, respectively (Table 3.1).

LINX-II $^{15}NO_3$-N injection experiments were performed on three stream reaches each year of stream network NO_3-N sampling and on an additional three stream reaches for one more year. We used published uptake rates from North Carolina (Earl et al. Submitted) in addition to LINX-II data. For a detailed description of techniques used in the LINX-II $^{15}NO_3$-N field experiments to determine uptake rates, see Mulholland et al. (2004). Vertical velocity (v_f) was

parameterized for each site as the slope of the linear relationship forced through zero between measured areal NO_3-N uptake rates and in-stream NO_3-N concentrations ($U = v_f [NO_3\text{-}N]$; Table 2.1).

Scenario descriptions and model runs

The model was implemented for both the North Carolina and Kansas stream networks for both years of sampling. For each model run, modeled discharge and NO_3-N were initialized to zero for each stream segment. NO_3-N and water were allowed to accumulate from the landscape through the stream network until the model reached steady state conditions. Model results from each model run represent environmental conditions during the time of sampling each year.

We used a model-independent parameter optimser, Parameter ESTimation (PEST; Version 10.1, S.S. Papadopoulos and Associates, Inc. 2006) to determine the spatially-explicit pattern of NO_3-N loading rates required to reproduce the observed patterns of in-stream NO_3-N concentrations across each stream network. PEST determined areal NO_3-N loading rates for the contributing area of each sampling location and assigned the loading rate to each stream segment within a sampling location's contributing area (Figure 3.4b). Loading rates were not permitted to drop below zero because we assumed that streams experienced a net gain from rather than loss to their adjacent drainage areas.

Model Output Analyses

We analyzed model results from the Kansas and North Carolina stream networks to determine the total proportion of NO_3-N removed from each network in order to compare network-scale results among sites and years. We also determined the patterns of removal throughout each network in order to examine the spatial distribution of NO_3-N removal within each stream network. Total NO_3-N load to the stream network was calculated by summing the

mass of NO_3-N loads to stream segments across the entire network. The total NO_3-N removed was calculated by summing the mass of NO_3-N removed from each stream segment across the entire network. Then, we calculated the percent of the load removed by the whole network by dividing the total NO_3-N removed by the total NO_3-N load and multiplying by 100%.

Patterns of in-stream NO_3-N removal throughout the stream networks were analyzed using various descriptors of in-stream removal. We used basin area for each stream segment as a surrogate for stream size, which was determined from the watershed delineations as described above (see Parameterization). To determine the relative proportion of total network removal occurring in different sized streams, we calculated the cumulative fraction of NO_3-N removed from small to large streams. The cumulative fraction of NO_3-N removed was calculated by dividing the mass of NO_3-N removed from each stream segment by the total NO_3-N removed from the network and then, for each stream segment, adding its fraction to the sum of fractions of all stream segments with smaller basin areas. Cumulative stream length was calculated similarly. For each stream segment, its length was added to the sum of the lengths of all segments with smaller basin areas.

To examine the magnitude of removal occurring in different sized streams, we determined the mass of NO_3-N removed and the NO_3-N removal efficiency for each stream segment, which were both normalized by segment length. The mass of NO_3-N removed per unit length for each segment was calculated by dividing the mass removed in each stream segment by that segment's length. The removal efficiency per unit length for each segment was calculated by dividing the fractional removal (R from equation 1) by the segment's length, which is equal to the fraction of direct inputs removed per unit length by each stream segment. We also calculated

the mass of NO_3-N per unit length within each stream segment to illustrate the distribution of NO_3-N availability from small to large streams.

Results

Both stream networks removed a substantial proportion of their NO_3-N (Table 3.2). However, both the North Carolina and Kansas stream networks removed different proportions of incoming NO_3-N each year and the Kansas stream network removed a much higher proportion of its NO_3-N input than did the North Carolina stream network. The North Carolina stream network removed 16 and 28 percent of the total NO_3-N load in 2003 and 2004, respectively. The Kansas stream network removed 80 and 71 percent of the total NO_3-N load in 2003 and 2004, respectively.

Although inter-annual differences in overall removal existed (Table 3.2), patterns of NO_3-N removal remained consistent for both years for both networks. Thus, here we present results from the year 2004 for each stream network. The North Carolina and Kansas stream networks removed substantially different proportions of incoming NO_3-N overall, but they followed very similar patterns of removal (Figures 3.5 – Figure 3.10). In the North Carolina stream network, small streams make up a large proportion of cumulative stream length (Figure 3.5a). Over 80% of stream length occurs in stream segments with basin areas less than 20 km^2. As a result, 50% of NO_3-N removal occurred in streams with catchment areas less than 20 km^2 (Figure 3.5b). Removal efficiency or the proportion of direct inputs removed per meter of stream length, decreased as stream size increased (Figure 3.6). Yet because large stream segments tended to have more in-stream NO_3-N mass available per unit length (Figure 3.7a), large stream segments tended to remove more NO_3-N mass than small stream segments per unit length (Figure 3.7b).

Similarly, in the Kansas stream network, small streams make up a large proportion of cumulative stream length. 80% of stream length occurred in stream segments with basin areas less than 10 km^2 (Figure 3.8a). As a result, 50% of NO_3-N removal occurred in stream segments with catchment areas less than 10 km^2 (Figure 3.8b). Removal efficiency or the proportion of direct inputs removed per meter of stream length, decreased as stream size increased (Figure 3.9). As in North Carolina, because large stream segments tended to have more in-stream NO_3-N mass available per unit length (Figure 3.10a) large stream segments tended to remove more NO_3-N mass than small stream segments per unit length (Figure 3.10b).

Discussion

In-stream NO_3-N removal was substantial for both the North Carolina and Kansas stream networks during base flow conditions. The percentages of NO_3-N removed in the stream networks were similar to those reported in the literature for larger river basins, and suggest that smaller stream networks also remove a substantial proportion of their incoming NO_3-N. However, the stream networks exhibited inter-annual, inter-catchment, and stream size differences.

Inter-annual variation of in-stream NO_3-N removal

NO_3-N loading rates to streams and the proportion of NO_3-N removed within each stream network exhibited different degrees of inter-annual variation. Model results for each year represent in-stream conditions during the particular time of sampling so that variation in model results for each stream network represent variation in environmental conditions during the different sampling times. For the North Carolina stream network, NO_3-N loading rates to streams were greater in 2003, but the proportion of NO_3-N removed was lower (Table 3.2). For the Kansas stream network, NO_3-N loading rates were greater in 2004, but the proportion of

NO_3-N removed was lower. Flow was higher throughout the stream network during 2003 in North Carolina and higher during 2004 for the Kansas stream network. Higher flow conditions may have resulted in decreased NO_3-N removal because high flow decreases water residence time and increases water depth in stream channels. Decreasing water residence time and increasing stream depth decreases overall NO_3-N removal because contact between N and the benthic sediments is reduced (Alexander et al. 2000). Previous research has also shown that N loading to streams tends to increase during wet years but the fraction of N removed across networks decreases (Donner et al. 2004). This dependence on flow conditions suggest that NO_3-N removal may not only vary between years, but may also vary throughout the year with fluctuation in stream flow. Since high flow may decrease the fractional N removal in stream networks and higher flows contribute most of the annual N load to streams (e.g., Arheimer et al. 1996), decreased in-stream removal may occur during periods with the highest NO_3-N loading rates to streams.

Other sources of variation driving annual differences in stream network removal may include varying sources of NO_3-N during the sampling times or other temporal differences in NO_3-N distribution within the landscape (e.g., fertilizer application). In-stream biological differences may also drive inter-annual variation. For example, higher whole-stream uptake rates of phosphorus and ammonium were associated with the observed presence of stream autotrophs (e.g. algae and macrophytes; Bernot et al. 2006), and biological uptake rates in systems with a natural abundance of litterfall was higher than in experiments where leaf litter was excluded from streams (Webster et al. 2000). The variation in NO_3-N delivery rates and in-stream removal between years for the Kansas and North Carolina stream networks illustrates the

importance of understanding temporal variation in stream network dynamics in order to accurately predict N delivery to, transport and processing within streams.

Inter-catchment variation of in-stream NO_3-N removal

The North Carolina and Kansas stream networks both removed substantial, but different, proportions of their NO_3-N. The North Carolina stream network removed much less NO_3-N than the Kansas stream network for both years (Table 3.2). Variation in stream length, biological activity and water residence time in the channels are the drivers of inter-catchment variation observed among the Kansas and North Carolina networks. All else being equal, catchments with more total stream length should remove a higher proportion of in-stream NO_3-N. Indeed, the Kansas stream network had a longer stream length and a higher drainage density than did the North Carolina stream network (Table 3.1). Seitzinger et al. (2002) found that simulated network N removal increased with total stream length ($r^2 = 0.84$), and that increasing the drainage density in a watershed (e.g., increasing map scale of hydrography from 1:500,000 to 1:100,000) increased the simulated proportion of N removed by 8 to 31 percentage points. The Kansas stream network also had substantially higher biological activity than did the North Carolina stream network. Networks with greater biological activity (i.e., v_f) remove greater proportions of their incoming N (Wollheim et al. 2006). Furthermore, the Kansas stream network had an overall lower slope in its drainage basin (Table 2.2), resulting in longer water residence times in stream channels, which increased simulated NO_3-N removal from streams.

Thus, Kansas streams are inherently more efficient at removing NO_3-N since biological activity in the Kansas network was greater and there was a greater opportunity for in-stream removal to occur since there is more total stream length available for processing and water remains in the channels for longer periods of time. Seitzinger et al. (2002) suggest that the

relationship between total stream length and percent removal they observed may provide an approach for estimating network-scale N removal in watersheds with hydrological and physiographic characteristics similar to their study watersheds. We suggest an approach that would allow one to estimate network-scale removal even in networks that differ in physiographic characteristics. On a catchment-scale, there are four qualities that may determine how important in-stream removal is for any particular stream network, including stream length, biological activity, and water residence time as well as channel geometry. Since Kansas and North Carolina had similar channel geometry, this factor did not drive differences in this study. However, because the proportion of NO_3-N removed in any stream segment depends on discharge and the surface area of the streambed (e.g., $H_L = Q/A$), longer streams with wider channels and lower flow relative to their surface area (e.g., a high width to depth ratio) process N more efficiently. Streams with relatively high width to depth ratios remove higher proportions of their NO_3-N, since a high streambed width relative to the depth of water provides more streambed per unit of water, which increases contact between N and the streambed. An approach that incorporated information about total stream length and biological activity as well as residence time (hydrology) and downstream trends in channel geometry could be used across physiographic regions to determine the potential for in-stream N removal at the stream network scale.

NO_3-N removal and stream size

Although the Kansas stream network removed a higher proportion of in-stream NO_3-N than the North Carolina network, both streams had similar spatial patterns of removal. On a network scale, small and large streams both removed a substantial amount of NO_3-N; however, small and large streams played different roles in network-scale removal. Cumulatively, small

streams removed a substantial amount of NO_3-N inputs (Figure 3.5b and Figure 3.8b) and a higher proportion of their direct NO_3-N inputs than did large streams (Figure 3.6 and 3.9). This agrees with previous studies which have established that small streams remove a greater percentage of their direct N inputs (Alexander et al. 2000; Seitzinger et al. 2002; Wollheim et al. 2006).

Large streams also played an important role in stream network-scale removal. Large stream segments in the two networks generally removed a greater mass per unit length than did smaller streams, and the mass of removal in large streams was less variable than in small streams (Figure 3.7b and 3.10b). Large streams removed a greater mass of NO_3-N per unit length on average because NO_3-N accumulates downstream so that even though large streams removed a smaller proportion of their NO_3-N, more incoming NO_3-N to large stream segments (Figure 3.7a and 3.10a) resulted in greater masses removed by large streams (Figure 3.7b and 3.10b). This agrees with findings from Seitzinger et al. (2002) that show large streams remove more NO_3-N because more NO_3-N passes through them. However, although individually small streams received less NO_3-N and thus removed less NO_3-N mass on average, small stream segments are so abundant in the networks and process NO_3-N so efficiently that, combined, they remove a high proportion of stream network NO_3-N removed relative to individual stream segment removal. Ultimately, patterns of NO_3-N removal in this study were similar to patterns observed in previous studies of large river systems. However, this study illumines the importance of including small streams in analyses of stream network NO_3-N dynamics across stream sizes since they have a substantial cumulative effect on catchment-scale in-stream NO_3-N removal.

Recent research has shown that developed stream networks lose drainage density (Meyer and Wallace 2001), and that loss of small streams can decrease diversity of biota (Meyer et al.

2005). The current study suggests that eliminating small streams could also decrease the capacity of the overall network to remove N and other nutrients. Eliminating small streams reduces the total surface area in the network available for removal, reducing the effects of in-stream removal on catchment wide N removal.

The relative importance of small and large streams varies with biological activity and downstream trends in channel geometry (Wollheim et al. 2006). Width coefficients were relatively similar among the stream networks, but the Kansas stream network had higher biological activity (v_f) than did the North Carolina stream network (Table 3.1). Small streams in networks with higher biological activity have an elevated role in network-scale removal (Wollheim et al. 2006). Thus, not only are Kansas streams inherently more efficient at removing NO_3-N, but small streams in Kansas remove a higher proportion of direct inputs. As a result, a smaller proportion of NO_3-N inputs to small streams were passed on to larger rivers, and thus larger streams removed less NO_3-N relative to small streams in the Kansas network than in the North Carolina network. This suggests that the role of small streams was slightly greater in the Kansas stream network; however, the differences between the removal patterns among the two steam networks were small.

Conclusions

Stream network removal of NO_3-N was substantial across the two catchments in North Carolina and Kansas. Catchment-scale in-stream removal varied between years and between the two stream networks. The observed inter-annual and inter-catchment variation may be due to one or a combination of differences in channel geometry, stream length, flow conditions and biological activity. These catchment-scale variables should be useful for predicting network-scale potential of in-stream removal across physiographic regions.

Small and large streams both play important roles in stream network-scale NO_3-N removal. Small streams removed the majority of in-stream NO_3-N removal because they are abundant and efficient at removing NO_3-N. Although large stream segments removed a greater mass of NO_3-N per unit length, small stream segments removed more NO_3-N cumulatively. The spatial patterns of removal were similar to patterns observed in previous studies; however, findings here underscore the importance of the cumulative effects of very small streams in network-scale N dynamics.

References

Alexander, R. B., P. J. Johnes, E. W. Boyer, and R. A. Smith. 2002. A comparison of models for estimating the riverine export of nitrogen from large watersheds. Biogeochemistry **57**:295-339.

Alexander, R. B., R. A. Smith, and G. E. Schwarz. 2000. Effect of stream channel size on the delivery of nitrogen to the Gulf of Mexico. Nature **403**:758-761.

Arheimer, B., L. Andersson, and A. Lepisto. 1996. Variation of nitrogen concentration in forest streams -- influences of flow, seasonality and catchment characteristics. Journal of Hydrology **179**:281-304.

Bernot, M. J., J. L. Tank, T. V. Royer, and M. B. David. 2006. Nutrient uptake in streams draining agricultural catchments of the Midwestern United States. Freshwater Biology **51**.

de Wit, M. J. M. 2001. Nutrient fluxes at the river basin scale. I: the PolFlow model. Hydrological Processes **15**:743-759.

Donner, S. D., C. J. Kucharik, and M. Oppenheimer. 2004. The influence of climate on in-stream removal of nitrogen. Geophysical Research Letters **31**:doi: 10.1029/2004GL020477.

Earl, S. R., H. M. Valett, and J. R. Webster. Submitted. Nitrogen saturation in stream ecosystems. Ecology.

Fisher, S. G., R. A. Sponseller, and J. B. Heffernan. 2004. Horizons in stream biogeochemistry: Flowpaths to progress. Ecology **85**:2369-2379.

Howarth, R. W. 1998. An assessment of human influences on fluxes of nitrogen from the terrestrial landscape to the estuaries and continental shelves of the North Atlantic Ocean. Nutrient Cycling in Agroecosystems **52**:213-223.

Howarth, R. W., G. Billen, D. Swaney, A. Townsend, N. Jaworski, K. Lajtha, J. A. Downing, R. Elmgren, N. Caraco, T. Jordan, F. Berendse, J. Freney, V. Kudeyarov, P. Murdoch, and Z. Zhao-Liang. 1996. Regional nitrogen budgets and riverine N and P fluxes for the drainages to the North Atlantic: Natural and human influences. Biogeochemistry **35**.

Meyer, J. L., G. C. Poole, and K. L. Jones. 2005. Buried alive: Potential consequences of burying headwater streams in drainage pipes. *in* K. J. Hatcher, editor. Proceedings of the 2005 Georgia Water Resources Conference, Athens, GA.

Meyer, J. L., and J. B. Wallace. 2001. Lost linkages and lotic ecology: rediscovering small streams. Pages 295-317 *in* M. C. Press, N. J. Huntly, and S. Levin, editors. Ecology: Achievement and Challenge. Blackwell Science.

Mulholland, P. J., H. M. Valett, J. R. Webster, S. A. Thomas, L. W. Cooper, S. K. Hamilton, and B. J. Peterson. 2004. Stream denitrification and total nitrate uptake rates measured using a field 15N tracer addition approach Limnology and Oceanography **49**:809-820.

Peterson, B. J., W. M. Wollheim, P. J. Mulholland, J. R. Webster, J. L. Meyer, J. L. Tank, E. Marti, W. B. Bowden, H. M. Valett, A. E. Hershey, W. H. McDowell, W. K. Dodds, S. K. Hamilton, S. Gregory, and D. D. Morrall. 2001. Control of Nitrogen Export from Watersheds by Headwater Streams. (Cover story). Science **292**:86.

Seitzinger, S. P., R. V. Styles, E. W. Boyer, R. B. Alexander, and G. Billen. 2002. Nitrogen retention in rivers: model development and application to watersheds in the northeastern U.S.A. Biogeochemistry **57**:199-237.

Turner, R. E., and N. N. Rabalais. 1994. Coastal eutrophication near the Mississippi river delta. Nature **368**:619-621.

Turner, R. E., N. N. Rabalais, E. M. Swenson, M. Kasprzak, and T. Romaire. 2005. Summer hypoxia in the northern Gulf of Mexico and its prediction from 1978 to 1995. Marine Environmental Research **59**:65-77.

Van Breemen, N., E. W. Boyer, and C. L. Goodale. 2002. Where did all the nitrogen go? Fate of nitrogen inputs to large watersheds in the northeastern U.S.A. Biogeochemistry **57**:267-293.

Vitousek, P. M., J.D. Aber, R.W. Howarth, G.E. Likens, P.A. Matson, D.W. Schindler, W.H. Schlesinger, D.G. Tilman. 1997. Technical Report: Human alteration of the global nitrogen cycle: sources and consequences. Ecological Applications **7**:737-750.

Webster, J. R., J. L. Tank, J. B. Wallace, J. L. Meyer, S. L. Eggert, T. P. Ehrman, B. R. Ward, B. L. Bennett, P. F. Wagner, and M. E. McTammany. 2000. Effects of litter exclusion and wood removal on phosphorus and nitrogen retention in a forest stream. Verh. Internat. Verein. Limnol. **27**:1337-1340.

Wollheim, W. M., B. J. Peterson, L. A. Deegan, J. E. Hobbie, B. Hooker, W. B. Bowden, K. J. Edwardson, D. B. Arscott, A. E. Hershey, and J. Finlay. 2001. Influence of Stream Size on Ammonium and Suspended Particulate Nitrogen Processing. Limnology and Oceanography **46**:1-13.

Wollheim, W. M., C. J. Vorosmarty, B. J. Peterson, S. P. Seitzinger, and C. S. Hopkinson. 2006. Relationship between river size and nutrient removal. Geophysical Research Letters **33**:doi:10.1029/2006GL025845.

Table 3.1: Geographic descriptions of study sites. %Ag = % reclassified agricultural land cover, %Urb = % reclassified urban land cover. The mass transfer coefficient (vf) is equal to the slope of the linear regression between measured areal uptake rates and NO_3-N concentrations (U = vf [NO_3-N], Chapter 1). The width coefficient (a) and width exponent (b) are derived from this equation parameterized for each stream network from measured stream width (w) and discharge (Q), $w = aQ^b$.

[1]See Fenneman 1914 for a description of physiographic provinces within the United States

Site Location	Stream	Physiographic Province [1]	Watershed Area (km^2)	Drainage Density (km km^{-2})	Minimum Elevation (meter)	Maximum Elevation (meter)	% Ag	% Urb	Mass transfer coefficient (m s^{-1})	Width Coefficient	Width Exponent
Western North Carolina	Little Tennessee River	Southern Appalachians	361	1.23	603	1651	10.4	6.5	1.99E-06	6.27	0.44
										7.30	0.45
Central Kansas	Mill Creek	Great Plains	1008	1.87	276	489	26.7	0.62	5.90E-06	7.17	0.35

Table 3.2: In-stream NO_3-N removal for both model scenarios. [1]Reported as mean (range).

Stream Network	Year Sampled	Sampling dates	Number of Observations	Observed flow at outlet during sampling ($L\ s^{-1}$)	Total NO_3-N Load to streams (kg N day^{-1})	Percent NO_3-N load to stream removed	NO_3-N loading to streams (kg N km^{-2} day^{-1})[1]
North Carolina	2003	6/6/2003	55	12962	230	16	0.58 (0.02 - 3.14)
	2004	5/26/2004	57	5550	75	28	0.20 (0 - 0.86)
Kansas	2003	5/16-17/2003	25	3477	135	80	0.13 (0 - 0.61)
	2004	7/12/2004	25	10709	1207	71	0.92 (0.01 - 2.88)

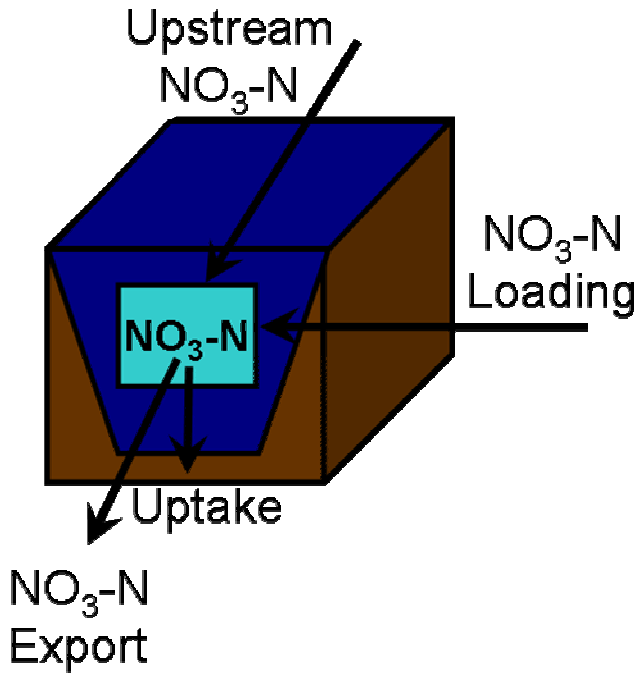

Figure 3.1: Box-and-arrow diagram of NO_3-N flow through a stream segment.

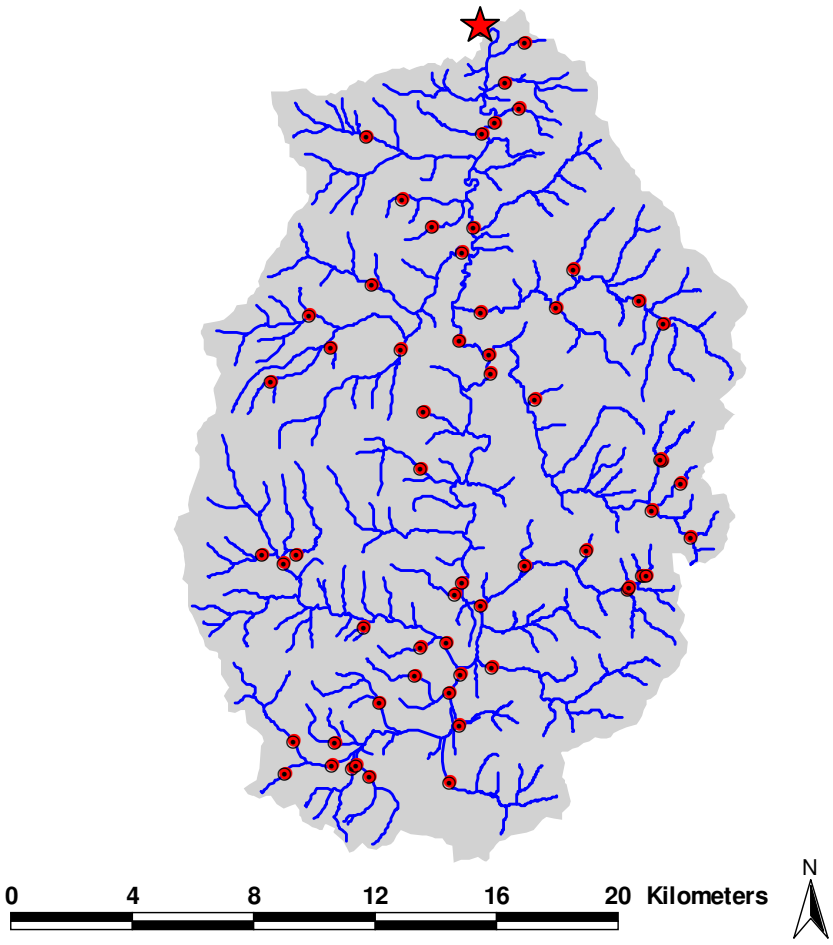

Figure 3.2: Map of the Little Tennessee River catchment, North Carolina. Red circles represent synoptic sampling locations. Star represents outlet.

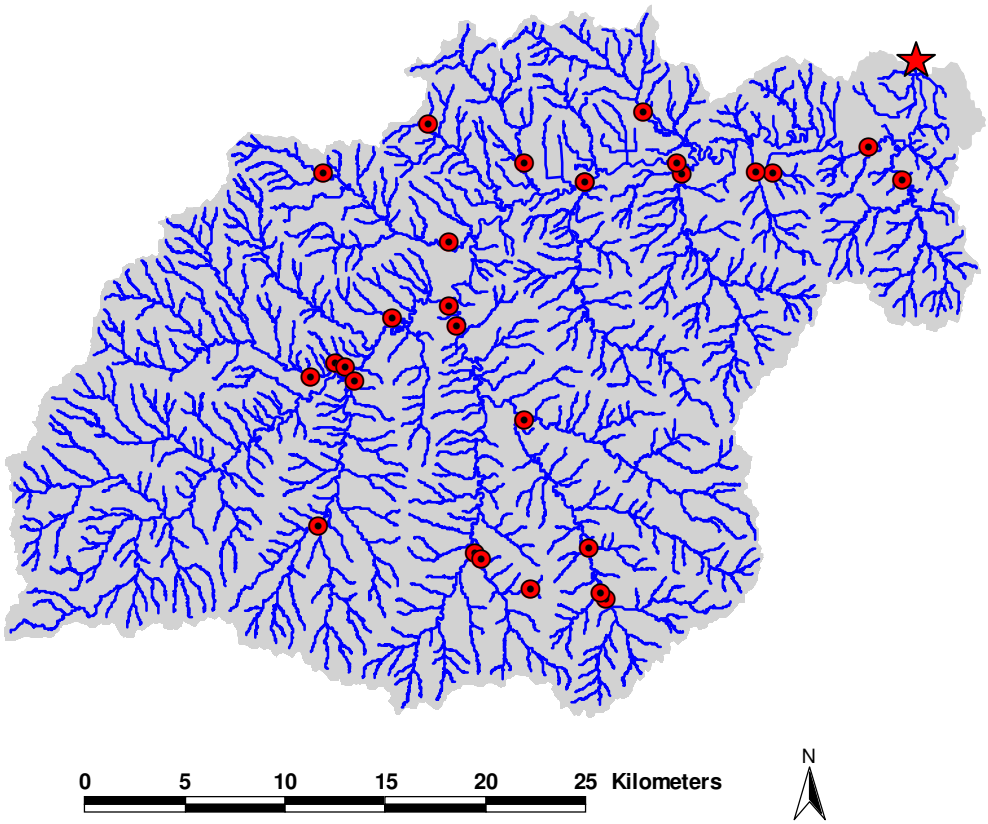

Figure 3.3: Map of the Mill Creek catchment, Kansas. Red circles represent synoptic sampling locations. Star represents outlet.

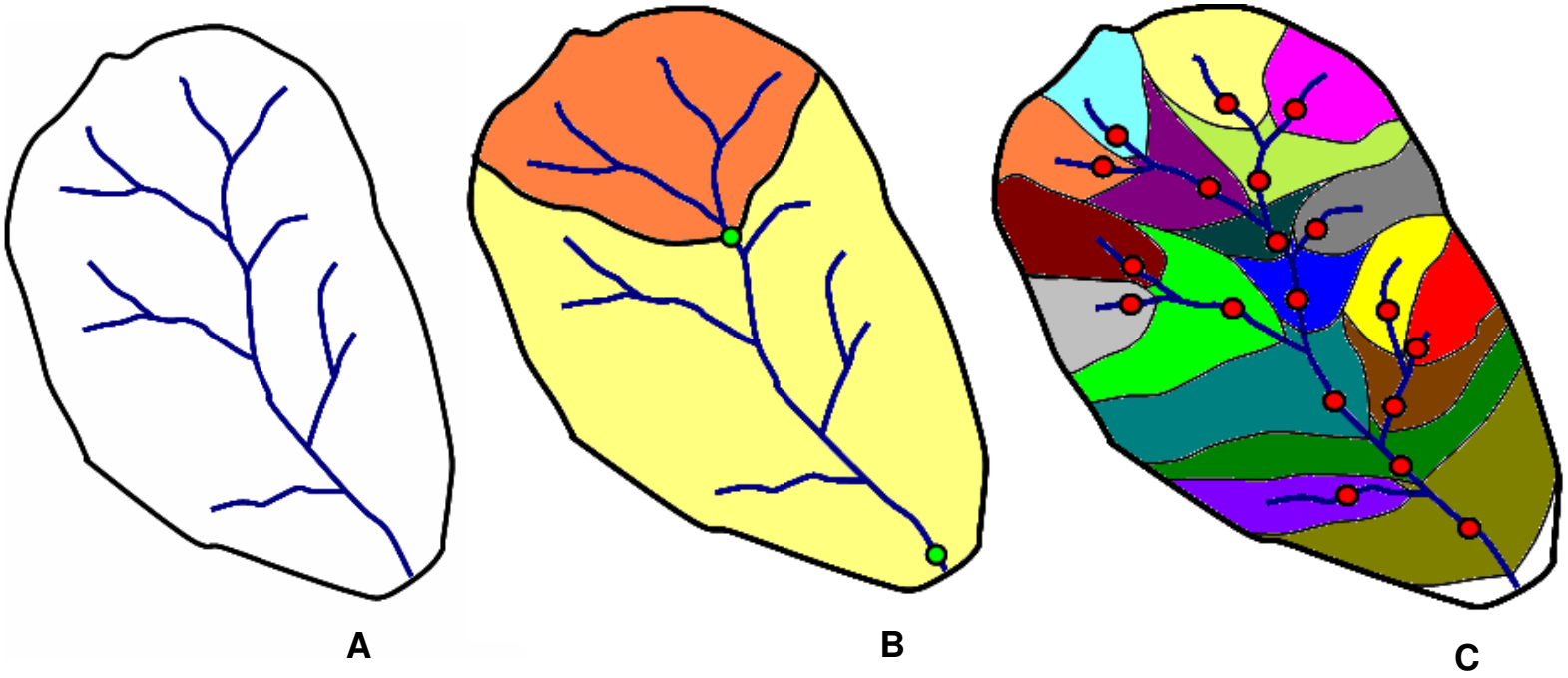

Figure 3.4: Example of watershed area, contributing drainage area and adjacent area. A) Watershed area for the entire network. B) Contributing drainage areas for each sampling location (represented by green circles). Stream segments within the same contributing areas have equal NO_3-N loading rates. C) Adjacent drainage areas for each stream reach.

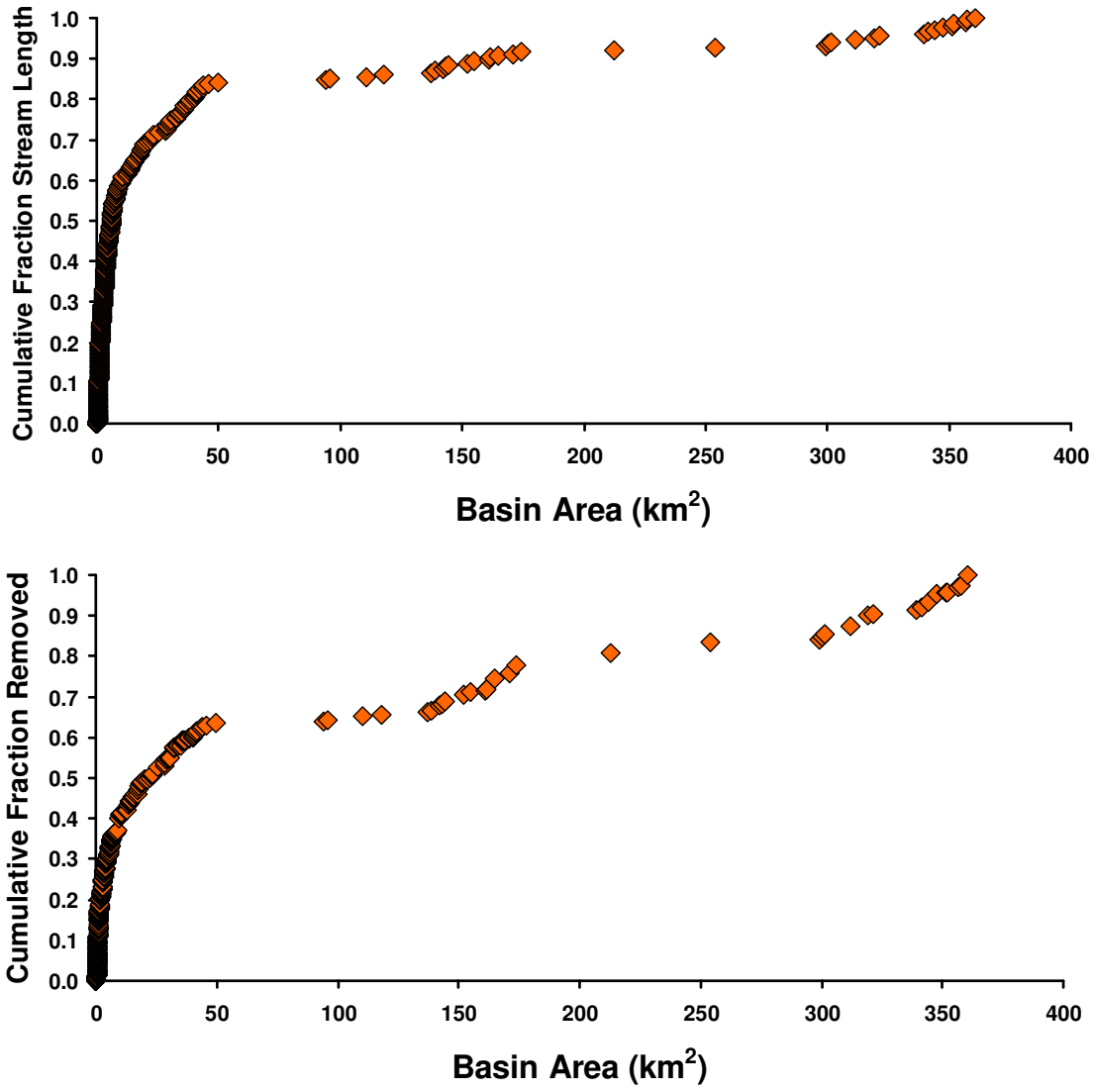

Figure 3.5: A) Cumulative fraction of stream length versus basin area and B) cumulative fraction of NO_3-N removed versus basin area for the Little Tennessee River, North Carolina for 2004.

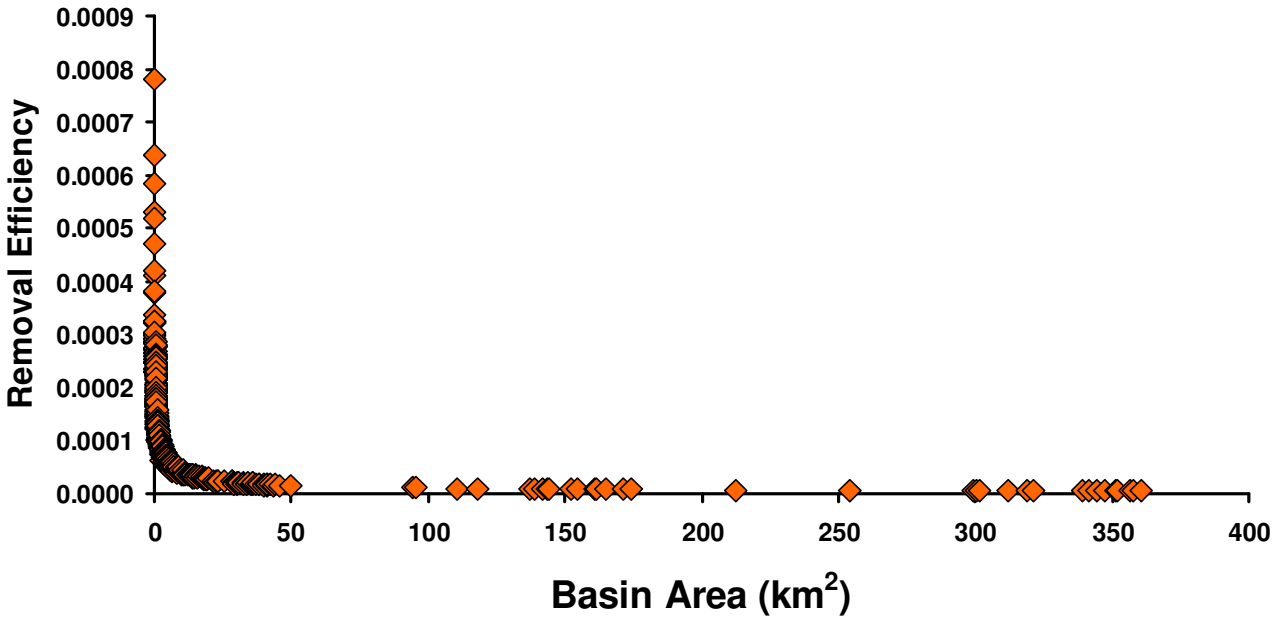

Figure 3.6: Removal efficiency for the North Carolina stream network for 2004. Removal efficiency represents the fraction of direct NO_3-N inputs to a stream segment, including input from upstream segments and input from the landscape, removed per meter of stream segment.

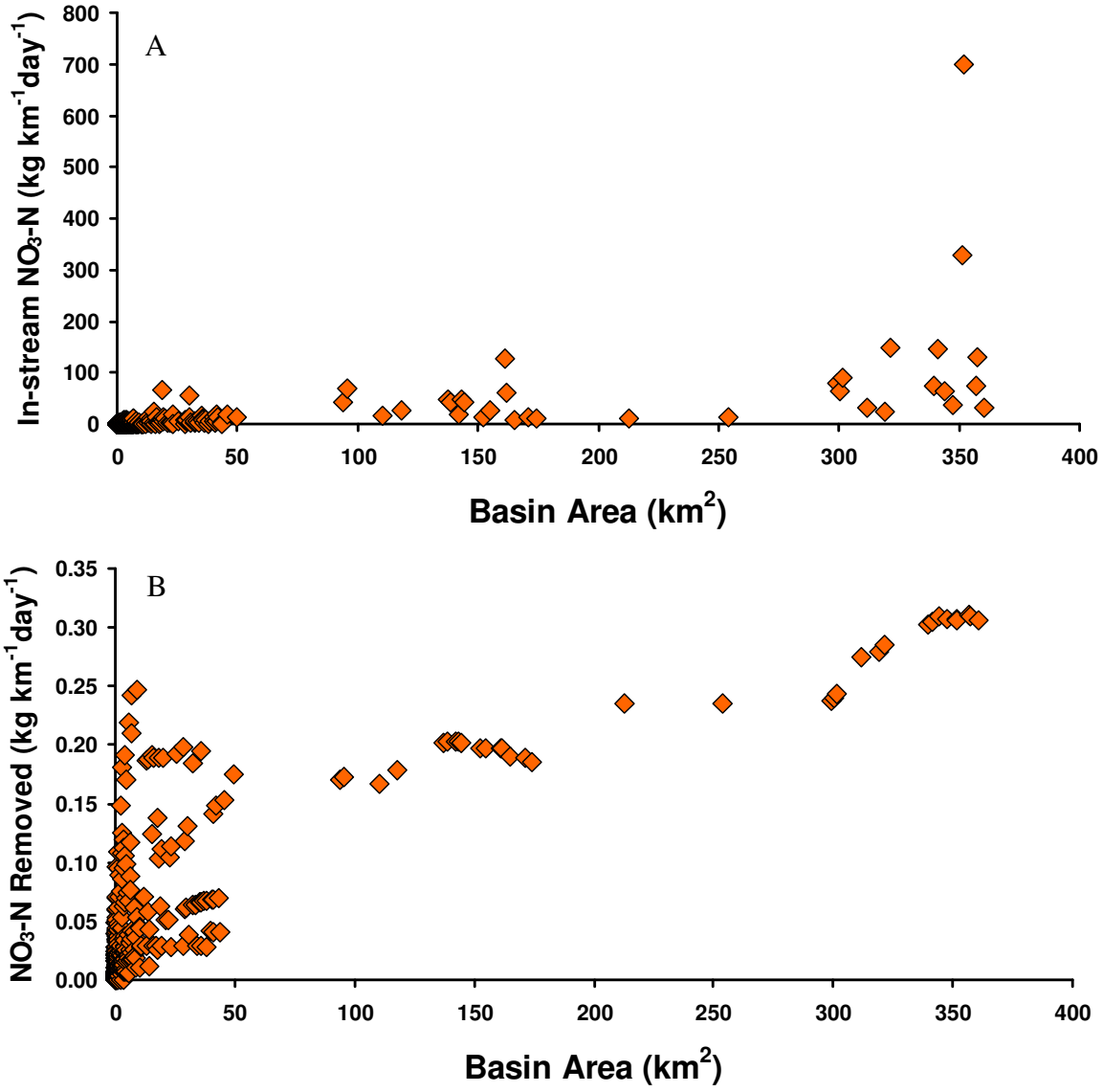

Figure 3.7: A) In-stream NO_3-N mass available per unit length versus basin area, and B) In-stream NO_3-N mass removed per unit length versus basin area for the Little Tennessee River in North Carolina for 2004.

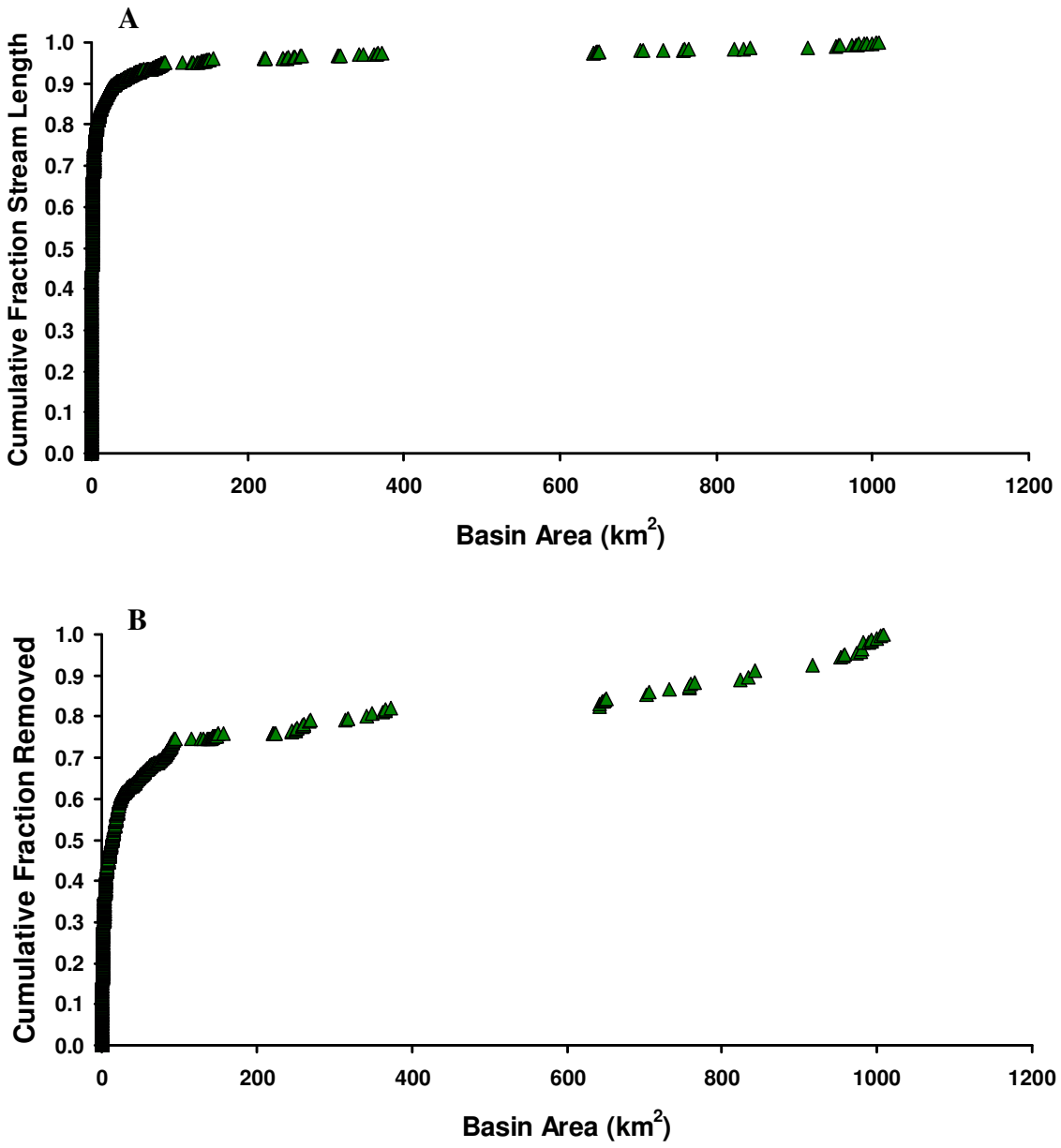

Figure 3.8: A) Cumulative fraction of stream length versus basin area and B) cumulative fraction of NO_3-N removed versus basin area for the Mill Creek, Kansas for 2004.

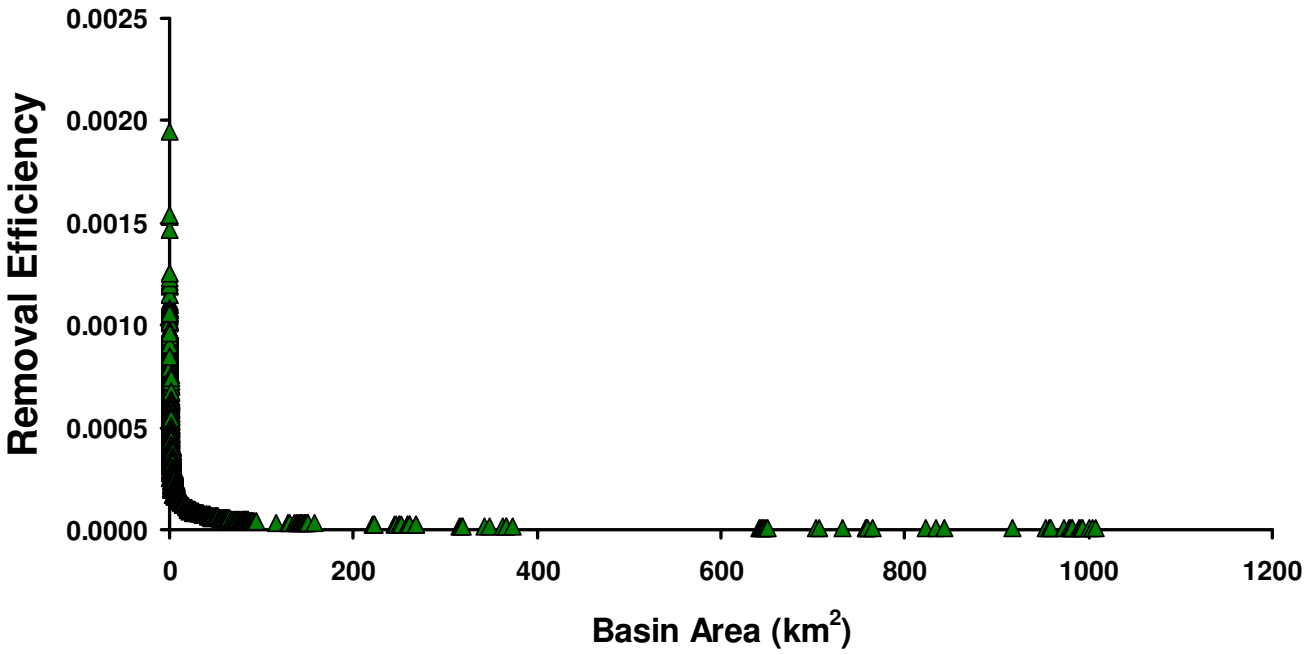

Figure 3.9: Removal efficiency for the Kansas stream network for 2004.

Removal efficiency represents the fraction of direct NO_3-N inputs to a stream segment, including input from upstream segments and input from the landscape, removed per meter of stream segment.

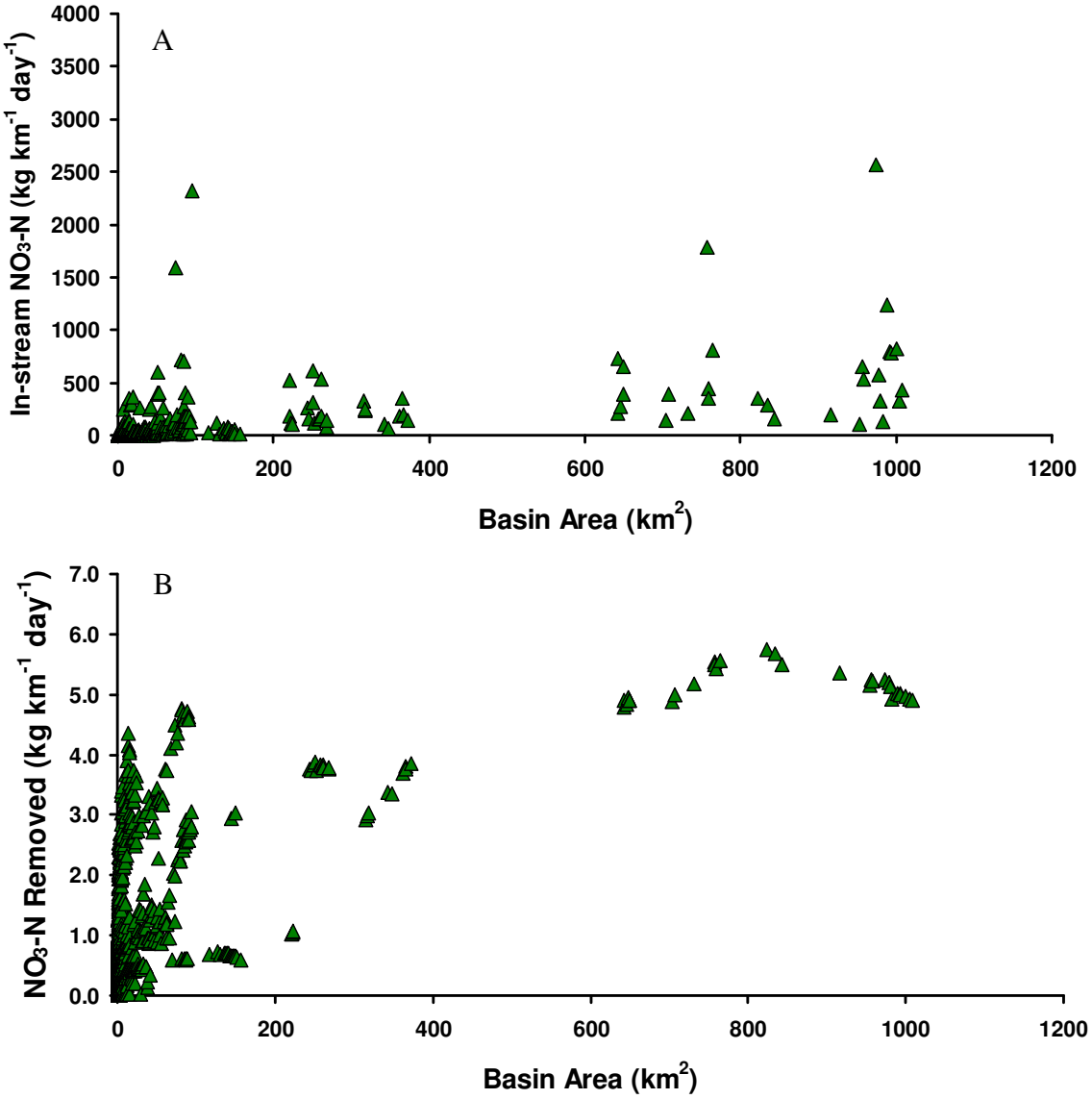

Figure 3.10: A) In-stream NO_3-N mass available per unit length versus basin area, and B) In-stream NO_3-N mass removed per unit length versus basin area for the Mill Creek, Kansas for 2004.

CHAPTER 4

CONCLUSIONS

Streams play an important role in landscape nitrogen (N) dynamics because they act to store, transport and transform N from uplands to coastal areas, where effects such as eutrophication and hypoxia have been well documented (e.g., Turner et al. 2005). In order to more accurately predict the downstream transport of nutrients and their effects on receiving water bodies, we must have a mechanistic understanding of the processes that control in-stream transport. We must be able to link small scale mechanistic studies (e.g., Mulholland et al. 2004) to large-scale statistical studies (e.g., Alexander et al. 2000). This research was a first attempt to scale up reach-scale measurements of NO_3-N uptake across biomes to stream networks to identify landscape-scale drivers of stream network NO_3-N dynamics.

In Chapter 2, I developed a simulation model of stream network NO_3-N loading, transport, and processing based on common conceptualizations of stream networks. I used this model as a frame of reference to compare differences in drivers of NO_3-N dynamics across biomes. My simulation model was insufficient to scale up reach-scale measurements of biological NO_3-N uptake in five out of seven stream networks in this study, revealing differences across biomes in the drivers of network-scale patterns of NO_3-N dynamics. Where the model adequately described NO_3-N dynamics, I found that uptake was a much stronger driver of stream network patterns of NO_3-N in the Kansas stream network than in North Carolina stream network because the North Carolina stream network removed a much smaller proportion of its NO_3-N inputs than did the Kansas stream network. Where the simulation model was insufficient to describe network-scale NO_3-N dynamics, I identified biological, hydrologic and

geomorphologic aspects of each stream network not incorporated into the simulation model to help explain additional drivers of NO_3-N dynamics across these catchments. The analyses of each catchment revealed different landscape drivers of NO_3-N dynamics for each stream network. The following aspects of stream networks were strong drivers of NO_3-N dynamics in different catchments: 1) the spatial distribution of anthropogenic sources of N to streams; 2) the influence of multiple hydrologic pathways of nutrient delivery to streams (e.g., tile drainage systems); 3) the relative roles of the hyporheic zone versus the stream bed in nutrient processing; 4) discontinuities and abrupt changes in downstream channel geometry and flow because of urbanization (channalization) and natural features (wetlands); and 5) variation in biological uptake across stream networks. This suggests that a more complete understanding of stream networks that encompasses hydrologic, geomorphologic and chemical drivers of in-stream processes must be incorporated into the core conceptual model of stream network loading, transport and processing in order to reliably scale up site-level measurements.

In Chapter 3, I used model results from Chapter 2 to analyze differences in network scale removal among stream networks and sampling years and to estimate the distribution of in-stream NO_3-N removal among streams of different sizes in each of the two networks that fit the simulation model well, Little Tennessee River in North Carolina and Mill Creek in Kansas. Stream network removal of NO_3-N was substantial across the two catchments in North Carolina and Kansas, but catchment-scale in-stream removal varied between years and between the two stream networks. The observed inter-annual and inter-catchment variation was most likely due to one or a combination of differences in channel geometry, stream length, flow conditions and biological activity. These catchment-scale variables should be useful for predicting network-scale potential of in-stream removal across physiographic regions.

In Chapter 3, I also found that small and large streams both play important roles in stream network-scale NO_3-N removal. Small streams removed the majority of in-stream NO_3-N removal because they are abundant and efficient at removing NO_3-N. Although large stream segments removed a greater mass of NO_3-N per unit length, small stream segments removed more NO_3-N cumulatively. The spatial patterns of removal were similar to patterns observed in previous studies; however, findings here underscore the importance of the cumulative effects of very small streams in network-scale N dynamics.

The stream networks in this study represented a wide range of naturally occurring variation in hydrology, geomorphology and biology. However, my conceptual model (and hence similar common conceptualizations of stream networks) did not encompass the range of possible conditions represented by stream networks. This study highlights the reality that different streams have very different hydrologic, geomorphologic and biological drivers of in-stream processing, and that integrating a more diverse array of possible drivers into our conceptual thinking about streams at the landscape scale will improve our ability to understand, explain and predict landscape-scale nutrient processing. For any stream network, considering the unique distribution of N in streams, channel geomorphology, residence time (hydrology), biological activity, and network topology (sensu, Poole 2002) will increase our understanding of stream N dynamics on a landscape-scale, which is a key to understanding N export from a diversity of landscapes through rivers to estuaries and coastal ecosystems.

References

Alexander, R. B., R. A. Smith, and G. E. Schwarz. 2000. Effect of stream channel size on the delivery of nitrogen to the Gulf of Mexico. Nature **403**:758-761.

Mulholland, P. J., H. M. Valett, J. R. Webster, S. A. Thomas, L. W. Cooper, S. K. Hamilton, and B. J. Peterson. 2004. Stream denitrification and total nitrate uptake rates measured using a field 15N tracer addition approach Limnology and Oceanography **49**:809-820.

Poole, G. C. 2002. Fluvial landscape ecology: addressing uniqueness within the river discontinuum. Freshwater Biology **47**:641-660.

Turner, R. E., N. N. Rabalais, E. M. Swenson, M. Kasprzak, and T. Romaire. 2005. Summer hypoxia in the northern Gulf of Mexico and its prediction from 1978 to 1995. Marine Environmental Research **59**:65-77.

APPENDICES

Appendix A, Table 1: Sampling locations in the Mill Creek watershed, Kansas. Datum: NAD27

Site ID	X-Coordinate	Y-Coordinate	Location
KS-01	-96.273	38.8902	s branch mill e
KS-02	-96.2697	38.8872	s branch mill w
KS-03	-96.2416	38.873	s branch mill ww
KS-04	-96.1991	38.8673	e branch mill below waubunsee
KS-05	-96.202	38.8701	e branch mill w
KS-06	-96.3537	39.0628	hendricks cr up
KS-07	-96.2925	39.0834	pretty cr
KS-08	-96.2829	39.0305	hendricks cr down
KS-09	-96.3167	38.9969	unamed branch near alma
KS-10	-96.3501	38.9776	w mill above IL
KS-11	-96.3442	38.9757	lower IL
KS-12	-96.3648	38.9712	spring cr
KS-13	-96.0204	39.0519	dry cr
KS-14	-96.0392	39.0668	lower mill cr
KS-15	-96.0951	39.0576	stuckys
KS-16	-96.1046	39.0577	dog cr
KS-17	-96.1474	39.0577	snokomo cr
KS-18	-96.1686	39.0861	mulberry cr
KS-19	-96.1498	39.0631	mill cr paxico
KS-20	-96.2381	39.0651	pawpaw cr
KS-21	-96.2793	38.9927	mill cr alendorf
KS-22	-96.2835	39.0014	lower w branch mill cr
KS-23	-96.3627	38.9041	upper IL
KS-24	-96.2077	38.8906	mill cr at Hesdale
KS-25	-96.2428	38.9506	nehring cr
KS-26	-96.2023	39.0559	kuenzli cr
KS-27	-96.2027	39.0556	mill cr above kuenzli
KS-28	-96.3396	38.9689	

Appendix A, Table 2: Sampling locations in the Ipswich River watershed, Massachusetts. Datum: NAD27

Site ID	X-Coordinate	Y-Coordinate	Location
BB-PR	-71.04263	42.6335	Pond Rd.
BBYr1	-71.00337	42.61726	Peabody Rd. at Boston Brook
BBYr2	-71.094	42.55856	Bear Brook at Haverill
FB-BV	-71.02798	42.66502	Fish Brook at Brookview
FB-LOCK	-70.98917	42.64526	Fish Brook at Lockwood Rd.
FB-WA	-70.97365	42.63051	Fish Brook at Washington St.
HB-01Yr1	-70.91704	42.65501	Howlett Brook at Ipswich Rd.
HB-01Yr2	-70.93103	42.66023	Howlett Brook at Rt. 1
HB-DR	-70.98041	42.67426	Howlett Br., off Depot Rd, Boxforf
IP00	-71.14364	42.55376	Woburn St. Bridge (downstream)
IP01	-71.11067	42.56117	Mill St. Bridge
IP04	-71.06973	42.57637	Rt. 62 bridge
IP04Yr2	-71.07308	42.57463	
IP06	-71.02923	42.56981	Boston St. Bridge
IP10	-70.99655	42.59574	Rt. 62 bridge
IP20	-70.89073	42.65893	Winthrop St. Bridge
IP24	-70.83826	42.67487	Sylvania Dam at Rt. 1A
IR-97	-70.93528	42.62384	Ipswich River at Rt. 97 (High St.)
IS_102	-71.18372	42.52422	Sawmill Brook at Mill St.
IS_104	-71.20841	42.53919	Last Year's 15N addition
IS_110	-71.13613	42.54524	Kilmarnock St.
IS_115	-71.09828	42.5511	Eastway west of Haverill St.
IS_118	-71.07422	42.58136	Duane Dr.
IS_120	-71.00571	42.57145	River St.
IS_127	-71.06287	42.60094	Marblehead Rd.
IS_128	-71.09412	42.59313	Jenkins Rd.
IS_129	-71.08954	42.60446	
IS_131	-71.10596	42.62909	Salem St.
IS_132	-71.0985	42.63195	Gray Rd.
IS_135	-71.10696	42.66384	Chestnut St.
IS_141	-71.01277	42.65686	
IS_142	-70.99106	42.64494	Middleton Rd.
IS_143	-70.99223	42.64224	Yr 2 Forest 15N addition
IS_145	-70.99295	42.65935	
IS_148	-70.94563	42.67182	Boxford Rd off of Linebrook Rd.
IS_161	-70.88725	42.61643	Highland St.
IS_163	-70.95971	42.59573	
IS_166	-70.84374	42.58127	Essex St.
IS_167	-70.82895	42.5855	Hull St.
IS_170	-70.84323	42.64725	Long Causeway Brook-- Appleton
IS_172	-70.84323	42.64725	Fellows Rd.
LB-62	-71.18308	42.56587	Lubber's Brook at Rt. 62

Appendix A, Table 2 (continued)

Site ID	X-Coordinate	Y-Coordinate	Location
LBYr1	-70.83649	42.65621	Lubbers Brook at Glen Rd. or Harn St.
LBYr2	-71.14363	42.55387	Lubber's Brook before enters Ipswich R.
LMB	-70.84572	42.65225	Long Meadow Brook Yr 2 Ag #2 15N addition
MB	-71.15806	42.57009	Martin's Brook before enters Ipswich-- Park St.
MB-PR	-71.10142	42.57157	Martins Brook of Parker Rd, Andover
MB-SAL	-71.09897	42.61155	Martin's Brook at Salem St. (Rt. 62)
MMB-38	-71.15653	42.55282	Maple Meadow Brook at Rt. 38
MMB-CHEST	-71.16139	42.53605	
MMBYr1	-71.13904	42.57973	Maple Meadow Brook at Wildwood
MMBYr2	-71.14363	42.55387	Maple Meadow Brook before Ipswich (same stop as
MPO	-71.17232	42.52722	Mill St. draining Mill Pond
MR-1A	-71.00126	42.60951	Miles River at Rt. 1A
MR-BR	-70.8515	42.61634	Miles River at Bridge St.
MR-LR	-70.87252	42.58979	drainage of Longham Reservoir
NB	-71.00352	42.55389	Norris Brook at Russell St.

Appendix A, Table 3: Sampling locations in the Rabbit River watershed, Michigan.
Datum: NAD27

Site ID	X-Coordinate	Y-Coordinate	Location
MI-01	-85.663	42.74928	Upper Little Rabbit, Allegan County (Hwy A45, S of 146th St)
MI-02	-85.8631	42.71007	Little Rabbit at mouth, Allegan County (140th Ave, W of 32nd St)
MI-03	-85.8006	42.75409	Trib to Little Rabbit, Allegan County (32nd St., S of 142nd Ave)
MI-04	-85.8598	42.71941	Trib to Little Rabbit, Allegan County (142nd Ave, E of 32nd St.)
MI-05	-85.8562	42.72452	Trib to Little Rabbit, Allegan County (143rd Ave., E of 32nd St.)
MI-06	-85.8505	42.73181	Trib to Ritz Dr., Allegan County (146th Ave, E. of 30th)
MI-07	-85.8343	42.75368	New Salem, Allegan County (146th Ave, W. of 26th)
MI-08	-85.7742	42.7544	near New Salem, Allegan County (146th Ave, E. of 24th St.)
MI-09	-85.7718	42.75446	near New Salem, Allegan County (147th Ave, W. of 22nd St.)
MI-10	-85.7859	42.73975	Trib to Little Rabbit, Allegan County (144th Ave, W. of 24th St.)
MI-11	-85.8091	42.73949	Trib to Little Rabbit, Allegan County (144th Ave, W. of 26th St.)
MI-12	-85.8352	42.73191	Ritz Drain, Allegan County (144th Ave, E. of 30th St.)
MI-13	-85.8314	42.7393	Ritz Drain, Allegan County (143 Ave., E. of 30th St.)
MI-14	-85.8402	42.72242	Little Rabbit River, Allegan County (142nd Ave, E of 30th St.)
MI-15	-85.8011	42.72995	Trib to Little Rabbit, Allegan County (26th St., N of 142nd Ave.)
MI-16	-85.7815	42.73253	Little Rabbit River, Allegan County (24th St, S. of 144th Ave.)
MI-17	-85.7813	42.72881	Trib to Little Rabbit, Allegan County (24th St, N. of 142nd Ave.)
MI-18	-85.7602	42.71795	Trib to Little Rabbit, Allegan County (141st. Ave, W. of 21st St.)
MI-19	-85.7615	42.73257	Little Rabbit River, Allegan County (22nd St., S. of 144th Ave.)
MI-20	-85.7516	42.73643	Red Run, Allegan County (21st St., S. of 144th Ave.)
MI-21	-85.753	42.73991	Dorr and Byron Cr., Allegan County (144th Ave., W. of 21st St.)
MI-22	-85.7507	42.76825	Trib to Dorr and Byron, Kent County (108th, E. of Homerich Rd.)
MI-23	-85.7421	42.77998	Trib to Dorr and Byron Cr., Kent County (Ivanrest Rd., S. of 100th)
MI-24	-85.7228	42.78094	Dorr and Byron Cr., Kent County (Byron Center Ave., S. of 100th)
MI-25	-85.7373	42.75434	Dorr and Byron Cr., Allegan County (146th Ave., W. of 18th St.)
MI-26	-85.7222	42.75333	Trib to Dorr and Byron Cr., Allegan County (18th St., S. of 146th)
MI-27	-85.7222	42.74725	Trib to Dorr and Byron Cr., Allegan County (18th St., N. of 144th)
MI-28	-85.722	42.74134	Trib to Dorr and Byron Cr., Allegan County (18th St., N. of 144th)
MI-29	-85.7417	42.73885	Trib to Dorr and Byron Cr., Allegan County (20th St., S. of 144th)
MI-30	-85.7418	42.73295	Red Run, Allegan County (20th St., N. of 142nd Ave.)
MI-31	-85.7219	42.72774	Wolf Drain, Allegan County (18th St., N. of 142nd Ave.)
MI-32	-85.7217	42.71465	Red Run, Allegan County (18th St., S. of 142nd Ave.)
MI-33	-85.9525	42.61559	Bear Creek, Allegan County (127th Ave., E. of Hwy 40)
MI-34	-85.919	42.6228	Trib to Bear Creek, Allegan County (38th St., S. of 128th Ave.)
MI-35	-85.9187	42.62171	Bear Creek, Allegan County(128th Ave., W. of 38th St.)
MI-36	-85.7284	42.71076	Trib to Red Run, Allegan County(140th Ave, W of 18th St.)
MI-37	-85.702	42.71212	Red Run, Allegan County (16th St., N. of 140th Ave.)
MI-38	-85.6886	42.72492	Red Run, Allegan County (142nd Ave., W of 14th St.)
MI-39	-85.6824	42.72172	Trib to Red Run, Allegan County (14th St., S. of 142nd Ave.)
MI-40	-85.6826	42.73407	Trib to Red Run, Allegan County (14th St., N. of 142nd Ave.)
MI-41	-85.6827	42.75094	Trib to Red Run, Allegan County (14th St., S. of 146th Ave.)
MI-42	-85.6752	42.58437	Miller Creek, Allegan County (122nd Ave, E of 14th St.)
MI-43	-85.7021	42.61738	Miller Creek, Allegan County (16th St., N. of 126th Ave.)
MI-44	-85.7147	42.62354	Pierce Drain, Allegan County (128th Ave., E. of 18th St.)

Appendix A, Table 3 (continued)

Site ID	X-Coordinate	Y-Coordinate	Location
MI-45	-85.7414	42.6219	Trib to Pierce Drain, Allegan County (20th St., S of 128th Ave.)
MI-46	-85.7633	42.62408	Bear Creek, Allegan County (128th Ave, W. of 22nd. St.)
MI-47	-85.7823	42.61972	Weick Drain, Allegan County (24th St., S of 128th Ave.)
MI-48	-85.8008	42.60798	Trib to Bear Creek, Allegan County (26th St., S of 127th Ave.)
MI-49	-85.8225	42.6886	Trib to Monterey Lake Outflow, Allegan County (137th Ave.)
MI-50	-85.8399	42.70348	Rabbit River, Allegan County (30th St., N of 138th Ave.)
MI-51	-85.8154	42.6958	Trib to Monterey Lake Outflow, Allegan County (138th Ave.)
MI-52	-85.8	42.69276	Rabbit River, Allegan County (26th St., N. of 138th Ave.)
MI-53	-85.7661	42.68164	Rabbit River, Allegan County (136th Ave., W. of 22nd St.)
MI-54	-85.7417	42.65817	Trib to Rabbit River, Allegan County (20th St., S. of 133rd Ave.)
MI-55	-85.7551	42.6386	Rabbit River, Allegan County (130th Ave., E. of 21st St.)
MI-56	-85.7586	42.63864	Bear Creek, Allegan County (130th Ave., E. of 22nd St.)
MI-57	-85.7278	42.63861	Rabbit River, Allegan County (120th Ave., W of 18th St.)
MI-58	-85.7122	42.64844	Buskirk Cr., Allegan County (17th St., S of 132nd Ave.)
MI-59	-85.6824	42.65796	Selkirk Cr,, Allegan County (14th St., N of 132nd Ave.)
MI-60	-85.6822	42.67433	Rabbit River, Allegan County (14th St., N of 135th Ave.)
MI-61	-85.662	42.67122	Mineral Springs Drain, Allegan County (12th St., S of 135th Av
MI-62	-85.6089	42.66285	Rabbit River, Allegan County (133rd Ave., E. of 7th St.)
MI-63	-85.6037	42.65885	Trib to Rabbit River, Allegan County (6th St., S. of 133rd Ave.)
MI-64	-85.6432	42.6854	Rabbit River, Allegan County (10th St., S of 137th Ave.)
MI-65	-85.6543	42.71055	Green Lake Cr., Allegan County (140th Ave., W. of Division St.)
MI-66	-85.6336	42.70667	Trib to Green Lake Cr., Allegan County (9th St., S. of 140th)
MI-67	-85.6335	42.70197	Haney Drain, Allegan County (9th St., N. of 139th Ave.)
MI-68	-85.5997	42.74295	Green Lake Cr., Allegan County (Kalamazoo St., N. of 144th)
MI-69	-85.6379	42.73947	Green Lake Cr., Allegan County (144th Ave., W. of 9th St.)
MI-70	-85.682	42.73377	Red Run, Allegan County (14th St., S. of 144th Ave.)
MI-71	-85.8866	42.81127	Trib to Black Creek, Ottawa County (Byron St., E. of 40th Ave.)
MI-72	-85.8278	42.78217	Black Cr., Ottawa County (Adams St., E. of 20th Ave.)
MI-73	-85.8416	42.77902	Shoemaker Dr., Ottawa County (24th Ave., S. of Adams St.)
MI-74	-85.8612	42.7716	Black Cr., Ottawa County (32nd Ave., S of Mason St.)
MI-75	-85.8764	42.78213	Trib to Black Creek, Ottawa County (Adams St., W. of 40th Ave.)
MI-76	-85.8934	42.73866	Black Cr., Allegan County (144th Ave., W. of 34th St.)
MI-77	-85.9003	42.7022	Black Cr., Allegan County (139th Ave., W. of 37th St.)
MI-78	-85.879	42.70567	Rabbit River, Allegan County (34th St., S. of 140th Ave.)
MI-79	-85.898	42.68141	Miller Creek, Allegan County (36th St., N. of 136th Ave.)
MI-80	-85.9372	42.68073	Silver Creek, Allegan County (136th Ave., E. of 41st St.)
MI-81	-85.9178	42.68804	Rabbit River, Allegan County (38th St., N. of 136th Ave.)
MI-82	-85.9522	42.69559	Trib to Rabbit River, Allegan County (138th Ave., W. of 40th St.)
MI-83	-85.9558	42.69562	Trib to Rabbit River, Allegan County (138th Ave., E. of 42nd St.)
MI-84	-86.0168	42.6821	Trib to Rabbit River, Allegan County (136th Ave., W. of 48th St.)
MI-85	-86.0723	42.66075	Rabbit River, Allegan County (133rd Ave., E. of 54th St.)
MI-86	-86.0037	42.67528	Rabbit River, Allegan County (Hwy 40 in Hamilton)
MI-87	-85.9893	42.67358	Trib to Rabbit River, Allegan County (135th Ave., E. of Hwy 40)

Appendix A, Table 4: Sampling locations in the Little Tennessee River, North Carolina. Datum: NAD27

Site ID	X-Coordinate	Y-Coordinate	Location
BTY-1	-83.3873	34.96698	Betty Creek, Betty Creek Outlet
BTY-2	-83.3965	34.96529	Betty Creek, Sutton Branch
BTY-3	-83.4172	34.97096	Betty Creek, Ledford Branch
BTY-4	-83.4547	34.99166	Betty Creek, Messer's Creek
BTY-5	-83.447	34.98947	Betty Creek, Upper Betty
BTY-6	-83.4423	34.99201	Betty Creek, Barkers Creek
CWT-1	-83.385	35.08335	Coweeta, Coweeta Outlet
CWT-2	-83.4066	35.05388	Coweeta, Dryman Fork
CWT-3	-83.4317	35.0539	Coweeta, Hugh White Creek
CWT-4	-83.453	35.04341	Coweeta, Upper Ball Creek
CWT-5	-83.4396	35.06359	Coweeta, Big Hurricane Branch
CWT-6	-83.4173	35.07283	Coweeta, Shope Creek
DMI-1	-83.3596	34.99052	Darnell-Mud Interbasin, Mud Creek Trib A
DMI-2	-83.3375	34.99544	Darnell-Mud Interbasin, Mud Creek Trib B
DMI-3	-83.3226	34.98393	Darnell-Mud Interbasin, S. Fork of Mud Creek
DMI-4A	-83.3159	34.98836	Darnell-Mud Interbasin, N. Fork Mud Cr, above pond
DMI-4B	-83.3169	34.98802	Darnell-Mud Interbasin, N. Fork Mud Cr, below pond
DMI-4C	-83.3173	34.98821	Darnell-Mud Interbasin, trib to N. Fork Mud, hole #4
DMI-4D	-83.3219	34.98486	Darnell-Mud Interbasin, N. Fork Mud Creek at Range
DMI-5	-83.3705	34.95985	Darnell-Mud Interbasin, Darnell Creek
DMI-6	-83.3975	35.03546	Darnell-Mud Interbasin, Bradley Branch
DMI-7	-83.3982	35.0184	Darnell-Mud Interbasin, Mulberry Creek
DMI-8	-83.3845	34.98131	Darnell-Mud Interbasin, Lamb Creek
DMI-9	-83.3756	34.97828	Darnell-Mud Interbasin, Mouth of Mud Creek
HLT-1	-83.3822	34.94234	Headwaters Upper Little T, Blacks Branch
HLT-10	-83.4419	34.93653	Headwaters Upper Little T, Keener Creek
HLT-11	-83.4202	34.92904	Headwaters Upper Little T, Pitt Branch
HLT-12	-83.4186	34.92986	Headwaters Upper Little T, Taylor Creek down
HLT-2	-83.3983	34.9569	Headwaters Upper Little T, Jerry Branch up
HLT-3	-83.3852	34.92536	Headwaters Upper Little T, Blacks Creek
HLT-4	-83.414	34.92642	Headwaters Upper Little T, Taylor Creek up
HLT-5	-83.4277	34.92964	Headwater Upper Little TN
HLT-6	-83.4444	34.92686	Headwaters Upper Little T, Billy Creek
HLT-7	-83.3862	34.95224	Headwaters Upper Little T, Jerry Branch down
HLT-8	-83.4112	34.94859	Headwaters Upper Little T, Rickham Creek
HLT-9	-83.4268	34.93622	Headwaters Upper Little T, Wolf Creek Church
LLT-1	-83.3641	35.14634	Lower Upper Little T, North of Clark Chapel
LLT-2	-83.3712	35.1342	Lower Upper Little T, Hayes Mill Creek
LLT-3	-83.3655	35.12675	Lower Upper Little T, Fulcher Branch
LLT-4	-83.379	35.11848	Lower Upper Little T, Dowdle Branch
LLT-5	-83.4206	35.11699	Lower Upper Little T, N. Fork Skeenah
LLT-6	-83.4071	35.09853	Lower Upper Little T, Bates Branch
LLT-7	-83.3961	35.09069	Lower Upper Little T, Hog Lot Branch
MDL-1	-83.3743	35.05271	Outlet of Middle Creek

Appendix A, Table 4 (continued)

Site ID	X-Coordinate	Y-Coordinate	Location
MDL-2	-83.3573	35.0403	Middle Creek, Smart Branch
MDL-3	-83.314	35.00795	Middle Creek, Lower Watkins Creek
MDL-4	-83.2999	34.99991	Middle Creek, Upper Watkins Creek
MDL-5	-83.3041	35.01594	Middle Creek, Jake Branch
MDL-6	-83.3108	35.02288	East Fork Middle Creek
MDL-7	-83.3116	35.0231	West Fork Middle Creek
MST-1	-83.3797	35.14983	Main Stem, Little T Prentiss Gauge
MST-2	-83.3743	35.12204	Main Stem, Prentiss Bridge
MST-3	-83.3813	35.09067	Main Stem, Riverside Park
MST-4	-83.3855	35.05711	Main Stem, Little T at Otto
MST-5	-83.3736	35.04749	Main Stem, Little T:DMI outlet
MST-6	-83.3822	34.98479	Main Stem at Route 246
MST-7	-83.3822	34.95757	Main Stem, Fruit-o-loom Factory
PSO-1A	-83.4027	35.17825	Parasynoptic, Crawford Br: Hemlock Hills
PSO-1B	-83.3893	35.17984	Parasynoptic, Crawford Br: Frank.Mem Park
PSO-1C	-83.3839	35.17899	Parasynoptic, Crawford Br: Mi Casa
PSO-1D	-83.3753	35.18421	Parasynoptic, Crawford Br: Depot St
PSO-2	-83.4641	35.17201	Parasynoptic, Mill Creek
PSO-3	-83.3129	35.24716	Parasynoptic, Watauga Creek
TST-1	-83.3779	35.06539	Outlet of Tessentee Creek
TST-2	-83.3507	35.06752	Tessentee, Evans Creek
TST-3	-83.3447	35.07883	Tessentee, Buckeye Branch
TST-4	-83.3206	35.07029	Upper Tessentee Creek
TST-5	-83.3118	35.06347	Tessentee, Nichols Branch

Appendix A, Table 5: Sampling locations in the Tualatin River watershed, Oregon. Datum: NAD27

Site ID	X-Coordinate	Y-Coordinate	Location
3500035	-122.78281	45.42961	Unknown trib to Fanno at Walnut
3701002	-122.65341	45.33963	Tualatin R. at Weiss Br.
3701054	-122.69665	45.37967	Tualatin R. at Stafford
3701087	-122.75648	45.38625	Tualatin R. at Boones Ferry
3701165	-122.85069	45.3885	Tualatin R. at Elsner
3701271	-122.91964	45.41522	Tualatin R. at Scholls Ferry
3701333	-122.94922	45.44962	Tualatin R. at Farmington
3701391	-122.9502	45.48988	Tualatin R. at Rood
3701450	-122.99002	45.50023	Tualatin R. at Hwy. 219
3701528	-123.05482	45.50209	Tualatin R. at Golf Course
3701612	-123.12393	45.47487	Tualatin R. at Springhill
3701715	-123.23895	45.44392	Tualatin R. at Cherry Grove
3805017	-123.15377	45.45899	Scoggins Cr. at Hwy. 47
3805048	-123.19441	45.46671	Scoggins Cr. at Stimson
3810015	-123.10819	45.50683	Gales Cr. near new Hwy. 47
3815021	-123.00964	45.52015	Dairy Cr. at Hwy. 8
3816020	-123.0028	45.54265	McKay Cr. at Horn.
3820022	-122.93262	45.5084	Rock Cr. at Brookwood
3820047	-122.90786	45.52367	Rock Cr. at Quatama
3821008	-122.90865	45.51951	Beaverton Cr. at Beaman
3821050	-122.85075	45.50097	Beaverton Cr. at 170th
3824001	-122.88464	45.52095	Bronson Cr. at 205th
3824015	-122.87157	45.52997	Bronson Cr. at Walker
3824018	-122.86635	45.5324	Bronson Cr. at 185th
3824020	-122.85561	45.53727	Bronson Cr. at Bronson Park
3824032	-122.83829	45.5449	Bronson Cr. at WU
3824050	-122.82885	45.5472	Bronson Cr. at 143rd
3824072	-122.80687	45.55525	Bronson Cr. at Saltzman
3827014	-122.83128	45.47488	Johnson Cr. at Davis
3835020	-122.8555	45.37486	Chicken Cr. at Sch-Sher
3838001	-122.73853	45.38381	Nyberg Cr. at Brown
3840012	-122.75365	45.40353	Fanno Cr. at Durham
3840074	-122.79548	45.45694	Fanno Cr. at Tuckerwood
3840095	-122.77428	45.47074	Fanno Cr. near Allan
3844009	-122.79879	45.43522	Summer Cr. at 121st
3845014	-122.76255	45.45	Ash Cr. at Hemlock
3850006	-122.93347	45.52402	Dawson Cr. at Brookwood
3859010	-122.80262	45.56109	Bannister Cr. at 124th
BLED	-123.0659	45.5933	Bledsoe Cr. at Br. 1300
BUR	-122.95956	45.42593	Burris at hwy 219 br
BV0	-123.2892	45.67099	Beaver Cr. at Br. 1431
CC1	-123.20428	45.70759	Cummings Cr at Br 04953A
CLD	-122.93267	45.46306	Colden Cr. at Jacktown Rd
CLR	-123.23555	45.56933	Clear Cr. above weir
CSTN	-122.98347	45.4425	Christiansen Cr. at Hwy 219

Appendix A, Table 5 (continued)

Site ID	X-Coordinate	Y-Coordinate	Location
EFD1	-123.06996	45.72291	East Fk. Dairy Cr. at Br. 1366
EFD2	-123.02769	45.62177	East Fk Dairy Cr. at Br.1358
EFD3	-123.06271	45.59297	East Fk. Dairy Cr. at Br. 1299
EFD4	-123.06959	45.57874	East Fk Dairy Cr. at Br. 1302
FA1	-122.77307	45.47071	Fanno Cr. near Allen (USGS)
FA2	-122.79307	45.459	Fanno Cr. at Farmhouse
GA1	-123.21113	45.58403	Gales Cr. at Gales Creek
GA2	-123.36026	45.64275	Gales Cr. at Gales Cr. CG
GA3	-123.27456	45.65123	Gales Cr. at Glenwood
HTN	-122.93754	45.38577	Heaton Cr. at Mountain Home
ILR	-123.21586	45.58511	Iler Cr. at Soda Springs Rd.
LDV	-123.35755	45.6424	Lwr Divide Cr. at Gales Cr. CG
LOU_CNL	-123.13699	45.57009	Lousignant Canal at Br. 1585
MCF1	-122.95878	45.40515	McFee Cr. at Midway Bridge
MCF2	-122.93726	45.40102	McFee Cr. at Hwy 219
MK1	-122.9907	45.57261	McKay Cr. at Br. 1314
MK2	-122.97381	45.62538	McKay Cr. at Br. 1353
MK3	-122.98501	45.66243	McKay Creek at Br 1425
ROD	-123.19467	45.55114	Roderick Cr. above quarry
RR1	-123.2597	45.45149	Tualatin R. at Lees Falls gate
SFD	-123.10824	45.57361	South Fk. Dairy Cr.at Hwy 47
SFGA	-123.31912	45.64818	South Fk Gales Cr at Hwy 8
THM	-123.23378	45.5647	Thomas Cr. at Br 1273 nr Clear
UBV	-123.28591	45.69977	Beaver Cr. upper Timber Rd.
UNK_CNL	-123.13137	45.59595	NoName Canal at Br 1286
WFD	-123.11542	45.62435	West F. Dairy in Banks
WFD1	-123.11542	45.62435	West Fork Diary at Br. 02303
WFD2	-123.18268	45.67529	West Fork Dairy Cr at Br 02672
WRBL1	-122.955	45.56968	NoName at Meeks R.Br 1611
WRBL2	-122.93612	45.57923	Culvert 24-1 Groveland Rd.

Appendix A, Table 6: Sampling locations in the Rio Pierdas watershed, Puerto Rico. Datum: NAD27

Site ID	X-Coordinate	Y-Coordinate
SYN1-0	-66.0674	18.40195
SYN1-1	-66.0686	18.39641
SYN1-3	-66.0657	18.39272
SYN1-4	-66.0724	18.37234
SYN1-5	-66.071	18.38216
SYN1-7	-66.0701	18.38539
SYN2-0	-66.0473	18.37948
SYN2-1	-66.042	18.37065
SYN2-2	-66.0418	18.37118
SYN2-4	-66.0359	18.37117
SYN2-5	-66.0379	18.37259
SYN2-6	-66.0417	18.37748
SYN2-7	-66.0358	18.37164
SYN3-0	-66.0529	18.38129
SYN3-2	-66.0508	18.3795
SYN3-3	-66.0531	18.37665
SYN3-4	-66.0526	18.36501
SYN4-0	-66.0647	18.35966
SYN4-2	-66.0561	18.35643
SYN4-3	-66.0435	18.35464
SYN4-4	-66.05	18.35715
SYN4-5	-66.0561	18.35691
SYN5-0	-66.0571	18.34566
SYN5-1	-66.0515	18.34429
SYN5-2	-66.0563	18.3454
SYN5-4	-66.0588	18.32976
SYN5-6	-66.0527	18.33038
SYN5-8	-66.0596	18.3386
SYN5-9	-66.0595	18.33855
SYN6-0	-66.0702	18.34643
SYN6-2	-66.0706	18.32918
SYN6-3	-66.0723	18.32763
SYN6-4	-66.0724	18.3301
SYN6-5	-66.072	18.33045
SYN6-6	-66.0738	18.34035
SYN6-7	-66.0708	18.34024
SYNP-1	-66.0653	18.40451
SYNP-2	-66.0567	18.39594
SYNP-3	-66.0592	18.38579
SYNP-4	-66.0591	18.37251
SYNP-5	-66.065	18.36052
SYNP-USGS	-66.0696	18.40971

Appendix A, Table 7: Sampling locations in the Flat Creek watershed, Wyoming. Datum: NAD27

Site ID	X-Coordinate	Y-Coordinate	Location
WY-01	-110.714	43.51985	Nowlin Cr.
WY-02	-110.601	43.54912	Upper Flat Cr.
WY-03	-110.62	43.55612	Middle Flat Cr.
WY-04	-110.663	43.5477	Lower Flat Cr.
WY-05	-110.71	43.56762	Ditch from Gros Ventre R.
WY-06	-110.732	43.5356	Outflow from Hatchery
WY-07	-110.736	43.52258	Flat Cr., S. of Hatchery
WY-08	-110.762	43.48857	Flat Cr. at Upper Jackson
WY-09	-110.73	43.46451	Cache Cr. at Trailhead
WY-10	-110.745	43.47324	Cache Cr. in Jackson
WY-11	-110.763	43.48514	Cache Cr. at Confluence with Flat Cr.
WY-12	-110.77	43.47905	Flat Cr. in Middle Jackson
WY-13	-110.778	43.47017	Flat Cr., ds of fairground
WY-14	-110.793	43.46199	Flat Cr. at Hwy 89, Lower Jackson
WY-15	-110.792	43.43284	Flat Cr. at Leeks Canyon, Rafter J
WY-16	-110.781	43.41467	Flat Cr. at Melody Ranch
WY-17	-110.759	43.39928	Flat Cr. ditch, south bend, north branch
WY-18	-110.759	43.39928	Flat Cr., south bend west branch
WY-19	-110.746	43.38887	Flat Cr. at Hwy 89, South Park

Appendix B

This appendix includes water chemistry parameters and indicates the subset of stream samples used in the simulation model. Sampling locations were not included in the model for the following reasons, indicated throughout this appendix using the following notation:

[*] Questionable sampling location that could not be verified on the ground.

[**] Sample taken on unmapped tributary and hydrologic connection could not be confirmed.

[+] A lab error occurred in processing the sample for [NO_3-N] or the [NO_3-N] measurement was questionable and could not be confirmed.

[++] A sub-watershed of the sampled watershed was used in the analysis and the sample fell outside of that sub-watershed.

[+++] Samples were collected more than a week before or after synoptic sampling.

Appendix B, Table 1: Water chemistry parameter key.

Parameter Abbreviation	Parameter Name	Units
Temp	Temperature	^{o}C
Cond	Conductivity	uS cm^{-1}
NO3-N	Nitrate-nitrogen concentration	ug L^{-1}
NH4-N	Ammonium-nitrogen	ug L^{-1}
SRP	Soluble reactive phosphorus	ug L^{-1}
TDN	Total dissolved nitrogen	ug L^{-1}
TDP	Total dissolved phosphorus	ug L^{-1}
TN	Total nitrogen	ug L^{-1}
TP	Total phosphorus	ug L^{-1}
DOC	Dissolved organic carbon	ug L^{-1}
DO	Dissolved oxygen	ug L^{-1}
DON	Dissolved organic nitrogen	ug L^{-1}
TKN	Total kjeldahl nitrogen	ug L^{-1}

Appendix B, Table 1: Kansas 2003 water chemistry data.

Site ID	Cl	Cond	DOC	NO_3-N	TDN	TDP	TN	TP
KS-01	5.72	320.0	1720	87.8	258.0	7.7	264.0	16.92
KS-02	5.25	350.0	1340	22.7	136.5	1.2	318.0	31.19
KS-03	6.08	280.0	2360	40.2	274.5	8.4	500.0	34.72
KS-04^{+}	5.50	210.0	1550	-	229.0	7.5	436.0	15.28
KS-05	5.01	250.0	1660	2.0	87.4	1.0	270.0	17.55
KS-06	7.68	360.0	2020	83.9	300.5	2.1	2084.0	49.37
KS-07	5.20	320.0	2040	596.9	1318.0	2.5	1320.0	46.21
KS-08	6.23	370.0	1740	161.9	327.0	1.9	348.0	16.41
KS-09	4.88	310.0	1870	52.9	193.0	4.0	242.0	20.08
KS-10	5.66	320.0	3700	166.8	424.0	2.2	521.0	42.05
KS-11	6.01	340.0	1900	0.5	164.7	2.0	485.0	27.40
KS-12	5.40	330.0	1770	62.2	219.6	2.4	249.0	24.49
KS-14	5.97	320.0	1840	81.0	316.3	3.7	669.0	56.06
KS-15	5.25	420.0	2520	80.5	-	-	182.0	30.18
KS-16	-	280.0	2720	222.4	843.9	5.0	1425.0	83.78
KS-17	5.29	270.0	1660	51.7	219.0	0.7	590.0	3.56
KS-18	6.75	410.0	2860	190.7	650.0	4.1	1229.0	50.67
KS-19	5.87	310.0	2710	51.0	363.8	4.3	627.0	5.11
KS-20	5.97	260.0	2970	561.8	957.4	26.9	2074.0	212.22
KS-21	5.80	340.0	1590	110.9	376.1	3.9	615.0	65.11
KS-22	5.87	300.0	1600	10.7	146.3	3.1	424.0	12.89
KS-23	5.16	280.0	2510	6.8	159.5	3.6	234.0	22.00
KS-24	5.40	280.0	2820	66.8	331.3	1.9	597.0	2.50
KS-25	4.82	230.0	1530	86.3	327.0	0.5	750.0	36.89
KS-26	5.43	270.0	2430	87.3	390.4	8.2	920.0	8.67
KS-27^{+}	5.64	320.0	2260	47.3	411.9	7.2	560.0	27.11
KS-28	4.86	250.0	1530	6.3	166.6	4.2	289.0	51.78

Appendix B, Table 2: Kansas 2004 water chemistry data.

Site ID	Cl	Cond	DOC	NH_4-N	NO_3-N	TDN	TDP	TN	TP
KS-01	3.45	370	1870	15.9	221.0	346.0	3.0	390.0	24.8
KS-02	4.73	370	1450	9.1	142.0	296.0	0.7	306.9	13.2
KS-03	5.71	340	2650	31.8	44.7	471.3	1.0	601.9	46.8
KS-04	4.67	210	2800	16.5	10.3	262.5	3.8	456.0	39.9
KS-05	4.97	320	1670	22.6	29.0	288.1	b.d.	439.8	3.7
KS-06	4.79	380	2080	8.5	184.0	86.9	0.4	379.0	28.9
KS-07	4.48	470	1500	5.9	1961.0	1732.4	1.4	2431.2	30.0
KS-08	5.42	370	1560	7	421.0	487.1	b.d.	559.5	21.1
KS-10	5.16	410	1890	12.7	1449.0	831.7	7.8	1035.6	37.3
KS-11	4.71	340	1510	21.9	214.0	548.2	3.4	716.9	23.2
KS-12	3.66	390	1860	22.6	393.0	740.0	1.8	885.0	18.9
KS-13^{++}	4.86	250	5670	30.1	570.0	911.7	31.9	1725.5	248.2
KS-14	4.30	360	3630	11.8	592.0	846.9	14.0	1184.7	193.0
KS-15	4.47	340	11560	35.8	212.0	938.3	124.8	1464.6	376.0
KS-16	-	170	14340	103.9	424.0	1264.0	189.2	2083.5	423.0
KS-17	4.29	360	2710	19.1	304.0	260.5	6.3	800.4	92.1
KS-18	5.83	420	5000	13.8	581.0	839.0	13.4	1082.5	109.6
KS-19	5.34	350	2250	7.8	715.0	803.1	0.4	957.0	84.0
KS-20	4.85	370	3690	75.4	1538.0	1876.6	36.2	2374.2	258.9
KS-21	4.88	360	1750	8.3	735.0	801.0	14.8	996.1	60.2
KS-22	4.90	390	2320	11.6	662.0	809.0	11.6	916.7	53.2
KS-23	4.62	320	2370	5.4	97.4	225.9	5.4	262.1	26.2
KS-24	3.30	320	1140	7.9	132.8	195.6	1.7	517.1	24.1
KS-25	5.13	390	2090	6.7	502.0	680.0	1.1	835.7	37.2
KS-26	4.89	370	2260	17.2	1050.0	1124.6	2.2	1406.5	53.2
KS-27	4.98	380	2490	21.1	736.0	948.7	b.d.	1118.6	73.4

Appendix B, Table 3: Massachusetts 2003 water chemistry data.

Site ID	Cl	Cond	DO	DOC	NH_4-N	NO_3-N	SRP	TDN	Temp	TP
BB-PR	72740	341	5450	9400	44.1	155.8	3.4	480	21.36	14
BBYr1	58240	313	4820	10200	28.6	59.5	0.6	440	22.57	16
FB-BV	43270	271	3440	14600	200.3	151.5	13.6	780	21.6	-
FB-LOCK	51470	251	6260	10900	24.2	166.4	4.6	500	23.11	21
FB-WA	67730	329	6880	9800	40.1	298.2	1.9	660	20.13	-
HB-01Yr1	56680	380	6700	6400	31.7	255.8	3.4	480	22.46	-
HB-DR	59700	326	7880	6000	36.7	11.3	4.6	280	24.47	16
IP00	85820	414	570	9200	151.9	13.0	8.1	400	19.61	89
IP01	75700	400	1180	12000	32.5	9.2	6.2	420	21.58	98
IP04	51850	346	3030	11900	169.7	209.1	8.4	730	20.91	-
IP06	52450	400	8980	11200	51.3	155.9	7.7	570	24.18	-
IP10	79220	444	6910	11100	22.0	186.6	9.3	600	24.01	-
IP20	62090	387	6650	12500	29.1	202.9	7.7	570	23.52	31
IP24	59390	376	6400	12500	25.9	202.5	7.7	630	24.15	30
IR-97	94590	419	8070	12300	30.4	220.2	6.5	660	22.23	28
IS_102	208600	857	6960	4000	77.9	929.2	5.0	1150	18.94	28
IS_104**	47580	306	4740	4400	104.1	1347.2	3.4	1470	17.17	11
IS_110	163660	804	1230	12500	653.0	81.6	9.0	850	20.41	84
IS_115	101960	595	4420	6200	136.6	801.2	15.2	1170	18.21	-
IS_118	53400	374	6500	5600	54.9	2177.0	5.9	3060	17.49	-
IS_120	57650	360	9140	10700	23.5	1095.5	24.8	870	20.73	-
IS_127	33010	193	2230	14000	112.1	8.7	16.4	590	20.18	99
IS_128	87670	405	7640	3500	116.0	2541.3	2.2	2720	16.47	17
IS_129	36830	248	1690	12800	979.6	15.8	39.6	1080	20.03	205
IS_131	66150	417	6990	8900	119.2	207.5	12.7	600	18.29	-
IS_132	22630	109	2200	-	55.8	10.7	17.7	-	20.44	-
IS_135	72210	447	1930	-	850.3	6.0	19.8	-	21.55	281
IS_141	14880	126	1700	-	86.9	58.0	4.6	-	20.25	460
IS_142	108820	423	5780	3400	42.6	225.1	3.1	340	19.27	2

Appendix B, Table 3 (continued)

Site ID	Cl	Cond	DO	DOC	NH_4-N	NO_3-N	SRP	TDN	Temp	TP
IS_148	35500	247	5660	-	67.8	225.3	16.1	-	22.59	40
IS_161	98030	500	1000	11700	785.4	1212.5	22.3	1960	19.47	176
IS_163	132310	914	6380	6900	66.8	482.9	14.2	700	22.13	-
IS_166	162140	753	7770	-	136.7	1465.5	10.2	-	20.04	48
IS_167	122650	481	1490	19600	-	3.4	10.8	1250	19.39	155
IS_170	22200	166	4350	13600	158.7	495.9	5.9	1050	21.11	54
IS_172	43470	427	4240	18000	155.9	47.9	35.9	790	20.57	106
LB-62	90790	412	600	10100	99.9	9.0	5.3	380	20.85	68
LBYr1	106120	482	4380	10500	170.5	380.1	3.7	850	19.69	19
MB	85680	423	2070	-	206.5	43.7	8.1	-	21.5	46
MB-PR	57470	275	7450	8900	33.2	304.3	8.1	660	19.64	17
MB-SAL	79570	365	540	8000	92.2	153.8	4.3	460	21.19	35
MMB-38^{+}	94980	-	-	9000	123.4	b.d.	2.2	370	20.71	55
MMB-CHEST	157430	807	4700	5600	150.9	362.3	2.5	620	20.71	23
MMBYr1	88620	-	-	8800	178.9	88.3	7.7	480	20.71	46
MPO	84080	343	6320	10300	39.4	121.2	3.4	460	24.94	32
MR-1A	46930	315	1250	11200	12.9	7.3	5.6	420	22.11	67
MR-BR	71310	352	3810	10200	19.3	6.1	37.5	490	22.46	115
MR-LR	46100	315	1910	9000	106.8	9.9	3.7	450	22.34	52
NB	126660	525	2630	5300	39.4	120.9	9.3	330	22.99	23

Appendix B, Table 4: Massachusetts 2004 water chemistry data.

Site ID	Cl	Cond	DOC	NH_4-N	NO_3-N	TDN	TP
BBYr2	38000	190.1	28980	75.96	150.68	1140	104.3
FB-BV	47000	213.4	16120	41.42	75.68	700	51
FB-LOCK	47000	215.7	13380	34.14	159.86	690	48
FB-WA	74000	299.5	11360	32.38	270.97	720	140
HB-01Yr2	59000	310.3	3870	46.06	213.64	410	20
IP00	108000	386.4	6830	9.81	65.88	350	29
IP01	84000	405	6280	54	2.09	330	42
IP04Yr2	110000	377.5	7510	55.42	125.81	490	53
IP06	92000	342.8	8580	31.34	153.4	560	51
IP10	96000	359.8	7930	16.07	172.94	550	71
IP20	75000	308.5	7960	11.09	93.32	470	20
IP24	73000	300.3	7480	10.65	108.3	430	31
IR-97	56000	362.4	6420	14.05	195.52	530	26
IS_102	180000	654	1220	65.92	1106.74	700	7
IS_104**	56000	303.7	2810	87.08	1646.25	1760	15
IS_110	255000	796	11390	454.21	314.89	1200	80
IS_115	145000	583	5990	75.73	1082.76	1450	71
IS_118	55000	324	3210	71.91	791.76	800	33
IS_120	53000	327.3	9350	35.08	1065.07	1330	45
IS_127	55000	249	35630	233.79	407.01	1560	208
IS_129	38000	177.4	11710	133.03	69.4	630	60
IS_131	134000	491.7	7470	138.59	624.12	1060	45
IS_132	21000	105.8	13770	118.57	0.4	650	213
IS_135	162000	565	6600	559.46	4	830	129
IS_142	5500	103.8	9230	19.39	22.1	450	50
IS_143*	8300	82.4	5450	5.14	69.39	320	15
IS_148	19000	146.2	16940	49.79	200.65	860	94
IS_161	119000	593	2880	277.46	2578.98	1270	148
IS_166	166000	574	4270	182.62	950.94	840	81
IS_167	142000	550	6740	559.57	3.98	1110	138
IS_170	35000	211.5	10340	58.56	365.07	850	43
IS_172	76000	439.7	8640	86.22	84.95	640	98
LB-62	115000	430.4	6090	25.48	35.7	290	28
LBYr2+	93000	396.2	6040	0.16	2.09	270	28
LMB	28000	131	2760	79.72	1365.73	1590	61
MB	95000	365	8370	32.58	42.7	440	77
MB-SAL	60000	322.6	-	44.74	1.67	-	42
MMB-38	87000	338	5800	116.61	2.37	380	54
MMBYr2*	114000	386.1	6990	10.51	36.4	350	46
MR-1A	59000	289.8	6370	26.28	13.22	370	153
MR-BR	33000	311.7	2950	9.51	0.8	210	33
NB	66000	439.5	2460	19.09	73.09	240	15

Appendix B, Table 5: Michigan 2003 water chemistry data. *Samples not included in model.

Site ID	Cl	Cond	NH_4-N	NO_3-N	SRP	Temp	TN	TP
MI-01	25666.5	384.0	38.0	19.3	79.0	23.1	348.5	169.0
MI-02	26873.1	495.7	45.0	2898.0	19.3	18.3	1963.7	47.3
MI-03	60293.1	643.2	92.1	5255.3	67.9	18.5	3100.0	90.0
MI-04^{++}	131760.0	520.9	74.9	5234.0	92.2	21.5	3069.8	145.3
MI-05	102414.5	741.1	329.3	2197.1	44.4	23.0	2457.0	162.0
MI-06	41379.4	28.5	1913.8	541.2	1914.5	28.8	2006.0	756.6
MI-07	85780.7	550.9	246.5	1991.9	34.6	22.8	450.5	55.6
MI-08	42526.0	553.7	227.7	260.8	13.6	24.1	326.6	90.0
MI-09	27986.6	514.1	100.0	9532.1	14.9	30.9	11600.0	105.0
MI-10	54394.1	544.7	47.9	1373.7	31.6	25.7	1867.3	16.9
MI-11	53779.2	587.2	94.0	2884.4	24.5	21.2	3302.8	42.4
MI-12	41704.3	756.6	105.0	11148.0	76.0	28.3	4904.8	98.5
MI-13	137426.6	528.4	66.3	9673.3	41.5	23.3	1300.5	63.0
MI-14	61601.7	495.3	54.7	2664.4	13.8	20.1	925.6	37.7
MI-15	17204.4	301.9	162.2	251.5	14.6	18.1	564.0	290.0
MI-16	40769.0	481.0	47.1	1381.6	21.8	23.7	1788.6	12.4
MI-17	27213.8	355.8	107.3	53.9	12.2	24.5	232.5	26.0
MI-18	42633.9	390.7	86.9	803.2	35.1	25.4	1308.9	36.8
MI-19	36793.6	485.1	50.2	1313.8	14.6	25.3	943.0	19.1
MI-20^{++}	25590.1	456.1	82.2	876.4	13.1	15.8	839.7	30.4
MI-21	30512.2	542.2	87.7	1293.7	18.9	18.7	576.5	15.3
MI-22	88163.1	630.2	181.4	6380.3	44.8	18.8	3399.6	53.0
MI-23	31914.3	431.0	85.4	1960.0	48.7	19.8	1325.1	95.2
MI-24	33538.5	539.0	169.6	260.9	106.4	20.3	4191.2	29.9
MI-25	24233.7	491.0	98.3	1083.9	28.6	-	1250.9	23.6
MI-26	506000.0	201.0	67.4	2693.8	95.1	19.4	2685.4	58.4
MI-27	22605.2	458.1	174.4	4758.9	64.5	18.3	1257.0	101.3
MI-28	45506.7	491.0	97.1	1701.7	15.4	17.2	1271.3	9.0
MI-29	33341.8	472.5	118.4	772.3	16.7	18.0	944.4	16.3
MI-30	26124.8	453.0	83.5	871.6	10.4	15.9	1282.7	4.6
MI-31	27826.3	427.8	126.5	1211.4	15.0	16.2	1160.2	2.6
MI-32	31529.5	420.0	84.6	1615.2	13.5	15.2	1447.1	12.4
MI-33^{++}	14483.2	283.3	35.6	335.4	18.9	16.9	748.9	17.7
MI-34^{++}	15378.5	229.0	106.5	250.2	25.2	17.6	-62.0	12.5
MI-35^{++}	10090.0	298.0	85.7	517.1	22.3	16.8	16.8	10.0
MI-36	10367.1	266.3	147.3	489.4	36.0	19.7	452.6	70.0
MI-37^{++}	49482.7	382.0	61.5	2857.9	53.6	21.7	542.8	61.0
MI-38	94332.2	604.6	240.1	6118.6	325.0	19.2	8475.2	495.4
MI-39	15739.4	313.0	62.5	4230.9	23.8	18.3	2823.1	72.7
MI-40^{++}	169405.7	697.0	259.1	3737.9	170.3		2951.7	154.6
MI-41	158731.9	570.0	930.0	4444.7	513.2	19.9	3777.9	445.3
MI-42^{++}	25640.8	402.0	90.6	1431.3	11.5	20.8	687.7	16.2
MI-43^{++}	28691.1	398.4	43.7	1206.2	37.4	12.7	1165.8	18.2
MI-44^{++}	42295.8	497.1	131.1	3385.1	36.6	14.6	2263.2	69.2
MI-45^{++}	6412.6	417.8	119.7	253.2	58.1	17.7	738.3	14.6
MI-46^{++}	24096.3	474.5	157.9	3276.1	6.0	14.9	2049.9	67.6

Appendix B, Table 5 (continued)

Site ID	Cl	Cond	NH_4-N	NO_3-N	SRP	Temp	TN	TP
MI-47^{++}	27375.1	490.1	31.3	4497.9	17.4	15.9	3314.9	25.7
MI-48^{++}	34514.2	429.5	62.0	2248.0	48.2	15.2	1667.1	29.2
MI-49^{++}	9000.2	377.5	75.6	1056.2	36.0	14.2	1188.7	63.1
MI-50^{++}	24427.8	410.3	42.6	1554.2	24.7	18.5	1420.2	28.0
MI-51^{++}	14054.6	335.4	206.5	694.7	20.3	16.3	24.2	7.5
MI-52^{++}	8744.9	438.0	34.0	1617.4	10.9	18.7	1550.1	37.9
MI-53^{++}	24424.4	438.7	34.6	1913.4	20.0	19.9	1699.7	25.9
MI-54^{++}	35617.7	532.9	58.3	500.7	25.2	16.0	810.5	7.5
MI-55^{++}	23573.5	423.5	23.6	1152.9	15.7	22.4	1555.8	22.0
MI-56^{++}	38407.8	483.2	96.5	2745.9	24.9	18.5	1925.8	78.6
MI-57^{++}	33532.7	425.5	21.6	1767.9	22.7	20.4	1717.7	25.7
MI-58^{++}	33586.4	536.3	64.5	887.4	10.2	19.5	1010.6	12.3
MI-59^{++}	24095.6	505.2	31.8	145.8	18.9	22.0	439.4	7.5
MI-60^{++}	20814.0	413.1	51.2	2126.7	24.1	20.8	1444.6	34.2
MI-61^{++}	37081.9	554.8	423.7	697.1	11.8	27.7	596.5	12.5
MI-62^{++}	35124.2	388.1	29.8	1132.2	16.9	20.1	610.1	41.8
MI-63^{++}	61473.1	427.3	42.3	1321.2	7.8	18.9	926.6	43.5
MI-64^{++}	32563.8	385.1	35.6	1062.8	21.6	18.5	831.5	54.5
MI-65^{++}	117384.1	476.0	35.1	3073.3	20.6	21.5	1859.2	37.0
MI-66^{++}	22237.8	504.0	40.2	16953.5	11.0	23.5	5089.4	41.8
MI-67^{++}	23924.8	486.9	72.4	9405.9	12.5	25.8	4983.5	103.2
MI-68^{++}	24810.2	348.7	44.6	2922.9	14.5	30.0	1650.4	16.7
MI-69^{++}	53673.9	359.9	31.4	2859.1	24.9	25.3	1689.7	15.6
MI-70	26933.4	-	74.7	4193.6	46.5	-	2717.2	103.7
MI-71^{++}	24224.1	770.0	154.8	1536.5	30.7	15.7	1172.9	175.0
MI-72^{++}	17388.4	722.0	75.1	1994.1	10.5	18.0	2405.5	88.1
MI-73^{++}	20801.5	846.0	126.0	3096.0	14.4	15.6	2107.4	119.9
MI-74^{++}	235334.8	754.0	59.5	4274.3	139.6	17.4	2149.8	54.8
MI-75^{++}	37909.7	746.0	69.5	8085.2	55.0	17.6	3989.8	64.7
MI-76^{++}	15461.4	746.0	132.8	3009.4	102.9	19.5	2467.5	71.5
MI-77^{++}	44601.1	709.0	107.9	4266.2	67.7	18.2	2650.6	61.7
MI-78^{++}	32612.1	626.0	55.2	2177.4	82.2	18.0	1346.3	57.8
MI-79^{++}	43465.2	379.0	20.1	308.0	79.6	13.5	537.4	17.2
MI-80^{++}	29724.3	303.0	12.4	256.2	55.8	13.4	536.0	10.8
MI-81^{++}	33504.7	625.0	47.7	2180.6	43.0	18.6	1458.2	69.3
MI-82^{++}	43536.6	777.0	53.7	1291.0	28.1	15.8	1294.9	56.0
MI-83^{++}	8397.2	729.0	58.6	14577.3	22.3	16.9	7483.2	60.3
MI-84^{++}	7269.9	708.0	53.7	2078.9	9.5	17.0	1341.7	48.3
MI-85^{++}	42743.8	605.0	31.2	2000.8	34.2	19.8	964.9	23.1
MI-86^{++}	69354.9	616.0	37.6	2479.2	14.4	19.4	1697.3	28.8
MI-87^{++}	39363.0	322.0	42.4	491.5	28.5	17.4	727.6	40.9

Appendix B, Table 6: Michigan 2004 water chemistry data. *Samples not included in model.

Site ID	Cl	Cond	NH_4-N	NO_3-N	SRP	Temp
MI-01	99620	745	38.4	2888.0	50.9	21.2
MI-02	53350	686	83.6	3542.3	42.2	17.1
MI-03	70650	770	42.6	3690.0	43.0	16.3
MI-04^{++}	55740	658	33.9	2805.9	20.2	16.4
MI-05	47160	727	54.0	1210.0	28.9	17.0
MI-07	60700	782	61.1	2208.0	19.2	17.5
MI-09	60360	610	151.8	2704.9	65.6	19.2
MI-10	90520	751	115.8	4912.6	33.2	20.2
MI-11	354060	795	57.1	25141.1	10.5	17.0
MI-12	108430	981	80.1	12023.8	80.8	16.2
MI-13	52830	740	57.3	10506.1	57.3	15.7
MI-14	73750	674	92.6	4496.1	28.9	16.7
MI-15	197650	727	96.5	12528.5	25.9	17.1
MI-16	73130	765	102.3	4672.4	29.8	17.6
MI-17	42800	427	54.1	1668.3	13.3	17.4
MI-18	72730	413	68.8	683.7	11.9	20.0
MI-19	150550	767	110.7	9796.1	26.8	17.7
MI-20^{++}	74550	683	80.5	2878.4	25.1	17.6
MI-21	59900	844	67.0	5512.3	32.3	19.9
MI-22	55000	777	47.8	3162.9	12.9	18.1
MI-23	49680	605	22.1	3492.0	24.5	19.5
MI-24	31850	867	73.0	1185.6	20.8	20.5
MI-25	37780	873	92.6	4203.3	22.8	18.7
MI-26	70650	546	42.3	1801.1	85.6	20.5
MI-27	49580	602	59.9	3509.8	57.2	18.7
MI-28	54300	813	40.7	1308.8	22.5	17.4
MI-29	52200	795	254.0	3055.9	63.2	17.7
MI-30	70980	680	83.9	2710.4	32.0	17.6
MI-31	32210	659	84.9	1941.1	4.8	15.5
MI-32	73490	690	68.5	3656.9	24.8	17.2
MI-33^{++}	22740	354	17.3	310.9	11.3	16.7
MI-34^{++}	41700	376	28.9	62.5	9.1	16.4
MI-35^{++}	6480	380	39.8	311.8	13.3	16.1
MI-36	12530	367	52.7	486.2	23.7	18.9
MI-37^{++}	102190	763	67.7	6075.2	110.5	21.4
MI-39	53670	557	44.3	7118.6	14.3	19.4
MI-40^{++}	-	-	-	12858.2	-	-
MI-41	157870	870	26.7	4585.4	44.6	23.0
MI-42^{++}	20570	554	36.2	1141.1	4.0	25.6
MI-43^{++}	21490	575	38.1	984.4	8.8	23.0
MI-44^{++}	58920	780	97.9	7978.1	32.1	19.9
MI-45^{++}	16980	568	224.9	2837.8	22.8	24.7
MI-46^{++}	24310	696	70.5	7468.7	17.2	19.6
MI-47^{++}	18850	714	23.0	6385.3	9.1	20.3
MI-48^{++}	15130	615	27.5	3491.1	4.8	19.0
MI-49^{++}	33890	636	413.9	5597.0	64.5	16.2

Appendix B, Table 6 (continued)

Site ID	Cl	Cond	NH_4-N	NO_3-N	SRP	Temp
MI-50^{++}	36080	593	44.7	3543.3	24.4	19.2
MI-51^{++}	1230	567	304.4	145.8	27.3	16.6
MI-52^{++}	38690	616	28.7	3761.1	18.0	19.7
MI-53^{++}	37220	630	29.9	3633.0	22.6	19.8
MI-54^{++}	41180	760	64.8	1610.0	3.8	17.1
MI-55^{++}	41590	603	31.2	2602.1	21.6	21.9
MI-56^{++}	33130	714	71.8	8879.6	25.6	18.9
MI-57^{++}	57980	606	31.4	3345.7	22.2	20.0
MI-58^{++}	45740	789	27.6	5784.1	8.3	18.4
MI-59^{++}	75050	774	84.6	1338.9	7.1	18.1
MI-60^{++}	38410	602	32.5	2184.2	12.2	19.6
MI-61^{++}	103880	624	69.9	419.3	5.7	24.2
MI-62^{++}	33240	525	33.1	1790.6	8.8	19.5
MI-63^{++}	57170	570	34.2	3284.0	6.3	18.4
MI-64^{++}	33100	545	40.4	1228.8	7.6	18.5
MI-65^{++}	97670	627	31.2	4174.5	18.6	21.2
MI-66^{++}	55390	746	62.4	25689.3	32.0	21.2
MI-67^{++}	33150	648	46.3	7741.4	32.3	21.8
MI-68^{++}	42880	477	33.4	5083.0	7.1	22.6
MI-69^{++}	35430	567	24.2	2104.5	23.4	23.2
MI-70^{++}	298090	935	61.7	-	73.3	21.5
MI-71^{++}	72310	862	74.5	9472.3	53.9	15.1
MI-72^{++}	37430	736	51.9	3962.3	39.3	15.8
MI-73^{++}	47050	851	60.4	4011.8	22.0	14.7
MI-74^{++}	41140	768	49.2	4261.7	27.6	15.9
MI-75^{++}	114980	781	55.6	27985.5	37.3	15.2
MI-76^{++}	42580	771	96.9	5816.3	32.4	17.5
MI-77^{++}	41890	747	73.7	6834.8	30.6	17.0
MI-78^{++}	41150	639	37.9	2713.8	13.6	17.2
MI-79^{++}	11640	381	14.6	520.5	11.6	12.3
MI-80^{++}	14610	302	11.0	471.3	6.3	12.2
MI-81^{++}	36840	636	106.6	2292.5	21.2	17.8
MI-82^{++}	81570	787	46.5	4148.6	2.4	13.8
MI-83^{++}	51140	758	26.0	21867.9	14.4	14.6
MI-84^{++}	51350	722	9.0	4746.6	7.7	15.7
MI-85^{++}	39600	610	38.1	3584.0	18.1	18.8
MI-86^{++}	39540	618	43.7	3315.4	24.2	18.7
MI-87^{++}	6130	313	48.1	517.8	31.0	15.0

Appendix B, Table 7: North Carolina 2003 water chemistry data. *Samples not included in model. **Cond = Conductance (umho cm^{-1})

Site ID	Cl	Cond**	DOC	NH_4-N	NO_3-N	SRP	TN	TP
BTY-1	709	22.2	740	5	30.6	78.4	258.89	0.33
BTY-2	714.8	16.8	810	11.4	80.1	6.1	202.21	2.61
BTY-3	439.7	11	510	3.1	5.9	0.7	7.79	0.87
BTY-4	455.5	14.2	640	3.6	21	1.8	10.9	b.d.
BTY-5	496	16.1	610	1.1	38.9	3.5	192.4	0.13
BTY-6	553.8	19.5	580	5.5	36.6	5.2	47.42	3.95
CWT-1	623	17.7	620	4.7	36.6	1.7	248.38	b.d.
CWT-2	556.4	14.4	670	5	36.2	2.5	98.26	1
CWT-3	459.2	10.1	750	2.9	16.7	1	9.25	1.94
CWT-4	385.4	9	880	1.9	15.3	1.3	234.67	0.94
CWT-5	501.2	12.1	400	3.1	165.2	0.7	119.44	b.d.
CWT-6	616.3	22	700	3.1	22.8	3.1	25.31	3.5
DMI-1	663.9	18.5	670	5	35.8	9.4	15.49	12.25
DMI-2	2521.4	27.4	570	10.8	172.2	15.7	223.75	2.77
DMI-3	794.2	14.7	750	8.7	50	2.1	2.73	b.d.
DMI-4D	1146	19.6	660	21.4	102.2	3.8	118.43	b.d.
DMI-5	915	27.5	780	27.2	84.4	12	159.77	3.55
DMI-6	547.7	19.7	460	5.2	36.2	7.7	29.35	2.34
DMI-7	642.9	20.5	640	3.5	39.7	12.2	150.66	1.07
DMI-8	563.1	17.8	530	3.1	42.4	3.6	117.03	11.45
HLT-1	1117	28.8	1170	21	83.9	9.6	371.09	12.72
HLT-10	602	16.2	970	27.2	9.2	5.8	51.23	b.d.
HLT-11	734	22.2	950	30.1	45.2	4.2	41.97	1.81
HLT-12	1045	22.4	1340	17	46.8	9.4	77	1.14
HLT-3	901	24	930	13	84.6	10.3	83.7	3.21
HLT-4[+]	-	-	-	-	-	0.7	-	-
HLT-5	688	20.3	920	18.5	88.6	5.1	136.1	5.49
HLT-6	610	19.6	830	23.9	45.6	19.1	94.37	3.35
HLT-7	2026.6	43.1	3190	80.1	394.3	46.1	1125.93	88.77
HLT-8	704	17.3	890	17.1	13.2	3.6	46.02	0.07
HLT-9	2752	62.2	2100	192.3	1411.4	20.5	1531.38	10.04
LLT-1	1329	37.6	580	8.1	122.2	4	148.72	0.94
LLT-2	1635	42.3	960	10.7	463.2	8	639.87	3.48
LLT-3	1229	36.5	710	12.1	121.7	6.4	202.6	18.88
LLT-4	2541	51.8	1020	32.3	561.2	8.7	647.96	2.68
LLT-5	920.3	33.8	750	5.1	77.8	5.2	79.17	4.61
LLT-6	770.1	23.4	580	5.2	70.9	3	312.15	1.87
LLT-7	966.2	21.6	700	13.6	129.4	6.6	91.1	1.27
MDL-1	1706.7	24.1	650	4.3	284.3	4.6	331.07	2.41
MDL-2	583	14.2	770	0.9	6.3	2.5	180.33	0.13
MDL-3	1586	28.8	820	23.6	596.1	7.4	634.26	2.34

Appendix B, Table 7 (continued)

Site ID	Cl	Cond**	DOC	NH_4-N	NO_3-N	SRP	TN	TP
MDL-4	795	14.4	770	9.7	183.1	7	316.9	0.6
MDL-5	4549.4	34.7	750	5.9	263.6	3.9	315.81	0.33
MDL-6	1844	21.9	580	11.8	237	0.7	285.47	8.11
MDL-7	3241	42.5	670	17.3	1005.3	8.5	1015.1	26.92
MST-1	14087.8	86.5	790	4.3	173.3	57.5	317.29	45.26
MST-2	14379.4	87.9	820	5.1	158.5	82.7	86.82	44.59
MST-3	14259	86.2	940	4.1	137.5	69.8	187.49	51.82
MST-4^{+}	19853.6	116.2	840	2.4	200.1	118.8	288.24	123.7
MST-5	23362.2	137.9	910	6.2	158.4	125.5	243.29	156.33
MST-6	28274	174.8	1530	29.5	147	187.5	201.68	204.91
MST-7	1027.6	27.6	920	16.8	205.2	14.8	215.05	6.49
PSO-1A**	1047.5	33.2	780	4.1	104.7	2.7	128.4	3.23
PSO-1B**	1777.3	37.4	680	7.2	367.9	5	296.73	2.14
PSO-1C**	2016	43.4	600	17.1	423.2	1.3	510.3	5.76
PSO-1D**	2395.2	52.4	690	28	434	6.8	592.55	2.67
PSO-3**	3702	46.8	600	3	96.3	3.6	101.38	2.08
TST-1	731	18.2	690	2.7	37.2	3.9	111.41	9.86
TST-2	798	20.5	680	5.7	32	6.7	105.11	1.54
TST-3	609.7	14.8	570	3.3	27.2	14.2	43.68	2.01
TST-4	687	16.6	670	2.8	55.4	5.5	37.37	1.67
TST-5	852	18.6	560	3.2	145.5	4.8	354.7	3.4

Appendix B, Table 8: North Carolina 2004 water chemistry data.
***Cond = Conductance (umho cm^{-1})

Site ID	Cl	Cond***	DOC	NH_4-N	NO_3-N	SRP	Temp
BTY-1	604	19.4	610	0.9	59	4	16.7
BTY-2	606	19.5	710	7.05	31	9.9	16.2
BTY-3	438	15.3	490	4.17	15	4.3	16
BTY-4	452	17.3	590	8.21	44	0.7	15.8
BTY-5	490	18.8	520	6.28	59	1.8	16.6
BTY-6	609	22.2	920	0.9	50	0.7	15.9
CWT-1	558	17.6	950	0.9	38	0.7	27.7
CWT-2	476	18.1	560	4.35	51	0.7	15.9
CWT-3	437	12.7	610	0.9	40	3.1	16
CWT-4	347	10.9	610	0.9	24	0.7	14.7
CWT-5	508	18	340	0.9	129	0.7	15.3
CWT-6	484	27.7	330	3.13	37	0.7	16.2
DMI-1	656	21.6	1160	0.9	49	0.7	17.4
DMI-2	2966	30.6	1090	0.9	147	0.7	18
DMI-3	677	15.5	650	8.63	35	0.7	20.7
DMI-4D	1027	20.6	1250	34.8	84	0.7	20.8
DMI-5	591	17.5	650	3.39	22	0.7	16.2
DMI-6	548	21.6	1200	0.9	26	0.7	16.3
DMI-7	624	22.8	1120	0.9	57	0.7	17.4
DMI-8	553	19.3	1490	0.9	21	0.7	19.1
DMI-9	1383	26	1090	-	154	-	20
HLT-1	814	26.5	720	6.73	103	0.7	16.9
HLT-10	571	13.9	670	0.9	14	0.7	16.7
HLT-11	749	20.5	770	13.83	42	0.7	23.9
HLT-12	740	21.6	650	7.94	24	2.4	23.5
HLT-2	2462	34.7	3080	242.6	249	85	17.6
HLT-3	847	24.1	1270	10.4	80	0.7	17
HLT-4	940	20.1	620	8.89	10	71.1	22.6
HLT-5	820	19.4	930	16.51	78	3.4	18.8
HLT-6	667	17.9	620	18.99	51	14.1	16
HLT-7	1622	36.6	1950	323.97	321	15.8	23.7
HLT-8	514	15	1470	0.9	19	0.7	15.8
HLT-9	2498	72.1	3400	789.25	340	16.3	23.1
LLT-1	1270	40.9	470	7.81	107	7.3	15.8
LLT-2	1516	43.1	1200	4.6	304	0.7	17.6
LLT-3	1137	46.3	1160	18	122	0.7	18.9
LLT-4	2209	57.1	1280	20.7	479	2.5	17.2
LLT-5	827	40.9	1520	3	70	0.7	19.7
LLT-6	735	29.2	590	6.93	70	2.8	18.8
LLT-7	811	23.5	1070	9.9	61	0.7	19.5
MDL-1	1584	23.1	1170	0.9	209	0.7	21.5

Appendix B, Table 8 (continued)

Site ID	Cl	Cond**	DOC	NH_4-N	NO_3-N	SRP	Temp
MDL-2	578	17.2	1780	0.9	15	6	16.2
MDL-3	1627	28.9	1320	11.8	470	0.7	20.8
MDL-4	669	14.5	1450	0.9	99	0.7	21.4
MDL-5	5629	39.1	1070	0.9	253	0.7	17.6
MDL-6	1611	22.5	630	7.09	164	0.7	19.2
MDL-7	1612	22.5	1230	0.9	162	0.7	19.2
MST-1	26330	163.2	1820	0.9	112	166.9	19.8
MST-2	25896	165.9	1000	5.14	116	176.7	19.2
MST-3	28617	171.8	1700	79.3	107	101.5	21.7
MST-4	41468	229.7	1640	2.9	109	294.8	20.9
MST-5^{+}	55999	309.5	1590	22.53	126	406.7	19.3
MST-6	66514	354	1580	16.38	108	433.6	18.9
MST-7	994	26.9	710	21.57	146	10.2	16.9
PSO-1A^{++}	1205	40.4	1140	10	108	2.2	16.9
PSO-1B^{++}	1564	45.1	1590	4.5	301	0.7	17
PSO-1C^{++}	1759	48.4	1120	20	311	0.7	17.1
PSO-1D^{++}	2317	55.1	1550	67.4	343	4.3	17.1
PSO-2^{++}	705	34.6	1840	2	80	0.7	19.2
PSO-3^{++}	4819	53.7	1560	0.9	81	0.7	17.8
TST-1	722	18.1	640	7.21	28	34.4	21.1
TST-2	580	17.3	1320	0.9	24	0.7	16.4
TST-3	742	24	1300	0.9	37	0.7	17.6
TST-4	680	19.5	1110	0.9	45	0.7	16.7
TST-5	754	20.4	1290	0.9	115	0.7	15.5

Appendix B, Table 9: Oregon 2003 water chemistry data.

Site ID	Cl	Cond	DON	NH_4-N	NO_3-N	SRP	TDN	TDP	Temp	TKN	TN	TP
3701002	19100	319	600	69	2540	51	3210	93	23.6	672	-	-
3701054	21300	344	580	68	2790	27	3430	78	22.4	643	-	-
3701087	19000	324	550	85	2630	31	3270	79	21.7	637	-	-
3701165	15600	276	580	11	2860	20	3460	90	21.8	595	-	-
3701271	17500	294	470	47	2610	47	3130	92	21	517	-	-
3701333^{+++}	20200	291	450	42	4330	39	4820	62	19.5	493	-	-
3701450	2890	92	290	19	566	37	880	63	16	310	-	-
3701528	2630	76	110	11	197	11	320	27	13	118	-	-
3701612	2130	65	100	10	189	8	300	25	10.6	110	-	-
3701715	2900	61	70	10	74	7	150	25	11.5	78	-	-
3805017	1820	67	100	10	201	5	310	25	9.3	110	-	-
3805048	1830	67	320	10	209	5	540	25	9	329	-	-
3810015	5980	145	160	24	175	28	360	51	19.8	186	-	-
3815021	3510	150	290	25	1170	66	1480	119	18.6	314	-	-
3816020	5500	185	360	38	335	64	730	125	18.9	397	-	-
3820022	20400	324	420	41	326	175	790	224	19.1	463	-	-
3820047	11000	314	420	43	206	88	670	147	18.4	465	-	-
3821008	11800	270	460	37	348	189	850	245	20.1	499	-	-
3821050^{+++}	11400	248	370	52	303	97	720	150	19.4	418	-	-
3824001^{+++}	21700	273	960	60	122	54	1140	282	19.2	1020	-	-
3824015^{+++}	23200	266	960	99	101	54	1160	146	20.9	1060	-	-
3824018^{+++}	23600	263	760	56	67	33	880	94	23.5	811	-	-
3824020^{+++}	40800	325	310	25	157	44	490	83	16.1	337	-	-
3824032^{+++}	40100	314	330	49	364	52	740	113	15.2	376	-	-
3824050^{+++}	40200	392	350	80	406	29	840	147	14.7	432	-	-
3824072^{+++}	6920	164	180	14	1050	79	1250	104	13.7	195	-	-
3827014^{+++}	7510	180	720	62	47	40	820	133	20	777	-	-
3835020	3040	149	270	33	332	42	640	111	17.8	306	-	-
3838001^{+++}	5090	260	350	63	453	69	860	136	18.6	411	-	-
3840012	10500	267	310	47	449	105	800	152	18.7	352	-	-
3840074	10500	244	370	32	139	119	540	215	18.6	401	-	-
3840095	7870	205	370	48	216	135	630	207	19	414	-	-

Appendix B, Table 9 (continued)

Site ID	Cl	Cond	DON	NH_4-N	NO_3-N	SRP	TDN	TDP	Temp	TKN	TN	TP
3844009	8920	235	830	68	41	38	940	258	20.7	895	-	-
3845014	3730	162	200	33	362	72	590	124	16.9	228	-	-
3850006^{+++}	15100	409	320	83	281	108	690	168	16.8	405	-	-
3859010^{+++}	4460	130	160	11	412	92	580	99	13.7	167	-	-
BLED^{+}	7093	205.2	210	114	4483	13	4800	-	17.5	320	5770.33	18.8
BV0	5057.7	75.5	60	10	68	30	140	-	16.3	70	184.46	32.91
CLR	2245	175.1	90	10	40	22	140	-	15.8	100	113.61	9.13
EFD1	2407	63	50	2	390	40	440	-	13.3	50	669.53	43.32
EFD2	2447	66.1	70	8	259	29	340	-	17.9	80	411.33	21.48
EFD3	3623	71.4	90	3	544	29	630	-	17.4	90	682.24	22.77
EFD4	3135	73.5	110	9	334	29	450	-	18.3	120	514.43	23.97
FA1^{+++}	12429	206.8	290	54	220	136	560	-	19.5	340	577.53	85.35
FA2^{+++}	12328	233.5	260	38	145	120	450	-	20.1	300	348.58	61.02
GA1	3834	97.8	60	1	21	15	80	-	16.9	60	109.1	14.1
GA2	2733	74.1	50	b.d.	53	20	100	-	12.8	50	84.49	21.94
GA3	3137	89.4	40	3	32	21	70	-	16.2	40	119.85	17.51
ILR	3347	109.9	80	4	44	23	120	-	15.7	80	126.44	18.34
LDV	2940	100.4	20	1	63	26	80	-	12	20	120.43	16.68
LOU_CNL	3412	151.6	290	41	3	53	330	-	19	330	349.38	28.94
MK1	5991	134	260	23	372	41	650	-	19	280	665.83	20.28
MK2	2437	78.1	90	7	219	13	320	-	18.4	100	377.47	11.89
ROD	2582	142.4	50	1	280	36	330	-	13.2	50	357.01	18.16
RR1	3261	61.4	50	1	77	2	130	-	11.4	50	149.9	2.4
SFD	4174	94.3	190	15	416	35	620	-	18.5	200	672.88	23.23
SFGA	3105	78.2	40	1	76	7	120	-	14.1	40	138.81	4.24
THM	2781	145.7	50	5	70	22	120	-	14.2	50	139.96	41.02
UBV	12357	103.2	120	7	104	47	230	-	14.8	130	266.75	52.08
UNK_CNL**	7349	155.5	280	36	3751	6	4070	-	19.8	320	4368.86	15.21
WFD	4112	93.2	140	31	423	31	590	-	18.8	170	753.55	19.82
WRBL1	58166	484.2	780	63	508	927	1350	-	18.1	840	1183.61	774.56
WRBL2^{+++}	54306	458.1	660	40	915	882	1620	-	22.1	700	1750.85	760.91

Appendix B, Table 10: Oregon 2004 water chemistry data.

Site ID	Cl	Cond	DON	NH_4-N	NO_3-N	SRP	TDN	TDP	Temp	TKN	TN	TP
3500035	8730	270	281	54	930	99	1270	203	17.4	335	-	-
3701002	24000	300	489	21	2940	37	3450	72	23.7	510	-	-
3701054	22700	292	551	12	2660	32	3220	78	22.8	563	-	-
3701087	19600	261	451	53	2450	40	2950	93	22.1	504	-	-
3701165	17300	249	396	22	2800	36	3220	75	22.1	418	-	-
3701271	18100	263	342	41	2590	42	2970	71	20.5	383	-	-
3701333^{+++}	18200	175	488	27	3840	30	4360	70	18.9	515	-	-
3701391	3330	87	165	16	266	25	450	44	16.2	181	-	-
3701450	3190	82	126	12	195	19	330	36	14.6	138	-	-
3701528	2910	73	95	10	144	11	250	25	12.7	105	-	-
3701612	2650	68	81	10	99	9	190	25	11.7	91	-	-
3701715^{+++}	3580	62	40	10	50	5	100	25	12.3	50	-	-
3805017	2360	63	42	10	93	5	150	25	10.8	52	-	-
3805048	2370	68	77	15	110	7	200	25	10.5	92	-	-
3810015	9550	150	131	30	174	36	340	58	21.8	161	-	-
3815021	9800	223	455	42	3030	87	3530	158	20	497	-	-
3816020	6580	194	346	51	430	83	830	158	19.8	397	-	-
3820022	37100	343	416	44	653	209	1110	290	20.3	460	-	-
3820047	9200	307	423	104	229	126	760	247	19.4	527	-	-
3821008	51400	359	361	56	629	195	1050	274	20.9	417	-	-
3821050^{+++}	16700	205	427	117	202	120	750	216	22.6	544	-	-
3824001^{+++}	13400	226	501	42	30	88	570	195	21.7	543	-	-
3824015^{+++}	13300	226	487	53	30	95	570	177	22.3	540	-	-
3824018^{+++}	14100	212	496	28	37	101	560	162	24.7	524	-	-
3824020^{+++}	16700	247	319	19	176	68	510	116	18.1	338	-	-
3824032^{+++}	17600	248	204	58	234	71	500	160	18	262	-	-
3824072^{+++}	6450	178	237	22	1000	122	1260	181	17.9	259	-	-
3827014^{+++}	6670	130	646	133	30	55	810	206	22.8	779	-	-
3835020	4800	188	239	47	225	63	510	136	18.8	286	-	-
3838001	5420	265	449	141	227	86	820	315	19.6	590	-	-
3840012	12600	275	358	75	426	115	860	180	20.3	433	-	1696.62
3840074	25700	302	384	83	93	113	560	209	20	467	-	-

Appendix B, Table 10 (continued)

Site ID	Cl	Cond	DON	NH_4-N	NO_3-N	SRP	TDN	TDP	Temp	TKN	TN	TP
3840095	65500	443	448	67	424	98	940	160	18.8	515	-	-
3844009	8700	219	829	36	30	24	900	126	24.5	865	-	-
3845014	5710	250	181	33	329	96	540	154	18.5	214	-	-
3850006^{+++}	50500	375	382	60	183	124	630	229	19.6	442	-	-
3859010^{+++}	3970	190	39	11	222	130	270	160	15.2	50	-	-
$BLED^{+}$	10300	283.2	-12	43	13854	62	13890	-	19.5	30	25394.2	177.27
BUR	19500	308.8	298	52	183	60	530	-	20	350	262.19	54.02
BV0	2560	88.9	141	19	85	65	250	-	17.3	160	151.63	37.49
CC1	4440	116.5	131	9	175	32	320	-	17	140	367.58	23.74
CLD	4590	423.5	353	108	449	105	910	-	17.7	460	865.12	150.45
CSTN	17900	305	332	78	67	22	480	-	18.8	410	582.56	168.05
EFD1	1360	58	98	2	322	43	420	-	17	100	259.39	3.77
EFD2	1810	74.9	139	11	184	35	330	-	21.5	150	194.44	18.83
EFD3	2150	80.7	125	15	492	38	630	-	20.2	140	318.54	26.85
EFD4	2330	88.7	144	16	551	43	710	-	20.4	160	463.29	28.81
GA1	3770	106.2	91	9	52	15	150	-	18.9	100	108.83	4.09
GA2	3410	79.1	38	2	127	23	170	-	13.5	40	165.03	42.95
GA3	2120	95	52	8	115	25	180	-	16	60	149.48	4.58
HTN	8180	108.5	164	36	143	20	340	-	19.3	200	190.99	12.11
LOU_CNL	2150	161.4	241	19	10	28	270	-	20.6	260	354.72	121.22
MCF1	5630	18.6	246	84	196	66	530	-	22.6	330	442.39	137.56
MCF2	2080	128.5	212	39	285	50	540	-	21.3	250	307.14	35.36
MK1	6880	178.3	324	36	467	61	830	-	21.3	360	556.85	86.6
MK2	1940	93.4	141	19	152	22	310	-	20	160	210.35	9
MK3	1890	98.5	105	5	483	36	590	-	18.1	110	335.31	10.31
ROD	2170	159.2	86	4	232	36	320	-	14.7	90	180.45	14.73
SFD	3620	21.3	362	28	260	31	650	-	139.1	390	485.44	36.34
SFGA	5160	85.8	57	3	144	9	200	-	15.7	60	194	4.09
THM	2710	163.8	54	6	98	28	160	-	15.7	60	67.53	20.95
UNK_CNL**	11100	218.3	531	9	10	5	550	-	21	540	666.76	121.74
WFD1	4190	123	272	48	668	47	990	-	20.1	320	862.48	26.19
WFD2	3700	122.4	235	46	155	46	440	-	18.9	280	256.38	48.62
$WRBL2^{+}$	45800	480.3	810	40	873	673	1720	-	26.8	850	1696.05	1289.9

Appendix B, Table 11: Puerto Rico 2004 water chemistry data.

Site ID	Cl	Cond	DON	NH_4-N	NO_3-N	SRP	TDN	Temp	TP
SYN1-0	24800	330.1	90	1149.8	468	82	1712.7	25.3	290
SYN1-1	24970	318.2	80	982.1	421	56	1483.2	25.6	250
SYN1-3	21480	307.8	800	1489.2	277	66	2561.6	25.2	324
SYN1-4	23660	507	270	24.0	373	12	665.3	25	106
SYN1-5	22550	354	380	474.1	517	49	1373.2	25.3	218
SYN1-7	24710	371	860	1881.9	457	153	3201.9	25.3	417
SYN2-0	33260	457.6	400	146.1	892	44	1434.9	26.4	260
SYN2-1	40220	496	2320	918.4	107	56	3348.7	25.7	422
SYN2-2	24210	605	1720	791.2	118	53	2632.0	25.7	339
SYN2-4**	39370	397.3	590	1136.2	855	111	2578.3	26.8	279
SYN2-5	38920	468.2	700	1100.9	361	89	2163.4	27.7	302
SYN2-6**	14510	258.6	290	710.3	6	60	1010.4	25.8	215
SYN2-7	41460	501	800	901.6	438	66	2138.4	27.5	375
SYN3-0	41770	476	790	1991.5	380	34	3165.3	26	259
SYN3-2	54760	661	2060	8397.8	34	343	10492.5	25.8	1532
SYN3-3	36620	465	-	352.6	971	8	1230.1	25.6	89
SYN3-4	37870	436	340	184.9	932	19	1453.0	26.3	130
SYN4-0	23310	237.1	620	510.6	316	129	1450.4	25.6	1602
SYN4-2	41720	388	360	70.9	932	15	1364.7	25.1	75
SYN4-3	42460	526	300	118.1	410	6	830.6	25	96
SYN4-4	33110	460.9	240	26.5	867	10	1134.9	24.6	75
SYN4-5	29210	421.9	290	28.8	1094	20	1417.0	24.3	120
SYN5-0	21880	265.7	250	16.5	398	5	662.2	25.1	42
SYN5-1	18550	237.3	280	12.0	63	1	352.0	27.4	27
SYN5-2	24210	304.2	210	11.2	663	25	889.2	25	84
SYN5-4	31670	572	290	24.0	1192	24	1506.9	25.2	162
SYN5-6	31030	491.5	270	214.8	569	33	1051.2	24.9	181
SYN5-8	27930	410.9	230	8.6	848.5	13	1091.8	24	117
SYN5-9**	27540	388.3	410	26.9	762	16	1195.4	23.4	101
SYN6-0	21580	274.1	400	46.9	723	23	1165.5	23.3	206
SYN6-2	23330	385.7	400	125.7	522	16	1046.8	23.3	106
SYN6-3	22900	438.3	420	20.5	899	40	1335.6	22.2	151
SYN6-4	25170	360.7	350	95.9	469	5	911.1	22	55
SYN6-5	24190	377.2	470	114.8	643	18	1228.8	22.7	178
SYN6-6	29020	475.5	410	100.0	1004	22	1517.9	23.2	195
SYN6-7	20070	308.7	290	26.6	597	24	914.0	23	157
SYNP-1	25420	348.6	-	315.3	644.5	36	898.8	24.2	205
SYNP-2	24980	343.4	-	125.5	597	30	654.0	24.3	191
SYNP-3	33470	403	-	172.8	718	32	747.8	26	171
SYNP-4	31550	407	-	753.1	669	70	1242.5	27.1	205
SYNP-5	19030	317.7	40	16.0	404	19	458.2	25	105
SYNP-USGS	22560	312.2	-	668.5	523	68	1144.3	24.3	253

Appendix B, Table 12: Puerto Rico 2005 water chemistry data.

Site ID	Cl	Cond	DON	NH_4-N	NO_3-N	SRP	TDN	Temp	TP
SYN1-0	37600	466.1	790	3728	60	318	4570	24.1	611
SYN1-1	46800	537	2560	4635	30	302	7230	24.4	969
SYN1-3	69020	785	6670	11775	90	1457	18530	26.5	2468
SYN1-4	29230	547	290	40	870	30	1190	24.3	77
SYN1-7	39780	579	1440	3312	180	634	4940	24.8	2051
SYN2-0	35020	493	330	90	940	41	1360	24.8	133
SYN2-1	38180	489	560	61	1400	62	2020	24.7	165
SYN2-2	37160	521	170	27	750	21	950	26	89
SYN2-4**	32410	398.6	1040	711	1020	244	2780	26.4	360
SYN2-5	33760	437.8	620	693	560	59	1870	26.6	215
SYN2-6**	30020	634	120	6	1360	52	1480	27.2	57
SYN3-0	43820	509	650	2998	410	124	4060	24.5	499
SYN3-2+	52060	564	1610	3490	-	64	5100	24.4	388
SYN3-3	35080	452.1	150	11	1230	18	1390	24.9	88
SYN3-4	35570	417.4	390	279	840	28	1510	26.4	152
SYN4-0	34320	436.2	470	106	1390	67	1960	24.6	224
SYN4-2	29830	335.2	370	124	1240	40	1730	23.9	104
SYN4-3	42500	642	3570	1281	270	168	5120	25.1	469
SYN4-4	37490	483.2	270	66	1430	29	1760	24.4	92
SYN4-5	33370	402.1	170	9	1610	33	1790	24.6	118
SYN5-0	24780	299.4	210	12	1380	22	1600	25	43
SYN5-1	17150	239.7	210	11	320	3	540	27.7	10
SYN5-2	25550	311.2	100	5	1040	40	1140	24.4	72
SYN5-4	22200	688	270	39	770	27	1090	25.3	190
SYN5-6	29740	448	280	73	570	14	930	24.3	100
SYN5-9**	30420	264.6	190	-	1050	27	1240	24.6	66
SYN6-0	33310	473	210	14	940	21	1160	24.4	89
SYN6-2	29680	424.8	170	8	670	17	850	25.5	46
SYN6-3	31040	504	190	4	1000	21	1200	21.2	96
SYN6-4	33310	450.7	220	22	690	4	930	24.9	31
SYN6-5	31740	370.6	130	15	860	15	1000	23.3	68
SYN6-6	36950	613	390	3	230	21	620	24.9	86
SYN6-7	38650	522	980	250	90	127	1320	25.3	295
SYNP-1	32790	456.9	720	85	690	61	1490	24	205
SYNP-2	32410	444.1	290	126	730	33	1150	23.9	110
SYNP-3	31200	436.7	220	23	890	24	1130	24.5	109
SYNP-4	31610	384.3	160	23	940	30	1130	24.1	91
SYNP-5	29680	413.9	170	34	940	15	1140	24.6	90
SYNP-USGS	33160	444.1	1000	115	550	79	1670	23.8	202

Appendix B, Table 13: Wyoming 2005 water chemistry data.

Site ID	Cl	Cond	Flow	NH_4-N	NO_3-N	TDN	Temp
WY-01	1083.6	279.2	192.9	2.5	53.5	125.2	-
WY-02	893.9	198.8	2394.2	4.2	30.3	92.8	-
WY-03	415.4	200.6	2025.4	3.7	25.9	70.3	-
WY-04	386.1	206.1	77.6	8.1	10.4	70.0	-
WY-05**	2166.5	276.8	1749.6	7.1	25.3	87.3	-
WY-06**	1693.3	278.5	251.5	48.1	201.5	286.2	-
WY-07	753.5	277.8	3349.6	4.3	14.9	74.7	-
WY-08	1010.0	276.3	3830.3	3.4	11.1	88.1	-
WY-09	416.1	295.1	515.9	6.6	28.0	88.1	-
WY-10	740.2	294.4	500.0	10.1	29.5	79.1	-
WY-11	885.1	291.3	106.0	10.1	56.7	135.5	10.5
WY-12	841.0	279.6	3038.4	1.7	2.5	89.7	17.6
WY-13	2063.3	278.0	2693.8	3.5	8.8	105.3	17.7
WY-14	1300.3	277.2	2349.2	3.4	8.7	120.1	18.1
WY-15	1191.7	299.9	1949.0	2.8	14.4	133.2	18.4
WY-16	2169.8	320.1	2148.5	5.7	9.5	105.4	19.4
WY-17	2308.7	457.9	441.5	7.5	8.9	93.2	16.6
WY-18	3669.1	392.2	1919.7	10.2	67.4	209.2	18.2
WY-19	4410.2	406.2	2966.4	15.7	33.5	208.3	18.3

Appendix C, Table 1: Reclassification scheme for National Land Cover Data (NLCD).

Land Cover Description	Reclassification
Open Water	Water
Perennial Ice/Snow	Water
Low Intensity Residential	Urban
High Intensity Residential	Urban
Commercial/Industrial/Transportation	Urban
Bare Rock/Sand/Clay	Barren
Quarries/Strip Mines/Gravel Pits	Barren
Transitional	Barren
Deciduous Forest	Forested Upland
Evergreen Forest	Forested Upland
Mixed Forest	Forested Upland
Shrubland	Shrubland
Orchards/Vineyards/Other	Agriculture
Grasslands/Herbaceous	Herbaceous Upland
Pasture/Hay	Agriculture
Row Crops	Agriculture
Small Grains	Agriculture
Fallow	Agriculture
Urban/Recreational Grasses	Agriculture
Woody Wetlands	Wetlands
Emergent Herbaceous Wetlands	Wetlands

Appendix C, Table 2: Reclassification scheme for Massachusetts land cover.

Land Cover Description	Reclassification
water	Water
marine water	Water
developed	Urban
bare ground	Barren
upland deciduous forest	Forested Upland
upland mixed forest	Forested Upland
upland coniferous forest	Forested Upland
upland scrub/shrubland	Shrubland
grassland	Agriculture
cultivated	Agriculture
wetland	Wetlands
lake, fresh marsh, or pond, emergent vegetation	Wetlands
coniferous forested wetland	Wetlands
deciduous shrub wetland	Wetlands
coniferous shrub wetland	Wetlands
deciduous forested wetland	Wetlands
riverine tidal unconsolidated bottom	Wetlands
estuarine, riverine intertidal rocky shore	Wetlands
estuarine, riverine intertidal unconsolidated shore	Wetlands
estuarine intertidal aquatic vegetation	Wetlands
estuarine subtidal aquatic vegetation	Wetlands
marine intertidal unconsolidated shore	Wetlands
estuarine intertidal emergent vegetation	Wetlands
marine intertidal aquatic vegetation	Wetlands
marine intertidal rocky shore	Wetlands
estuarine intertidal scrub/shrub	Wetlands

Appendix C, Table 3: Reclassification scheme for Oregon land cover.

Land Cover Description	Reclassification
Stream orders 5-7	Water
Permanent lentic water	Water
Residential 0 - 4 DU/ac, 4-9 DU/ac, 9-16DU/ac, >16DR/ac	Urban
Commercial	Urban
Commercial/Industrial	Urban
Industrial	Urban
Residential and Commercial	Urban
Urban non-vegetated unknown	Urban
Rural structures	Urban
Railroad	Urban
Primary and secondary roads	Urban
Light duty roads	Urban
Rural non-vegetated unknown	Barren
Topographic shadow	Barren
Upland forest open	Forested Upland
Upland forest semi-closed mixed	Forested Upland
Forest closed hardwood	Forested Upland
Forest closed mixed	Forested Upland
Upland forest semi- close conifer	Forested Upland
Conifers 0-20yrs	Forested Upland
Forest closed conifer 21-40yrs, 41-60yrs, 61-80yrs, 81-200yrs, >200yrs	Forested Upland
Upland forest semi closed hardwood	Forested Upland
natural shrubland	Shrubland
hybrid poplar	Agriculture
berries and vineyards, nursery	Agriculture
hops	Agriculture
orchard	Agriculture
christmas trees, conifer woodlot	Agriculture
natural grassland	Herbaceous Upland
urban tree overstory	Agriculture
grass seed rotation	Agriculture
irrrigated annual rotation	Agriculture
grains	Agriculture
double cropping	Agriculture
mint	Agriculture
radish seed	Agriculture
sugar beet seed	Agriculture
row crop	Agriculture
grass, turfgrass	Agriculture
field crop, late field crops	Agriculture
hayfield, pasture	Agriculture
bare/fallow	Agriculture
irrigated perennial	Agriculture
flooded/marsh	Wetlands

Appendix C, Table 4: Reclassification scheme for Puerto Rico land cover.

Land Cover Description	Reclassification
Water	Water
Urban and barren	Urban
Salt and mud flats	Barren
Sand and rock1	Barren
Sand and rock2	Barren
Quarries	Barren
Lowland dry semideciduous forest	Forested Upland
Lowland dry semideciduous woodland/shrubland	Forested Upland
Lowland dry mixed evergreen drought-deciduous shrubland with succulents	Forested Upland
Lowland dry and moist, mixed seasonal evergreen sclerophyllous forest	Forested Upland
Lowland moist seasonal evergreen forest	Forested Upland
Lowland moist seasonal evergreen forest/shrub	Forested Upland
Lowland moist coconut palm forest	Forested Upland
Lowland moist semi-deciduous forest	Forested Upland
Lowland moist seasonal evergreen and semi-deciduous forest	Forested Upland
Lowland moist seasonal evergreen and semi-deciduous forest/shrub	Forested Upland
Submontane and lower montane wet evergreen sclerophyllous forest	Forested Upland
Submontane and lower montane wet evergreen sclerophyllous forest/shrub	Forested Upland
Submontane and lower montane wet evergreen forest/shrub	Forested Upland
Lower montane wet evergreen forest - tall and palm cloud forest	Forested Upland
Lower montane wet evergreen forest - elfin and palm cloud forest	Forested Upland
Lower montane wet evergreen forest - elfin and palm cloud forest	Forested Upland
Seasonally flooded rainforest	Forested Upland
Lowland moist evergreen hemisclerophylous shrubland	Shrubland
Lowland moist semi-deciduous forest/shrub	Shrubland
Active sun/shade coffee, submontane and lower montane wet forest/shrub	Agriculture
Pasture	Agriculture
Agriculture/hay	Agriculture
Agriculture	Agriculture
Submontane wet evergreen forest	Wetlands
Tidally and semi-permanently flooded evergreen sclerophyllous forest	Wetlands
Tidally flooded evergreen dwarf-shrubland and forb vegetation	Wetlands
Other emergent wetlands (including seasonally flooded pasture)	Wetlands